

A peer-reviewed version of this preprint was published in PeerJ on 7 December 2018.

[View the peer-reviewed version](https://doi.org/10.7717/peerj.5964) (peerj.com/articles/5964), which is the preferred citable publication unless you specifically need to cite this preprint.

Raselli I. 2018. Comparative cranial morphology of the Late Cretaceous protostegid sea turtle *Desmatochelys lowii*. PeerJ 6:e5964
<https://doi.org/10.7717/peerj.5964>

Comparative cranial morphology of the Late Cretaceous protostegid sea turtle *Desmatochelys lowii*

Irena Raselli ^{Corresp. 1}

¹ Departement of Geosciences, University of Fribourg, Fribourg, Switzerland

Corresponding Author: Irena Raselli

Email address: irena.raselli@hotmail.com

Background. The phylogenetic placement of Cretaceous marine turtles, especially Protostegidae, is still under debate among paleontologists. Whereas protostegids were traditionally thought to be situated within the clade of recent marine turtles (Chelonioidae), some recent morphological and molecular studies suggest placement along the stem of Cryptodira. The main reason why the evolution of marine turtles is still poorly understood, is in part due to a lack of insights into the cranial anatomy of protostegids. However, a general availability of high quality fossil material, combined with modern analysis techniques, such as X-ray microtomography (μ CT), provide ample opportunity to improve this situation. The scope of this study is to help resolve its phylogenetic relationships by providing a detailed description of the external and internal cranial morphology of the extinct protostegid sea turtle *Desmatochelys lowii* Williston, 1894 . **Material and Methods.** This study is based on the well-preserved holotype of *Desmatochelys lowii* from the Late Cretaceous (middle Cenomanian to early Turonian) Greenhorn Limestone of Jefferson County, Nebraska. The skulls of two recent marine turtles, *Eretmochelys imbricata* (Cheloniidae) and *Dermochelys coriacea* (Dermochelyidae), as well as the snapping turtle *Chelydra serpentina* (Chelydridae) provide a comparative basis. All skulls were scanned using regular or micro CT scanners and the scans were then processed with the software program Amira to create 3D isosurface models. In total, 81 bones are virtually isolated, figured, and described, including the nature of their contacts. The novel bone contact data is compiled and utilized in a preliminary phenetic study. In addition, an update phylogenetic analysis is conducted that utilizes newly obtained anatomical insights. **Results.** The detailed examination of the morphology of the herein used specimens allowed to explore some features of the skull, to refine the scoring of *Desmatochelys lowii* in the recent global matrix of turtles, and develop five new characters. The alleged pineal foramen in the type skull of *Desmatochelys lowii* is shown to be the result of damage. Instead, it appears that the pineal gland only approached the skull surface, as it is in *Dermochelys coriacea*. Whereas

the parasphenoid is confirmed to be absent in hard-shelled sea turtles, its possible presence in *Desmatochelys lowii* is unclear. The results of the phenetic study show that *Desmatochelys lowii* is least similar to the other examined taxa in regards to the nature of its bone contacts, and therefore suggests a phylogenetic placement outside Americhelydia for this protostegid sea turtle. The phylogenetic study results in a placement of Protostegidae along the stem of Chelonioidea, which is a novel position for the group more congruent with recent molecular calibration analyses.

1 **Comparative Cranial Morphology of the Late Cretaceous**
2 **Protostegid Sea Turtle *Desmatochelys lowii***

3 Irena Raselli

4 Department of Geosciences, University of Fribourg, Fribourg, Switzerland

5

6 Corresponding Author:

7 Irena Raselli

8 Chemin du Musée 6, Fribourg, 1700, Switzerland

9 Email address: irena.raselli@hotmail.com

10

ABSTRACT

Background. The phylogenetic placement of Cretaceous marine turtles, especially Protostegidae, is still under debate among paleontologists. Whereas protostegids were traditionally thought to be situated within the clade of recent marine turtles (Chelonioidae), some recent morphological and molecular studies suggest placement along the stem of Cryptodira. The main reason why the evolution of marine turtles is still poorly understood, is in part due to a lack of insights into the cranial anatomy of protostegids. However, a general availability of high quality fossil material, combined with modern analysis techniques, such as X-ray microtomography (μ CT), provide ample opportunity to improve this situation. The scope of this study is to help resolve its phylogenetic relationships by providing a detailed description of the external and internal cranial morphology of the extinct protostegid sea turtle *Desmatochelys lowii* Williston, 1894.

Material and Methods. This study is based on the well-preserved holotype of *Desmatochelys lowii* from the Late Cretaceous (middle Cenomanian to early Turonian) Greenhorn Limestone of Jefferson County, Nebraska. The skulls of two recent marine turtles, *Eretmochelys imbricata* (Cheloniidae) and *Dermochelys coriacea* (Dermochelyidae), as well as the snapping turtle *Chelydra serpentina* (Chelydridae) provide a comparative basis. All skulls were scanned using regular or micro CT scanners and the scans were then processed with the software program Amira to create 3D isosurface models. In total, 81 bones are virtually isolated, figured, and described, including the nature of their contacts. The novel bone contact data is compiled and

utilized in a preliminary phenetic study. In addition, an update phylogenetic analysis is conducted that utilizes newly obtained anatomical insights.

Results. The detailed examination of the morphology of the herein used specimens allowed to explore some features of the skull, to refine the scoring of *Desmatochelys lowii* in the recent global matrix of turtles, and develop five new characters. The alleged pineal foramen in the type skull of *Desmatochelys lowii* is shown to be the result of damage. Instead, it appears that the pineal gland only approached the skull surface, as it is in *Dermochelys coriacea*. Whereas the parasphenoid is confirmed to be absent in hard-shelled sea turtles, its possible presence in *Desmatochelys lowii* is unclear. The results of the phenetic study show that *Desmatochelys lowii* is least similar to the other examined taxa in regards to the nature of its bone contacts, and therefore suggests a phylogenetic placement outside Americhelydia for this protostegid sea turtle. The phylogenetic study results in a placement of Protostegidae along the stem of Cheloniodea, which is a novel position for the group more congruent with recent molecular calibration analyses.

INTRODUCTION

All recent marine turtles (i.e., turtles that permanently live in fully marine environments) are currently accepted to form a monophyletic group, Chelonioidea Baur, 1893, that consists of two clades: the hard-shelled Cheloniidae Bonaparte, 1832 and the leathery-shelled Dermochelyidae Lydekker, 1889 (e.g., Crawford et al., 2014; Pereira et al., 2017). Whereas the former group consists of six species distributed across all tropical to warm temperate oceans, the latter group is represented only by one species with a global distribution, the leatherback turtle *Dermochelys coriacea* (TTWG, 2017). The ancestry of marine turtles, however, is controversial for paleontologists, because relationships are unclear between extant marine turtles and various groups of fossil turtles adapted to marine environments (see Cadena and Parham, 2015, for recent summary). The following groups of fossil turtles are currently thought to be marine: the Late Jurassic Eurysternidae Dollo, 1886, Plesiochelyidae Baur, 1888, and Thalassemydidae Zittel, 1889 (Anquetin et al., 2017), which were recently grouped as Thalassochelydia Anquetin et al., 2017, the Cretaceous Protostegidae Cope, 1872 (Cadena and Parham, 2015) and certainly paraphyletic or polyphyletic Toxochelyidae Cope, 1873 (Parham and Pyenson, 2010), the Early Cretaceous to Paleogene Bothremydidae Baur, 1891 (Gaffney et al., 2006) and Sandownidae Tong & Meylan, 2012 (Cadena, 2015), and, finally, the Tertiary Stereogenyina Gaffney et al., 2011. Whereas it is apparent that the two clades of marine pleurodires, Bothremydidae and Stereogenyina, have no immediate relationships with their extant cryptodiran cousins, all other fossil groups have at one point or the other been suggested to be ancestral or related to extant marine turtles.

Recent discussions have focused on the phylogenetic position of protostegids. On the one hand, some studies suggest that protostegids are situated within crown Chelonioidea (e.g.,

Gaffney & Meylan, 1988; Hirayama, 1998; Cadena and Parham, 2015), while others place them outside of crown Cryptodira (e.g., Joyce, 2007; Anquetin, 2012; Rabi et al., 2013; Parham et al., 2012). The latter hypothesis is concordant with molecular calibration analyses, as these suggest a divergence of crown Cheloniodea near the K/T boundary event (Joyce et al., 2013). One of the primary reasons why the interrelationships of marine turtles remain unresolved is because only few specimens from the Mesozoic have been described in detail, even though much interesting material is available for study and new methods available to access anatomical information. As a consequence, modern studies using cladistic methodologies still often rely on outdated literature that often provides simplified or incomplete illustrations of specimens. A good example is the holotype of the Late Cretaceous protostegid *Desmatochelys lowii* Williston, 1894. The specimen was collected in 1893 near Fairbury, Jefferson County, Nebraska from the Late Cretaceous Greenhorn Limestone (formerly Benton Cretaceous) in sediments that had once been deposited in the Western Interior Seaway. The ‘Benton Cretaceous’ is now regionally classified as the Greenhorn Limestone, which is middle Cenomanian to lower Turonian in age (Hattin, 1975). Even though the specimen includes the best-preserved skull of *Desmatochelys lowii* in particular, but also one of the best preserved protostegid skulls in general, it was only superficially described by Williston (1894), Zangerl and Sloan (1960), and Elliott et al. (1997).

The purpose of this study is to document in detail the cranial morphology of the holotype of *Desmatochelys lowii*. As the detailed cranial anatomy is not yet available for any other species of protostegid, the skull is here compared on a bone-by-bone basis to the extant marine turtles *Eretmochelys imbricata* (Cheloniidae) and *Dermochelys coriacea* (Dermochelyidae), as well as the freshwater snapping turtle *Chelydra serpentina* (Chelydridae). All specimens were CT scanned and their bones 3D visualized to provide the greatest amount of possible new insights

96 into their cranial morphology. The resulting data was then used to update the scoring of
 97 *Desmatochelys lowii* in the latest available global matrix of marine turtle relationships (Cadena
 98 & Parham, 2015). In addition, an exploratory phenetic study is conducted that seeks phylogenetic
 99 information from bone contacts.

100

MATERIALS AND METHODS

Material

The osteology of the fossil marine turtle *Desmatochelys lowii* is herein described in detail based on CT scans. For comparison, the study includes scans of two recent marine turtles, *Eretmochelys imbricata* and *Dermochelys coriacea*, and *Chelydra serpentina* as the “outgroup.”

Desmatochelys lowii Williston, 1894

The description of this species is based KUVP 1200, which is the holotype *Desmatochelys lowii*, currently housed in the collection of the University of Kansas in Lawrence, Kansas, USA. The skull is 21.5 cm long and has a maximum width of 14 cm. It is posteroventrally crushed and its basicranium is pierced by a hole of 1.5 cm in diameter that was drilled into the skull for mounting following its initial description. Although this specimen is lightly damaged and internally filled with matrix, it is the best-preserved skull of this species known to date (Everhart & Pearson, 2009; Elliott et al., 1997).

Eretmochelys imbricata (Linnaeus, 1766)

The species is represented by NMB C.2417, which is housed in the collection of the Naturhistorisches Museum Basel, Switzerland. The skull is 12.5cm long and has a maximum width of 6.5cm. The specimen lacks locality information.

Dermochelys coriacea (Vandellius, 1761)

The description of this species is based on SMF 62797 of the Department of Herpetology at the Senckenberg Naturmuseum Frankfurt, Germany. The skull is 25 cm long and has a maximum

width of 21 cm. It was collected in 1966 near the Hebrides in the North Sea by the Institut für Meeresforschung in Bremerhaven and donated to the Senckenberg in 1967.

Chelydra serpentina (Linnaeus, 1758):

This species is based on UFR VP1, which is currently housed at the Department of Geosciences at the University in Fribourg in Switzerland. The specimen lacks locality data, but likely originates from the USA. The skull is 12 cm long and has a maximal width of 9 cm.

Digital Data Generation

X-ray computed tomography and reconstruction

The four selected specimens were scanned at three different CT scanning facilities, mostly due to logistic demands and size constraints. The raw data was afterwards converted into slices using in-house software associated with the CT scanners. The most important scanning and reconstruction parameters are provided in the Tables 1 and 2. The original CT scan images are available on Morphobank (see link in Appendix).

Segmentation and generation of 3D models

Virtual isolation of the skull bones was performed with the software Amira (version 6.0.0) (Fig. 1 and Supplementary Material, Appendix S2, Tables S2.1). Segmentation was implemented from all perspectives by hand, mostly with the brush tool and, occasionally, with the magic wand, drawing the limits by hand. Each bone was labeled using a different color and the same color was applied to homologous structures in different specimens. Depending on the complexity of bone morphology, every third or fifth slice was labeled, followed by interpolation of the

marked areas. The segmentation process was performed applying the masking option for the pixels belonging to the grey scale range of the bone. The 3D models used herein were generated in Amira as well. The 3D models of the skulls were left unaltered with exception of that of *Dermochelys coriacea*, which was smoothed using a factor of 2 to cache stepping caused by disproportionally large voxel size. The images provided in the text were generated using the screenshot function of Amira.

Bone contact analysis

The use of CT data allows studying the detailed nature at which bones contacts each other within a skull, which is a novel source of data that may prove valuable in the future in phylogenetic or biomechanical analyses. The following classification was developed to provide a standardized nomenclature and to help generate data. Two different morphological aspects are addressed in this classification. On the one side, contacts can be described in regards to the spatial relationships of the involved structures. Bones can contact each other in a suture that stands perpendicular to their surfaces (i.e., “parallel”), they can broadly overlap each other (i.e., “overlapping” or “underlying”), or one bone can clasp another (i.e., “clasping”). On the other side, the actual contact between two bones can vary in regards to the depth of the suture, ranging from blunt (i.e., “smooth”) to strongly interfingering (i.e., “faintly interfingering,” “moderately interfingering,” and “strongly interfingering”). These categories are figured in Figure 2 and examples provided in Figure 3.

The varying contacts that can be observed in each of the four scanned specimens were documented in the Description using the newly developed nomenclature (see below) and tabulated for analysis (Supplementary Material, Appendix S3, Tables S3.1-3.4). Whenever contacts vary between two bones the different kinds of contacts are listed from the anterior to

posterior, also in the tables. Some bone contacts are not clear in the scanned specimen of *Desmatochelys lowii* and the spatial relations of these bones are therefore determined, but not the type of suture. The contacts of the nasal were excluded from the table as this bone only occurs in *Desmatochelys lowii*.

To explore if bone contact data contains a signal, a similarity matrix was calculated that expresses the percentage of bony contacts that are similar between two given species. Any difference in spatial relationships of bones is hereby considered to constitute dissimilarity. However, to be considered dissimilar, the suture depth has to be different by at least two categories. Along those lines, a faintly interfingering clasping suture is considered to be similar to an intermediately interfingering clasping suture, but not with a strongly interfingering clasping suture.

Phylogenetic analysis

A phylogenetic analysis was performed herein to explore if the new insights gained into the anatomy of *Desmatochelys lowii* have an impact on its phylogenetic placement. For this purpose, the global character/taxon matrix of Cadena & Parham (2015) was utilized, which in return is a combination of previously published matrices of marine turtle relationships (Hirayama, 1994; Hirayama, 1998; Kear & Lee, 2006; Parham & Pyenson, 2010; Bardet et al., 2013; Lapparent de Broin et al., 2014b) and global turtle phylogenies (Joyce, 2007; Sterli, 2008; Joyce et al., 2011; Anquetin, 2012; Rabi et al., 2013; Sterli & de la Fuente, 2013; Zhou et al., 2014). The matrix was adjusted using the following modification. First, the codings were updated for 13 characters for *Desmatochelys lowii* (see Results for list of changes). Second, the matrix was expanded by seven characters, of which five have previously not been used in phylogenetic analyses. The

matrix was assembled in Mesquite 3.31. The final matrix consists of 154 taxa and 263 characters provided in nexus format in Appendix 4. The phylogenetic analysis was performed using TnT 1.1 (Goloboff et al., 2008). *Odontochelys semitestacea* was defined as the out-group. Characters 7, 17, 22, 44, 49, 52, 55, 57, 59, 66, 70, 71, 76, 79, 89, 101, 106, 118, 122, 128, 135, 138, 144, 148, 171, 174, 189, 191, 211, 223, 225, 229, 244, 256, 257, 258 and 262 form morphoclines and were therefore run ordered. Following Cadena & Parham (2015), 81 taxa were deactivated and a backbone constraint tree topology was used that constrains the topology of extant turtles based on the molecular analysis of Crawford et al. (2015) (see Appendix 5). The matrix was subjected to 1000 replicates of random addition sequences followed by a second round of tree bisection-reconnection. The full strict consensus tree and a list with all common synapomorphies are attached in Appendix 7 and 8.

209 DESCRIPTION

210

211 Abbreviations used in figures

212	bo	basioccipital	pal	palatine
213	bs	basisphenoid	pc	processus clinoideus
214	b. col	basis collumelae	pf	prefrontal
215	ccc	canalis caroticus cerebialis	pm	premaxilla
216	col	columella	po	postorbital
217	epi	epipterygoid	pr	prootic
218	exo	exoccipital	pt	pterygoid
219	f	foramen	qj	quadratojugal
220	fna	foramen nervi abducentis	qu	quadrate
221	fr	frontal	so	supraoccipital
222	ju	jugal	st	sella turcica
223	mx	maxilla	tb	tuberculum basioccipitale
224	na	nasal	vo	vomer
225	op	opisthotic		
226	pa	parietal		

227

228 Quality of CT Data

229 *Desmatochelys lowii*—Although the relatively large skull of *Desmatochelys lowii* was
230 scanned using a μ CT scanner and therefore has a relatively high resolution, many details are

obscured by crushing, fractures, and, more importantly, a lacking contrast between matrix and bones, especially towards the back of the skull (Fig 4 and Appendix S1, Figure S1.2).

Eretmochelys imbricata—The resolution and contrast of the CT scans of *Eretmochelys imbricata* (and *Chelydra serpentina*) were the best in this study, as they are based on recent material and were scanned using a μ CT scanner (see Material and Methods).

Dermochelys coriacea —The CT scans of *Dermochelys coriacea* were produced using a medical CT scanner and the voxel are therefore disproportionally large relative to the skull size, which obscures the details of some structures (see Appendix S1, Figure S1.6.).

Chelydra serpentina—The skull of *Chelydra serpentina*, is characterized by a strong ornamentation on the skull roof and most contacts are tight sutured (see Appendix S1, Figures S1.7 and 1.8), which lead to difficulties in determining the exact limits of the bones in some parts of the skull.

Skull Shape

Desmatochelys lowii—The skull of *Desmatochelys lowii* has a rather narrow rostrum, large, laterally facing orbits, a prominent lateral protuberance that spans from the jugal to the squamosal, and a median bulge formed by the parietals (Figs 5, 6). The cavum tympani is notably elongate, but the antrum postoticum is not developed. The palate is relatively narrow, but nevertheless shows well-developed lingual ridges.

Eretmochelys imbricata—The skull of *Eretmochelys imbricata* has a narrow rostrum, the orbits are large and facing laterally, and the width of the skull is rather constant (Figs 7, 8). The cavum tympani is rounded, but the antrum postoticum is not developed. A modest secondary palate is developed that includes low lingual ridges.

Dermochelys coriacea—The skull of *Dermochelys coriacea* is rather short relative to its width and has laterally facing orbits (Figs 9, 10). The middle ear lacks either a well-defined cavum tympani or an antrum postoticum. The anterior part of the labial ridge is marked by a notch and tooth on each side. The crista supraoccipitalis is short. A broad median depression on the skull roof is formed by the parietals.

Chelydra serpentina—The skull of *Chelydra serpentina* is characterized by a V-shaped outline and strong ornamentation of the skull roof (Figs 11, 12). The orbits face laterodorsally and the crista supraoccipitalis is long. This skull is further marked by a deep upper temporal emargination that exposes the prootic and opisthotic in dorsal view. The jaws are narrow and lack lingual ridges.

Dermal roofing elements (Figs 13–21)

Nasal (Fig. 13)

Desmatochelys lowii—In *Desmatochelys lowii*, the nasal bone is well preserved, except for its anterior margin, which is slightly broken. The nasals contact each other medially in a parallel, slightly interfingering, short suture. The posterior limit of the nasal contacts to two-thirds the frontal and to one third the prefrontal. The frontal slightly overlaps the nasal dorsally, whereas the nasal overlaps the anterior half of the prefrontal ventrally. The lateral suture of the nasal contacts entirely the maxilla in a slightly interfingering, parallel, posteriorly transverse suture that overlaps the maxilla. The suture between the nasal and maxilla is twice as long as the suture at the midline contact of the nasals. Towards the midline, the nasal bone thins out. An anteromedioventral, hook shaped process and a posteromedioventral, wedge-shaped process form the anteriormost part of the sulcus olfactorius that possibly once supported the septum

nasalis (Gaffney, 1979). The nasals participate in the formation of the roof of the fossa nasalis and their anterior edges constitute the upper part of the apertura narium externa.

In *Eretmochelys imbricata*, *Dermochelys coriacea*, and *Chelydra serpentina*, the nasal bone is not present.

Prefrontal (Figs 14, 17)

Desmatochelys lowii—The prefrontal of *Desmatochelys lowii* is heavily sculptured. In anterior view, the prominences and bosses of the bone form a shape that is reminiscent of a lower-case lambda. Posterior, medial, and ventral views are dominated by concavities, as the prefrontal participates in the formation the fossa orbitalis posteriorly, the fossa nasalis medially and ventrally, and the foramen orbito-nasale lateroventrally. The lateral side of the prefrontal is marked by a concavity, of which the vast majority serves as the sutural articulation surface with the maxilla. The posterior process descends towards the palatine and has a tricuspid lower margin. The dorsal exposure of the prefrontal is rather small and appears to be a flat, triangular bone, which is mainly surrounded by the frontal and partly surrounded by the nasal and maxilla. The frontal underlies the prefrontal posteriorly. Medially, the anterior extension of the frontal almost reaches the middle of the height of the prefrontal and overlaps this bone in a rather steep angle. The two prefrontals do not contact each other, as they are separated by the long anterior processes of the frontals in a moderately interfingering suture. The nasal overlaps the anterodorsal half of the prefrontal. Posteroventrally, the prefrontal meets the palatine in a presumably transverse contact at which the palatine seems to overlap the prefrontal. This, however, is not certain as the bones are slightly detached and somewhat displaced along this suture. The anteromedially descending process of the prefrontal contacts the ascending lamellar

process of the vomer. The contact changes from anterior to posterior. In the anterior part, the vomerine process overlaps the prefrontal with a relatively smooth contact surface, while along the rest of the contact the two bones are strongly interfingering. However, for most of the anterior half of the contact, the prefrontal overlaps the vomer. In the middle part, the contact between the two bones is parallel, while in the posterior part the vomer once again overlaps the prefrontal. The posterolateral part of the prefrontal participates in the border of the orbit.

Eretmochelys imbricata—Contrary to the prefrontals of *Desmatochelys lowii*, the prefrontals of *Eretmochelys imbricata* contact each other medially, as the anterior processes of the frontals fully underlie the prefrontals instead of separating them. The contact between the two prefrontals is parallel and moderately interfingering. Each prefrontal participates to a large extent in the margin of the orbit, in the formation of the apertura narium externa, and its rectangular dorsal part is entirely exposed along the skull roof. The prefrontal shows rather simple, angular structures. It does not contact with the palatine and the suture with the maxilla takes up less than a half of the prefrontal's lateral side. The contact between the prefrontal and the maxilla interfingers strongly and the prefrontal vertically underlies the maxilla's medial side. The prefrontal meets the vomer in a parallel and strongly interfingering contact. Similar to *Desmatochelys lowii*, the prefrontal of *Eretmochelys imbricata* contacts the frontal in a transvers manner posteriorly. Its medially descending process strongly interlocks with the ascending process of the vomer and laterally meets the maxilla. The contact between the prefrontal and the frontal is moderately interfingering and transverse and the frontal underlies the prefrontal. The prefrontal partly forms the fossa nasalis, the fossa orbitalis, and the foramen orbito-nasalis.

Dermochelys coriacea—The prefrontals of *Dermochelys coriacea* contact each other anteromedially because the frontals partly separate them. The contact between the two

prefrontals is parallel and slightly S-shaped and faintly interfingering. The prefrontal forms the dorsal edge of the apertura narium externa. The subtriangular dorsal surface is fully exposed. The frontal clasps the prefrontal along the anterior half of the contact. The prefrontal does not contact the palatine. The suture with the vomer is extremely short, rather smooth, and vertically transverse, and the prefrontal faintly overlaps the vomer. Only approximately one third of the prefrontal's lateral side takes part in the narrow suture with the maxilla, while the rest of it forms the anterodorsal margin of the orbit. Posterolaterally, the prefrontal overlaps the postorbital in a rather strongly interfingering suture. Similar to the prefrontal of *Desmatochelys lowii*, the prefrontal of *Dermochelys coriacea* connects posteromedially with the frontal by overlapping it. Lateroventrally, the prefrontal meets the maxilla in a faintly interfingering and vertically transverse suture. As in all other here analyzed specimens, the prefrontal takes part in the formation of the fossa nasalis, the fossa orbitalis, and the foramen orbito-nasalis.

Chelydra serpentina—As in the other modern species herein examined, the prefrontals of *Chelydra serpentina* contact each other medially in a parallel, moderately interfingering suture. The prefrontal forms the dorsal edge of the apertura narium externa, which is different from the condition in *Desmatochelys lowii*. The dorsal part is entirely exposed and elongate. Posterolaterally, the prefrontal overlaps the postorbital in a short, faintly interfingering suture. The ascending process of the vomer is clasped by the descending process of the prefrontal in a rather strongly interfingering suture. Laterally, the prefrontal meets the maxilla in a broad suture. In the anterior part of the latter suture, the two bones meet in a strongly interfingering, vertically transverse suture, by which the prefrontal overlaps the maxilla's medial side. In the posterior part of this suture, the bones meet in a parallel, moderately interfingering suture. Near the midline, the prefrontal clasps the frontal posteriorly in a moderately interfingering suture, while further to

the outside, the two bones meet each other in a parallel, moderately interfingering suture. Similar to *Desmatochelys lowii*, the prefrontal contacts the palatine. The contact between these two bones is transverse and the prefrontal overlaps the palatine in a moderately interfingering suture. The prefrontal is rather strongly sculptured and the ventral concavity is remarkably pronounced.

Frontal (Figs 14, 15, 17)

Desmatochelys lowii—In *Desmatochelys lowii*, the frontal is well preserved, except for a small posterodorsal part that appears taphonomically deformed. The dorsally exposed part of the bone, the dorsal plate, is flat and its geometry resembles the letter “P”. The dorsal plate of the frontal is approximately four times larger than the dorsal plate of the prefrontal. The lateral extension of the posterior half of the dorsal plate is approximately three times wider than the dorsal part of the anterior process. The ventral part of the anterior process is as long as the anteriormost edge of the dorsal plate. A particularly notable structure is the suture of the frontal with the prefrontal which forms a shallow, bay-like depression in the anterolateral part of the frontal. Ventromedially, a parasagittal ridge is visible. Along the transverse plane, this ridge forms a step between the roof of the sulcus olfactorius and the lower situated bottom of the suture with the prefrontal. The frontal bones contact each other medially in a parallel, moderately interfingering suture. Posteromedially, the frontal overlaps the parietal in a moderately interfingering suture. Posterolaterally, the frontal underlies the postorbital in a moderately interfingering suture. Anterolaterally, the frontals underliy the prefrontals and separate them from one another with the anterior process. Anteriorly, the frontal meets the nasal in a smooth, parallel suture, and further laterally in a transverse suture, along which the frontal overlaps the

nasal. The frontal contributes in the dorsal margin of the orbit, the sulcus olfactorius, the fossa orbitalis, and the fossa nasalis.

Eretmochelys imbricata—The dorsal plate of the frontal of *Eretmochelys imbricata* shows a very rounded, subtriangular shape, which is different from *Desmatochelys lowii*. The dorsal plate of the frontal is approximately the same size as the dorsal plate of the prefrontal. The posterior half of the dorsal plate of the frontal is slightly broader than the anterior half. The anterior process of the frontal is not exposed on the skull roof, shows a tongue-like shape, and does not separate the prefrontals. The ventral part of the anterior process is much longer than the anteriormost edge of the dorsal plate. Further, the medial flank of the process is steeper than the lateral its lateral flank, but unlike *Desmatochelys lowii* does not form a step on the ventral surface of the frontal. Similar to the frontal in *Desmatochelys lowii*, the frontals contact each other medially in a parallel, moderately interfingering suture. The frontal contacts the parietal medially in a transverse, moderately interfingering suture, while in the more lateral part of the contact, the frontal is clasped by the parietal, while the suture is strongly interfingering.

Posterolaterally, the frontal is overlapped by the postorbital in a moderately interfingering suture. However, the sutures between these three bones are somewhat steeper than in *Desmatochelys lowii*. Anteriorly, the frontal underlies the prefrontal in a moderately interfingering suture. The frontal participates in the orbit, the sulcus olfactorius, the fossa orbitalis, and the fossa nasalis.

Dermochelys coriacea—The dorsal plate of the frontal of *Dermochelys coriacea* is elongate and subtriangular. The dorsal plate of the frontal is approximately the same size as that of the prefrontal. The posterior half of the dorsal plate of the frontal is slightly broader than the anterior half. Anteriorly, the frontal clasps the prefrontal. Therefore, the frontal separates the prefrontals only partially. The frontal is clasped by the parietal posteriorly and by the postorbital

posterolaterally in faintly interfingering sutures. As the prefrontal contacts the postorbital, the frontal is excluded from the margin of the orbit. As in *Desmatochelys lowii*, the two frontal bones contact each other medially in a parallel and moderately interfingering suture. The ventral part of the anterior process is as long as the anteriormost edge of the dorsal plate.

Chelydra serpentina—The frontal bones contact each other medially in a parallel, faintly interfingering suture. The dorsal plate of the frontal resembles the letter “D”. The posterior half of the dorsal plate of the frontal is almost as broad as the anterior half. The dorsal plate of the frontal is half the size of that of the prefrontal. The frontal clasps the prefrontal in a moderately interfingering suture and they further laterally meet in a parallel, moderately interfingering suture. The ventral part of the anterior process is much longer than the anteriormost edge of the dorsal plate. The tips of the anterior processes of the frontals are strongly curved and together form a tunnel through which the olfactory (I) nerve passes. Posteriorly, the frontal meets the parietal. Near the midline, the frontal overlaps the parietal in a strongly interfingering suture, while in the further lateral part, the two bones meet in a parallel, moderately interfingering suture. Laterally, the frontal meets the postorbital in a parallel, moderately interfingering suture. As the prefrontal contacts the postorbital, the frontal is excluded from the margin of the orbit.

Parietal (Figs 16, 17, 27)

Desmatochelys lowii—The parietal bone of *Desmatochelys lowii* is slightly damaged. The anterior part of the dorsal plate is considerably domed. The top of this doming has an oval hole, from which a few fractures radiate outwards. It is unclear if this hole is a pineal foramen or represents damage (see Discussion below). The tip of the posterior process of the parietal seems to be broken, which stands to reason as the posterior part of the crista supraoccipitalis is

415 damaged as well. The posterior suture with the supraoccipital is somewhat indistinct but still
 416 vaguely perceptible. The processus inferior parietalis is perforated by some small holes, which
 417 appears to be damage to this thinly laminar part of this bone. The two anterior thirds of the dorsal
 418 plate of the parietal are as broad as the dorsal exposure of the postorbital. The posterior third of
 419 the dorsal plate is much narrower than its anterior part, as it contributes to the formation of the
 420 upper temporal emargination. The processus inferior parietalis forms a lateral bulge in the middle
 421 and thins out towards its posterior end. On the opposite site of the bulge, on the medial part of
 422 the processus inferior parietalis, is a tongue-shaped concavity with a transverse crest that form
 423 the lateral wall of the cavum cranii. The dorsal plate of the parietal contacts the other parietal
 424 medially in a parallel, moderately interfingering suture. Further, it meets the postorbital laterally
 425 in a faintly transverse contact by which especially in the most anterior and posterior parts of the
 426 suture the postorbital overlaps the parietal in a faintly interfingering suture. Anteriorly, the dorsal
 427 plate of the parietal underlies the frontal in a rather flat angle. The extensive anterior part of the
 428 processus inferior parietalis meets the epipterygoid at its anteroventral edge in a transverse
 429 vertical contact. The rest of the extensive anterior part of the processus inferior parietalis meets
 430 the crista pterygoidea of the pterygoid on the lateral part of the margin in a vertically transverse,
 431 strongly interfingering suture. The posterior edge of the extensive anterior part of the processus
 432 inferior parietalis forms the anterodorsal margin of the foramen nervi trigemini. The lateral bulge
 433 of the processus inferior parietalis meets the prootic in a vertically transverse suture at which the
 434 parietal slightly underlies the medial part of the prootic in a moderately interfingering suture. In
 435 the anterior half of the suture with the supraoccipital, the parietal overlaps the lateral processes of
 436 the supraoccipital, while in the posterior half the parietal overlaps the ridge of the crista
 437 supraoccipitalis. The parietal contributes to the formation of the cavum cranii medially, the fossa

temporalis laterally, the foramen nervi trigemini ventrally, and the foramen interorbitale anteriorly. The parietal is not connected to the squamosal.

Eretmochelys imbricata—The parietals of *Eretmochelys imbricata* both show damage to the processus inferior parietalis where this bone is thinnest. The parietals do not form any hole or pineal foramen at the midline, nor does the dorsal plate form any remarkable elevation. The three anterior quarters of the dorsal plate are broader than the dorsal exposure of the postorbital. The processus inferior parietalis is straight. Laterally, the dorsal plate of the parietal contacts the postorbital in a parallel and moderately interfingering suture. The parietal does not contact the prootic directly. Instead, the two bones are separated from each other by an approximately 1 mm wide gap. The parietal contacts the squamosal posterolaterally in a very short, parallel, but strongly interfingering suture. The two parietals meet each other medially in a parallel and moderately interfingering suture. Anteriorly, the dorsal plate of the parietal underlies the frontal in a strongly interfingering suture with a rather flat angle. Epipterygoids are not apparent on either side of the skull in the examine specimen, but it is unclear if they never developed or fused with the surrounding bones. The extensive anterior part of the processus inferior parietalis therefore meets the pterygoid in a vertically transverse contact, by which the parietal overlaps the pterygoid's crista laterally and forms the anterodorsal edge of the foramen nervi trigemini. The posterior half of the parietal contacts the supraoccipital ventrally. Along the anterior part of this suture, the two bones meet each other in a smooth contact, where the parietal overlaps a part of the supraoccipital's lateral side. In the rest of the suture, the parietal overlaps the supraoccipital, but the two bones meet in a rather strongly interfingering suture.

Dermochelys coriacea—The dorsal plate of the parietal is generally twice as broad as the dorsal exposure of the postorbital. The posterior margin of the parietal is not as strongly curved

as in the other analyzed taxa, but forms a rather straight border. The processus inferior parietalis is very short and straight. The medial part of the processus inferior parietalis forms a strong concavity in its posterior part and a less pronounced concavity in its anterior part. The processus inferior parietalis only contacts the supraoccipital in a vertically transverse suture and the foramen nervi trigemini is therefore not developed. The postorbital overlaps the parietal in a flat angle along most of their contact, with the exception of the most anterior part of the suture where both bones meet each other in a parallel suture. Anteriorly, the dorsal plate of the parietal underlies the frontal in a steep angle. Posterolaterally, the parietal meets the squamosal. In the anterior part of this suture, the parietal and the squamosal meet each other in a blunt contact, while they both underlie the postorbital. Halfway along the suture, the parietal clasps the squamosal. Towards the posterior end of the suture, the connection between these two bones develops into a transverse contact, along which the squamosal overlaps the parietal. The dorsal plate of the parietal contacts the other parietal medially. The parietal bone contributes medially to the formation of the cavum cranii, laterally the fossa temporalis, and anteriorly the foramen interorbitale. The parietal ventrally overlaps the supraoccipital in a somewhat transverse, smooth to faintly interfingering suture.

Chelydra serpentina—The average width of the dorsal plate of the parietal is somewhat broader than the dorsal exposure of the postorbital. The anterior part of the processus inferior parietalis shows a negligible extension. On the opposite side of the lateral bulge, on the medial part of the processus inferior parietalis, is a tongue-shaped concavity forming a part of the cavum cranii, without any crest. Laterally, the parietal overlaps the postorbital in a moderately interfingering suture with a rather steep angle. Anteriorly, the parietal underlies the frontal with a rod-like elongation. The ventral part of the processus inferior parietalis meets the epipterygoid in

a vertically transverse, smooth contact, along which the parietal somewhat overlaps the epipterygoid's medial side. The parietal does not contact the pterygoid. The lateral bulge of the processus inferior parietalis meets the prootic. The parietal bones meet each other medially in a parallel, moderately interfingering suture. The posterior part of the dorsal plate is much narrower, as it contributes to the formation of the upper temporal emargination. The posteroventral edge of the processus inferior parietalis forms the dorsal margin of the foramen nervi trigemini. The processus inferior parietalis forms a lateral bulge in the middle and thins out towards its posterior end. In the anterior part of the suture with the supraoccipital, the parietal partly overlaps the lateral processes of the supraoccipital, while in the posterior half, the parietal shortly overlaps the ridge of the crista supraoccipitalis. In either case, the suture is developed in a moderately interfingering manner. The parietal bone contributes medially to the formation of the cavum cranii, laterally the fossa temporalis, ventrally to the foramen nervi trigemini, and anteriorly the foramen interorbitale. The parietal does not contact the squamosal.

Postorbital (Figs 17, 18)

Desmatochelys lowii—The left postorbital of KU VP1200 is damaged, but the right one is mostly intact. The description therefore mostly refers to the right side, although the left is shown in the figures. The postorbital of *Desmatochelys lowii* is a slightly convex to sub angular bone. The posterior part of the bone faintly bends downwards and participates in the margin of the upper temporal emargination. An arch-shaped, faintly angular process is developed along the anterior margin of the bone, which forms the posterior border of the orbit. A notch is situated halfway up the orbit. On the medial side of the postorbital, a rounded ridge follows the course of the anterior process. The dorsal part of the postorbital meets the parietal medially, by which especially on the

posterior and anterior part of the suture, the postorbital overlaps the parietal in a faintly interfingering suture. Anteriorly, the postorbital overlaps the frontal in a moderately interfingering suture in a flat angle. The bended, posterior part of the dorsal part of the postorbital partly covers the posteromedial ascending part of the squamosal. The suture between the postorbital and the squamosal varies along the sagittal plane. In the anterior part of the suture between those two bones, the postorbital overlaps the squamosal in a rather smooth contact. In the middle of this contact, the postorbital is clasped by the squamosal. Further posteriorly, the postorbital underlies the squamosal in a smooth contact but is clasped by the squamosal again towards the posterior. The anterior quarter of the lateral part overlaps the quadratojugal in a slightly interfingering suture with a rather flat angle. The anterior process of the postorbital clasps the posterior part of the jugal. The postorbital does not contact the palatine nor the prefrontal. The postorbital participates in the formation of the fossa orbitalis and the fossa temporalis.

Eretmochelys imbricata—The posterior part of the dorsal part is straight and does not participate in the rim of the temporal roof, as the parietal connects with the squamosal. The anterior margin of the lateral part is angled towards the outside. This protrusion is located at the top level of the orbit. The descending ridge that demarcates the posterior margin of the orbit is more pronounced than *Desmatochelys lowii*. The suture between the postorbital and the parietal is mostly parallel and interfingering, with parts where the parietal slightly overlaps the postorbital. The posterior part of the postorbital meets the squamosal in a parallel and strongly interfingering suture. The minority of the lateral part contacts the squamosal, while the rest of the lateral part posteriorly meets the quadratojugal in a parallel and strongly interfingering suture. Anteroventrally, the postorbital vertically overlaps the laterodorsal side of the jugal in a

moderately interfingering suture. Medially, a ridge follows the course of the anterior process. Anteriorly, the dorsal part of the postorbital overlaps the frontal in moderately interfingering suture with a flat angle. The postorbital does not contact the prefrontal. The postorbital participates in the formation of the fossa orbitalis and the fossa temporalis.

Dermochelys coriacea—The postorbital of *Dermochelys coriacea* does not participate in the rim of the upper temporal emargination, as the parietal connects with the squamosal. The notch in the posterior margin of the orbit is somewhat pointy to angled and located at the top level of the orbit. The anteromedial part of the postorbital contacts the frontal in a short and butting suture. Anteriorly, the postorbital underlies the prefrontal in a steep angle. In dorsal view, the suture between the postorbital and the squamosal is zigzagged. The postorbital overlaps the squamosal in a faintly interfingering suture. Medioventrally, the postorbital meets the quadratojugal in an extremely short, vertically transverse contact, along which the postorbital overlaps the quadratojugal's dorsolateral rim. The jugal bone contacts the entire ventral margin of the postorbital's lateral part. The postorbital clasps the jugal, except for the middle part of the suture, where the postorbital slightly underlies the jugal. The contact between those two bones is faintly interfingering. The posterior part of the bone (approximately two thirds) is bent downwards. On the medial side of the postorbital, a rounded, weakly noticeable ridge somewhat follows the course of the anterior process. The dorsal part of the postorbital overlaps the parietal especially posteriorly in a flat angle. Posteriorly the postorbital overlaps a considerable part of the posteromedial ascending part of the squamosal. The postorbital participates in the formation of the fossa orbitalis and the fossa temporalis.

Chelydra serpentina—The medial ridge of the postorbital of *Chelydra serpentina* is more pronounced than that of *Desmatochelys lowii*, has a broad base, and follows the course of the

orbit. The postorbital meets the parietal medially in a blunt and strongly interfingering suture. Anteriorly, the postorbital underlies the prefrontal. The postorbital meets the squamosal and quadratojugal posteriorly in parallel, moderately interfingering sutures. The anterior part of the postorbital contacts the jugal. In the anterior part of the suture between the postorbital and the jugal, the two bones contact each other in a vertically transverse, faintly interfingering suture, while in the posterior part, the two bones meet each other in a parallel, moderately interfingering suture. The postorbital contributes to the upper temporal emargination. The posterior margin of the orbit is faintly angled slightly above the midpoint of the orbit. The postorbital participates in the formation of the fossa orbitalis and the fossa temporalis.

Jugal (Figs 18, 19, 23)

Desmatochelys lowii—The posterior limits of the jugal of *Desmatochelys lowii* are a bit speculative, because of a lack of contrast in the scans. The bone consists of the evenly high, slightly convex lateral wall and the rather short, horizontal medial process. Posteriorly, the jugal probably contacts the quadratojugal in a transverse contact where the jugal overlaps the anterolateral part of the quadratojugal. Posterodorsally, the jugal seems to clasp the lower part of the anterior process of the postorbital. Anteriorly, the jugal overlaps the maxilla in a presumably moderately interfingering suture. The jugal neither contacts the squamosal nor the palatine or pterygoid.

Eretmochelys imbricata—The posterior half of the lateral wall of the jugal is strongly elevated and contributes to the margins of the light embayed lower temporal emargination and of the fenestra subtemporalis. Posterodorsally, the lateral wall of the jugal meets the postorbital in a moderately interfingering suture, where the postorbital mostly overlaps the jugal laterally.

Posteriorly, the jugal slightly overlaps the anterolateral part of the quadratojugal in a strongly interfingering suture. The medially thinning medial process of the jugal is broad and clasps the palatine. The medial process overlaps the maxilla in a moderately interfingering suture. The jugal neither contacts the squamosal nor the pterygoid.

Dermochelys coriacea—The jugal of *Dermochelys coriacea* is rather large and does not possess a medial process. While the upper margin of the lateral wall has a sinusoidal shape, the lower margin is noticeably curved. The jugal laterally covers the anterior half of the quadratojugal's lateral wall. The suture between the jugal and the postorbital is transverse and overlaps the ventrolateral part of the postorbital. Posteriorly, the jugal overlaps the anterior process of the squamosal. Ventrally, the jugal overlaps the maxilla in a strongly interfingering suture. The jugal neither contact the palatine nor the pterygoid.

Chelydra serpentina—Posteriorly, the jugal meets the quadratojugal in a parallel, faintly interfingering suture. The entire dorsal margin of the jugal contacts the postorbital. The contact is mainly slightly interfingering, except for a short anterior part of the suture where the postorbital somewhat overlaps the medial side of the jugal. The medial process of the jugal overlaps the anterior part of the processus pterygoideus externus. The tip of the medial process of the jugal connects with the palatine in a very short, blunt suture. Posteriorly, the jugal is somewhat clasped by the processus pterygoideus externus in a strongly interfingering suture. The jugal neither contacts the squamosal nor the quadrate. Anteriorly, the jugal overlaps the maxilla in a moderately interfingering suture.

Quadratojugal (Figs 18, 20)

Desmatochelys lowii—The contact of the quadratojugal with the jugal is somewhat obscure in the available material. As far as can be discerned, the quadratojugal in this specimen is a parasagittal, flat bone, which is approximately as long as the jugal. The posteroventral margin of the quadratojugal is infolded, but it is unclear if this is natural or caused by damage. The posterior half of the bone is a bit higher than the anterior half, as the dorsal outline of the bone is faintly ascending posteriorly. The lower border of the bone is slightly convex. Posteriorly, the quadratojugal covers the anterolateral part of the squamosal and at the very end, the ventral infolding contacts the ventral part of the squamosal. The contact between the quadratojugal and the squamosal is approximately at the same level as the cavum tympani. Dorsally, the quadratojugal meets the postorbital in a transverse, slightly interfingering suture, by which the postorbital overlaps the lateral part of the dorsal border of the quadratojugal bone. Anterolaterally, the quadratojugal is overlapped by the jugal. The quadratojugal forms a part of the lateral wall of the fossa temporalis inferior. Posteroventrally, the quadratojugal meets the quadrate in a short, angulated contact with a smooth suture. The quadratojugal does not participate in the formation of the cavum tympani.

Eretmochelys imbricata—The quadratojugal of *Eretmochelys imbricata* is extended vertically. The bone forms a lateral concavity in its lower third. The concavity somewhat affects the shape of the posterior margin of the bone, which is C-shaped, with a small, tricuspid bump in the middle. On the medial side of the bone, the curvature forms a bulge. The margin of this bulge contacts the anterolateral rim of the quadrate. The two bones meet in a moderately interfingering suture. The posteroventral part of the lateral wall of the quadratojugal forms a flat and rather broad process that descends obliquely. This process covers the anterolateral part of the processus articularis of the quadrate. Along the dorsal margin, the quadratojugal's lateral side is vertically

overlapped by the squamosal in a moderately interfingering suture. The contact between the two latter bones is at the level of the upper margin of the cavum tympani. The lower border of the quadratojugal is strongly curved, as it constitutes the posterior half of the lower temporal emargination. At the ventral part of the anterior border of this bone, there is a pointy process. The upper third of the anterior border of the quadratojugal contacts the postorbital in a parallel and strongly interfingering suture. Two thirds of the anterior border of the quadratojugal are in a transverse contact with the jugal, by which the jugal overlaps the quadratojugal's lateral side in a strongly interfingering suture. Noticeable foramina, especially on the lateral but also at the medial side of the bone, indicate canal systems within the quadratojugal. The quadratojugal forms the lateral wall of the fossa temporalis inferior.

Dermochelys coriacea—The shape of the quadratojugal of *Dermochelys coriacea* resembles the letter T. It consists of a flat, elongated, lateral wall that thins out dorsally and a posteroventral processus, which is directed ventrally. Medially, the anteroventral part of the quadratojugal overlaps the quadrate in a moderately interfingering suture. The posteriormost part of the quadratojugal is bent inwards and connects the quadrate in a parallel, horizontal manner in a faintly interfingering suture. Through this contact, the quadratojugal participate in the formation of the cavum tympani. The lateral wall of the quadratojugal thins out posteriorly and forms a dorsolateral sutural surface. The lower border of the bone is concave to subangular, as it constitutes half of the lower temporal emargination. The posterior half of the lateral wall is clasped by the anterior process of the squamosal in a faintly interfingering suture. The contact between these two bones is above the level of the upper margin of the cavum tympani. The anterior half of the dorsolateral suture surface is covered by the jugal in a faintly interfingering

suture, while only the medial edge of the surface connects with the postorbital. The quadratojugal forms the lateral wall of the fossa temporalis inferior.

Chelydra serpentina—The quadratojugal of *Chelydra serpentina* consists of a subtriangular lateral. The posterior margin is C-shaped. The ventral border of the quadratojugal forms a minor, sigmoidal curve, as the anterior half of this margin forms the posterior half of the lower temporal emargination. The posterior third of the dorsal margin of the quadratojugal clasps the squamosal in a faintly interfingering suture. The contact between the two latter bones is situated above the cavum tympani. The middle part of the dorsal margin contacts the postorbital in a parallel, moderately interfingering contact. Anterodorsally, the quadratojugal meets the jugal in a faintly interfingering and mostly parallel, slightly transverse contact, by which the jugal partly overlaps the medial side of the dorsal margin of the quadratojugal. The posterior margin of the quadratojugal meets the quadrate along the anterior margin of the cavum tympani. The two bones contact in a moderately interfingering suture. The quadratojugal builds the lateral wall of the fossa temporalis inferior.

Squamosal (Figs 18, 21)

Desmatochelys lowii—The squamosal of the available specimen is a bit deformed, especially the posterodorsal part. The course of the sutures between the squamosal and the quadrate and postorbital are somewhat obscure, but nevertheless perceptible. The squamosal consists of two posterior processes and an elongated, convex lateral wall, which is C-shaped in cross section. The squamosal forms an ascending medial process that is covered by the postorbital. The lower process of the squamosal descends anteroventrally and underlies the posterodorsal part of the quadrate in a faintly interfingering suture in an angle of approximately 45 degrees. As a

consequence of this contact, the squamosal participates in the formation of the cavum tympani. However, at the very posterior end of the quadrate, the squamosal clasps the quadrate. The entire squamosal is slightly bent anteriorly and posteriorly towards the midline. In addition to the ascending medial process, the squamosal bone meets the postorbital also along the dorsal margin of its lateral wall. This suture varies from anterior to posterior. Anteriorly, the postorbital seems to overlap the squamosal, while in the middle of the suture the squamosal clasps the ventral margin of the postorbital. In the posterior part, the squamosal appears to overlap the postorbital. The lower edge of the posteriormost part of the squamosal contacts the opisthotic in a short and parallel suture. The anteriormost part of the squamosals is laterally covered by the quadratojugal. The squamosal does not contact the parietal.

Eretmochelys imbricata—The posteromedial part of the squamosal in the available specimen has two holes caused by damaged to this fragile bone. Differently from the squamosal of *Desmatochelys lowii*, the squamosal of *Eretmochelys imbricata* consists of a tilted, laterodorsal plate, whose posterior part is strongly curved downwards and bent inwards at the same time, which results in a sub hemispherical structure. Interiorly, this structure builds the roof of the antrum postoticum. Exteriorly, the squamosal forms two main and one minor parasagittal protuberances with remarkable indentations between them. In medial view, this sub hemispherical structure appears as a medial bulge. The ventral margin of the medial bulge for contact with the opisthotic is strongly serrated, but the two bones are slightly detached from each other. It is unclear if this separation is natural or post mortem. Anteriorly, the squamosal meets the postorbital in a strongly interfingering suture. The anterior margin of the medial bulge connects the quadrate in a narrow suture and the two bones together form the roof of the antrum postoticum. Posteroventrally, the squamosal is detached from the quadrate by approximately 2

689 mm, but both bones show matching surfaces in the area of the corresponding contact.

690 Anteroventrally, the squamosal vertically overlaps the lateral part of the quadratojugal's dorsal
691 margin. The uppermost, medial part of the squamosal is somewhat elongated and contacts the
692 parietal in a short, parallel, and strongly interfingering suture.

693 *Dermochelys coriacea*—The squamosal bone of *Dermochelys coriacea* consists of a vertically
694 extended lateral wall and a posteroventral descending process, which is oriented nearly
695 transverse with an outward twist. The anterior half of the lateral wall shows a lowered surface
696 which is the medial suture area for the following bones: the jugal ventrally, the intermediate
697 postorbital, and the parietal dorsally. From medial view, the root of the process forms a medial
698 bulge, which forms an anteriorly thinning, sigmoidal margin along the medial side of the lateral
699 wall. The squamosal contacts the quadrate with the edge of the medial bulge in a rather loose
700 contact. In the anterior part of this contact the squamosal overlaps the quadrate in a faintly
701 interfingering suture. In the middle part of this suture, the two bones meet in a parallel,
702 moderately interfingering contact. In the posterior part, the quadrate clasps the squamosal. The
703 squamosal in this specimen does not contact the opisthotic. The lowermost part of the
704 anteromedial half of the lateral wall overlaps the quadratojugal. The squamosal participates in
705 the formation of the antrum postoticum. The posteroventrally descending process and the vertical
706 extension of the lateral wall in this specimen are somewhat similar to the two posterior processes
707 of the squamosal of *Desmatochelys lowii*.

708 *Chelydra serpentina*—The suture between the squamosal and the quadrate is a bit obscure as
709 the connecting parts of the bones are very thin and tightly sutured. The squamosal is prominently
710 cone-shaped and forms the apex of the antrum postoticum. The cone is directed medioventrally
711 with its apex pointing towards the opposite direction. The interior lateral wall of the cone has a

middle crest that reaches the mid-height of the chamber at its highest point. Further, the squamosal consists of a subtriangular lateral wall with a flat dorsal margin and a downwards-pointing process. The vast majority of the dorsal margin forms the upper temporal emargination. Anterodorsally, the squamosal contacts the postorbital in an approximately parallel and strongly interfingering suture. The cone clasps the upper part of the quadrate in a remarkably tight, faintly interfingering suture. The anteroventral margin of the lateral wall of the squamosal meets the quadratojugal in a predominantly parallel suture, while only in a minor posterior part of the suture, the squamosal laterally overlaps the posterior extension of the quadratojugal. The lower edge of the posteriormost part of the squamosal contacts the opisthotic in a short and parallel, moderately interfingering suture. The squamosal participates in the formation of the antrum postoticum.

Palatal Elements (Figs 22–25)

Premaxilla (Figs 22, 23)

Desmatochelys lowii—The premaxilla of the available specimen is relatively well preserved. The anterior lower margin of the bone is lightly convex in lateral view. The suture between the premaxilla and the vomer is difficult to locate precisely, as the contrast in the scans is low. The same issue applies to the suture between the premaxilla and the maxilla. The premaxilla consists of a slightly backwards tilted, frontal plate, which dorsally contributes to the lower edge of the apertura narium externa, and a short, posterior, sub horizontal process, which forms the bottom of the fossa nasalis together with the vomer. In ventral view, the premaxilla forms the anterior margin of the labial ridge, and a small, distinct depression for receipt of the median hook of the lower jaw. The premaxilla contributes to the anterior margin of the lingual ridge, which is higher than the labial ridge and therefore visible in lateral view. Medially, the two premaxillae contact

each other in a parallel, moderately interfingering suture. On the interior part of the frontal plate, there is a foramen, which is connected through a canal to a ventromedial foramen. Laterally, the premaxilla meets the maxilla in a broad, parallel suture. Posteriorly, the premaxilla apparently contacts the vomer in a parallel suture.

Eretmochelys imbricata—The premaxilla has a prominent ventral bulge, which is pierced by many canals. The anteroventral curvature of the premaxilla contributes to the labial ridge and the triturating surface. The ventral bulge is at the same level as the labial ridge. The height of the premaxilla measures half of the length of the bone. A canal exits the premaxilla anteroventrally at the posterior base of the frontal plate of the premaxilla. The upper margin of the frontal plate of the premaxilla contributes in the formation of the apertura narium externa. The lower margin ascends towards the midline, while the upper margin descends. Medially, the premaxillary bones meet each other in a parallel, strongly interfingering suture. Posteroventrally, the premaxilla overlaps the vomer in a strongly interfingering suture. Laterally, the premaxilla overlaps the maxilla in a moderately interfingering, broad suture.

Dermochelys coriacea—The premaxilla is as high as its length. The upper margin of the premaxilla contributes to the formation of the apertura narium externa. This margin rises medially and the two premaxillae therefore jointly form a median apex in the middle of the aperture. The ventral margin, which participates in the labial ridge, descends laterally, following the course of the rather deep maxillary part of the labial ridge, where it forms a notch. The posterior process of the premaxilla is rather short, bend upwards and slightly lateral, which results in an oval vacuity between the two premaxillary processes. These processes contact each other shortly with their posterior ends, laying on the highest point of the sulcus vomeri. Further, the two premaxillae contact each other medially with their anterior halves, in a parallel,

somewhat interfingering suture. The entire lateral surface of the premaxilla connects the maxilla in a parallel, faintly interfingering suture. The premaxilla overlaps the vomer in a rather smooth suture with a low angle.

Chelydra serpentina—The height of the premaxilla in this specimen measures half of the length of the bone. The foramen praepalatinum is located in the posterior part of the posterior plate of the premaxilla. The lower margins of the premaxillae jointly form a two-cusped median hook. The premaxilla of *Chelydra serpentina* shows a flat, plate-like posterior process. This posterior plate is slightly oblique, tilted lateroventrally, and thins out medially, while its posteriormost part is rather thick and pierced by the vertical foramen praepalatinum. The two premaxillae contact each other in a parallel, mostly moderately interfingering suture. Laterally, the premaxilla meets the maxilla in a moderately interfingering suture. Posteriorly, the vomer slightly clasps the premaxilla in a moderately interfingering suture.

Eretmochelys imbricata—The foramen supramaxillare is situated at the medial side of the bottom of the ascending process. Dorsomedially, the maxilla covers the prefrontal's anterolateral process in a strongly interfingering suture. The maxilla of *Eretmochelys imbricata* possess a sharp labial ridge as well as a rather pronounced, crisp lingual ridge. Posteriorly, the maxilla underlies the jugal in a moderately interfingering suture. Anteromedially, the maxilla meets the vomer in a moderately interfingering suture. In the anterior part of this contact, the two bones meet each other in a parallel suture, while in the posterior part the maxilla overlaps the vomer. Posteromedially, the maxilla meets the palatine. In the anterior part of the suture, the maxilla overlaps the palatine in a moderately interfingering suture. In the middle part of this contact, the maxilla is clasped by the palatine in a moderately interfingering suture. Finally, in the posterior part, the two bones meet in a parallel and moderately interfingering suture.

Dermochelys coriacea—Anteromedially, the maxilla meets the premaxilla in a parallel, faintly interfingering suture. At the very anterior part of the contact between the premaxilla and the maxilla, the short processus palatinus underlies the premaxilla and nearly contacts the vomer. The maxilla does not possess a lingual ridge, but a remarkably deep processus alveolaris with a notch in the anterior part. Approximately three third of the medial side of the maxilla contacts the palatine with its short processus palatinus in a mostly parallel, moderately interfingering suture. The prefrontal meets the maxilla at the posteromedial part of the processus praefrontalis in an interfingering and rather narrow suture. Posterodorsally and slightly laterally, the maxilla contacts the jugal in a strongly interfingering suture. At the lateral border of the foramen orbito-nasale the maxilla forms a cone, which points backwards and slightly inwards.

Chelydra serpentina—The maxilla of *Chelydra serpentina* has a labial ridge, but no lingual ridge. The processus alveolaris is rather short and anteriorly bent inwards. The processus praefrontalis is remarkably short. The posterior part of the palatine process forms a medially extending hook-shaped process, which contacts the jugal, palatine, and pterygoid. This part of the maxilla is medially clasped by the palatine in a faintly interfingering suture. Dorsally and ventrally this maxillary process is clasped by the pterygoid in a moderately interfingering suture. Posterodorsally, the maxilla's palatine process underlies the jugal in a moderately interfingering suture. This process constitutes the lateral margin of the foramen palatinum posterius. A little further to the anterior the maxilla forms together with the palatine and the prefrontal the lateral border of the foramen orbito-nasale. The triturating surface is rather broad. Laterally, the maxilla forms an elevated margin for the orbit. Anteromedially, the maxilla contacts the premaxilla in a moderately interfingering suture. Posterior to this contact, the maxilla overlaps the vomer's posterolateral process in a faintly interfingering suture. Along the medial edge of the processus

praefrontalis, the maxilla meets the prefrontal in a mostly broad and interfingering suture. In the posterior part of the suture, between the latter two bones, the contact thins out.

Vomer (Figs 23, 24)

Desmatochelys lowii—The unpaired vomer of *Desmatochelys lowii* consist mainly of two big bent lamellae, which are fused along the midline, and an anterior sub horizontal plate. On the anterior, sub horizontal plane of the vomer, a rugose elongated bulge is situated along the midline. The right lamella is anteriorly pierced by a vertical hole. Ventrally, the vomer forms a crest along the midline along its posterior three quarters, while at the anterior quarter, a triangular structure can be observed. This structure is made of a transverse bulge, in front of which a circular depression is situated. From this triangular structure, two ventral lamellae split off laterally that contact the lingual ridge of the maxilla. The contacts between the vomer and the premaxilla, maxilla, and palatine are difficult to determine in the available specimen. The dorsal edge of each lamella meets the prefrontal in a transverse suture. In the anterior part of this suture, the vomer slightly overlaps the prefrontal in a rather parallel suture, whereas in the middle of the contact, the prefrontal overlaps the vomer in a steep and strongly interfingering suture. Finally, at the posterior part of the suture, the vomer again overlaps the prefrontal in a moderately interfingering suture. At the very posterior, lower end of the lamella, the vomer meets the palatine in a short and interfingering contact. However, this contact is a bit uncertain as the palatine seems to be detached. The vomer meets the maxilla anteriorly and the two bones constitute the anterior rim of the apertura narium interna. It is difficult to determine the type of the contact between these two bones in this specimen, but it seems that the vomer slightly

828 overlaps or even clasps the medial margin of the maxilla's anterodorsal part of the lingual ridge.

829 Anteriorly, the vomer meets the premaxilla in a presumably parallel suture.

830 *Eretmochelys imbricata*—The anterior process of the vomer overlaps the palatine in a

831 moderately interfingering suture with a steep angle. In the middle part of the vomer, the palatine

832 shortly connects the vomer posteriorly on the ascending lamella in a smooth suture.

833 Posterolaterally, the palatine overlaps the vomer's posterior process to an extent that leaves out a

834 dorsally exposed ridge of the vomer and does therefore not contact the other palatine. The

835 posteriormost part of the vomer overlaps the pterygoid in a moderately interfingering suture with

836 a rather flat angle. The anteriorly elongated cone like process of the vomer connects with the

837 premaxilla anterodorsally in a rather flat angle and laterally it contacts the maxilla. The suture

838 between the vomer and the maxilla is transverse whereby in the posterior part of the suture, the

839 maxilla overlaps the vomer in a steep angle, but underlies the medial process of the maxilla

840 anteriorly. The ascending lamella dorsally contacts the prefrontal in a parallel, strongly

841 interfingering suture.

842 *Dermochelys coriacea*—The posteriormost part of the vomer overlaps the pterygoid, but the

843 two bones only barely touch each other in the available dry specimen. The vomer contacts the

844 palatine only with the lateral edge of its posterior process in a parallel, slightly interfingering

845 suture, except for the posteriormost part of the contact, where the vomer slightly overlaps the

846 palatines in a smooth suture. The premaxilla meets the vomer in a short suture, by which the

847 hook-like posterior process of the premaxilla connects with its tip to the bottom of the sulcus

848 vomeri, situated between the two lamellae. The anterolateral process of the vomer nearly

849 contacts the maxilla. The posterior process of the vomer is not covered by any other bone. The

850 dorsal process of the vomer contacts the prefrontal in a short parallel suture along paired

processes. The dorsal parasagittal bulge along the vomer corresponds to the ventral parasagittal groove.

Chelydra serpentina—The middle part of the vomer is square-shaped in cross sections. The morphology of the anterior process of the vomer is T-shaped. The two dorsal processes are directed forwards. The sulcus vomeri ends anterior to the dorsal processes in a ridge on the anterior process of the vomer. Laterally, the vomer forms a subhorizontal groove, which constitutes the medial wall of the apertura narium interna. Ventrally, the vomer has a crest along its posterior half. The lateral surface of the vomer's anterior process contacts the maxillary portion of the processus palatinus. The type of the contact of the latter two bones is transverse, by which the maxilla slightly overlaps the vomer in a steep angle. The palatine contacts the vomer laterally along its two posterior thirds in a faintly transverse, almost parallel suture, by which the palatine somewhat overlaps the vomer in a faintly interfingering suture. The frontal surface of the vomer's anterior process contacts the premaxilla in a strongly interfingering suture. The prefrontal meets the vomer in a strongly interfingering suture on the dorsal processes of the vomer as well as behind the dorsal processes (approximately one third of the dorsal exposure of the vomer). The posterior process of the vomer is basically clasped by the pterygoids from both sides in a moderately interfingering suture.

Palatine (Figs 23, 24, 25)

Desmatochelys lowii—The palatine of *Desmatochelys lowii* is tilted anteriorly by approximately 45° and consists of a main plate and a lateral horizontal plate. The palatine of the studied specimen is thin and therefore shows some erosional damage, including a transverse fracture. It furthermore is somewhat detached from the other palatal bones. The main plate is

874 domed along the parasagittal plane. The lateral plate of the left palatine exhibits a vertical
875 foramen, which is lacking on the right, an asymmetry also observed in *Chelydra serpentina* (see
876 below). It is unclear to me if this is a single foramen palatinum posterius, a foramen palatinum
877 accessorium, or a foramen unrelated to the inframaxillary artery. The lateral plate forms a lateral
878 thickening with a vertical component, which clasps the processus palatinus of the maxilla and
879 constitutes the posterior end of the lingual ridge. Posterolaterally, a thickened part of the palatine
880 participates in the formation of the vertical flange of the processus pterygoideus externus. The
881 two palatine bones meet each other medially in a parallel, rather broad, moderately interfingering
882 suture. Posteriorly, the palatine contacts the pterygoid in an interfingering, mainly transverse
883 suture by which the pterygoid overlaps the palatine. Anteriorly, the palatine meets the vomer in a
884 presumably transverse suture, by which the palatine probably overlaps the vomer. The palatine in
885 this specimen does not contribute to the triturating surface.

886 *Eretmochelys imbricata*—The posterior margin of the palatine forms a two-pronged
887 elongation in the middle, similar to a fish tail, which results in a strongly serrated suture between
888 the palatine and the pterygoid. The palatine overlaps the pterygoid in a moderately interfingering
889 suture. The palatines are separated from each other by the posterior process of the vomer.
890 Together with the vomer, the palatine forms a sharp ridge anteriorly and laterally to the apertura
891 narium interna. The anteromedial corner of the palatine is somewhat narrowed, elongated, and
892 elevated. Its tip therefore contacts the base of the vomer's dorsal processes, just underneath the
893 suture of the vomer and the prefrontal. This contact between the palatine's anteromedial process
894 and the vomer results in a cavity that is less than 0.5 cm large. Ventrally, the lateral process of
895 the palatine forms a prominent lingual ridge. Anterolaterally, the palatine contacts the maxilla in
896 a mostly parallel and moderately interfingering suture, except for the anteriormost part, where

897 the maxilla overlaps the palatine. The posterior quarter of the lateral edge of the palatine is
898 slightly clasped by the jugal in a very narrow suture. The palatine does not contact the prefrontal.
899 A foramen palatinum posterius is absent in this specimen.

900 *Dermochelys coriacea*—The palatine of this specimen has an overall subtriangular shape. The
901 anteromedial margin is elevated. There is an indentation in the middle of the posterior part of the
902 bone. This posterior margin interlocks with the pterygoid. Near the midline, the palatine overlaps
903 the pterygoid in a smooth suture, while further to the outside the palatine underlies the pterygoid
904 in a smooth suture. The lateral edge of the palatine contacts the maxilla in a parallel, moderately
905 interfingering suture. The palatine therefore does not contact the jugal. Medially, the two palatine
906 bones are separated from each other by the posterior process of the vomer. The palatine does not
907 contact the prefrontal. The lateral half of the posterior margin of the palatine forms a part of the
908 fossa temporalis inferior's border.

909 *Chelydra serpentina*—The palatine in this specimen is broken along a transverse plane.
910 Anteromedially, the dorsal surface of the palatine is overlapped by the prefrontal. Together with
911 the maxilla, the three latter bones form the foramen orbito-nasale and contribute to the apertura
912 narium interna. The middle part of the lateral border participates in the formation of the foramen
913 palatinum posterius. Medially, the two palatine bones are separated from each other by the
914 posterior process of the vomer. The anterolateral and the posterolateral processes of the palatine
915 both contact the maxilla in a transverse suture. The anterolateral process of the palatine is
916 overlapped by the maxilla, while the posterolateral process of the palatine overlaps the maxilla to
917 an extent that the palatine meets the jugal. The palatine and jugal jointly cover the posteromedial
918 process of the maxilla. Posteriorly, the palatine is clasped by the pterygoid in a moderately
919 interfingering suture.

920

921 **Braincase Elements (Figs 26–43)**

922 Pterygoid (Figs 26, 27, 30)

923 *Desmatochelys lowii*—The pterygoid of the available specimen of *Desmatochelys lowii* is
924 partially crushed, especially on the ventral side. In addition, it is extraordinarily difficult to
925 determine the limits of the pterygoid bone. This is due to the fact that in the posteroventral part
926 of this specimen's skull, the contacts are obscured by matrix. The posterior halves of the
927 pterygoids are medially pierced by a vertical, 1 cm wide hole, which was produced using a
928 mechanical drill to better mount the specimen. The two pterygoids contact each other medially in
929 a parallel, interfingering suture. The processus pterygoideus is rather large, angular, and its
930 lateral end is rather broad and tilted backwards by 60°. The crista pterygoidea is rather high and
931 posteriorly contributes to the foramen nervi trigemini. Anterodorsally, the crista contacts the
932 epipterygoid in a narrow, interfingering, transverse suture, by which the epipterygoid covers the
933 crista's lateral side. Posterodorsally, the crista pterygoidea meets the processus inferior parietalis
934 in a broad, strongly interfingering, vertically transverse suture, by which the parietal covers the
935 crista's lateral side. The crista pterygoidea participates medially in the sulcus cavernosus. On the
936 lateral side of the crista pterygoidea, next to its anterior base, is a parasagittal groove with a
937 posteriorly-situated foramen. This might be a foramen of the nervi vidiani, but as the canal
938 leading to it cannot be traced, this cannot be ascertained with confidence. Another foramen can
939 be observed behind the posterior base of the crista pterygoidea. Anteriorly, the pterygoid
940 overlaps the palatine in an interfingering suture. The lateral side of the pterygoid's posterolateral
941 process meets the quadrate in a rounded, faintly interfingering suture, where the pterygoid
942 slightly clasps the quadrate's medial side of the processus articularis. Medially, the pterygoid
943 meets the basisphenoid. The rostrum basisphenoidale lies on the contact between the two

pterygoids. It is unclear how the rest of the basisphenoid is sutured to the pterygoid as the contact is strongly obscured by matrix. The posterolateral process of the pterygoid meets the prootic anterodorsally. I am not able to observe whether the pterygoid contacts the basioccipital or not. Unfortunately, even the likely contact between the pterygoid and the opisthotic cannot be determined with confidence.

Eretmochelys imbricata—The rather flat anterior part of the pterygoid forms two prominent spikes that connect with the palatine. The processus pterygoideus externus forms a small vertical flange. The bone is ruttled by many grooves and pierced by many canals. Dorsally, several small crests, together with the prominent crista pterygoidea, shape the sulcus cavernosus, through which the vena capitis lateralis passes. Medially, a rather wide groove forms the lateral wall of the canalis caroticus lateralis. Ventrally, the pterygoid's posterior half forms a trough, as its elongated edges ascend medially on the well-developed crest of the basisphenoid and laterally on the processus articularis of the quadrate. However, the pterygoid does not reach the margin of the condylus mandibularis. Laterally, beneath the crista pterygoidea, a short but distinct groove bears the processus pterygoideus of the quadrate and forms the fossa cartilaginis epipterygoidei. In the posteriormost part of the pterygoid, the foramen posterior canalis carotici interni is situated. The pterygoids meet each other medially in a parallel, moderately interfingering suture. Ventrally, their contact results in a very weak ridge. In approximately the middle of the ventral surface of the pterygoid, there are two foramina pharyngeale. Anteriorly, the pterygoid meets the palatine in a moderately interfingering suture, by which the palatine overlaps the pterygoid. The anteromedial spike of the pterygoid underlies the vomer medially. The crista pterygoidea connects the processus inferior parietalis in a vertically transverse, strongly interfingering suture, by which the parietal overlaps the lateral upper side of the crista pterygoidea. Posterolaterally,

the pterygoid meets the quadrate in a moderately interfingering and slightly transverse suture by which the quadrate overlaps the pterygoid in a rather steep angle. The anteromedial wall of the pterygoid dorsally contacts the prootic in a rather loose, very short, parallel suture. The posterior end of the pterygoid is overlapped by the exoccipital in a rather strongly interfingering suture. In approximately the middle of the bone, the pterygoid meets the basisphenoid medially. In the anterior part of this suture, the rostrum basisphenoidale lies on the pterygoid. For the major, central part of the suture, the pterygoid meets the basisphenoid medially in a moderately interfingering contact, by which the pterygoid is somewhat bent towards the middle of the basisphenoid. Further anteriorly, the contact is rather straight but tilted, so the pterygoid faintly underlies the basisphenoid. In the posterior part of the suture, the basisphenoid clasps the pterygoid in a moderately interfingering suture. Behind the basisphenoid, the pterygoid is clasped by the basioccipital in a moderately interfingering suture. However, in the posterior part of the suture, the pterygoid overlaps the basisphenoid in a moderately interfingering suture. The pterygoid in this specimen does not contribute to the foramen palatinum posterius.

Dermochelys coriacea—The anterior margin of the anterior plate of the pterygoid is somewhat angular with an indentation in the middle. Laterally, a weak triangular structure follows the course of the margin of the fenestra subtemporalis. The dorsally dominant structures are the sulcus cavernosus and the crista pterygoidea, which has a horizontal foramen on the left side of the skull. Underneath the crista pterygoidea, on the lateral side, the fossa cartilaginis epipterygoidei is situated, which is dorsally bordered by a ridge. This ridge forms the ventral edge of the large foramen cavernosum. Ventrally, the posterolateral process forms a narrow subtriangular groove. The posterolateral process of the pterygoid does not reach the margin of the mandibular condyles. The anterior thirds of the anterior plate of the two pterygoid bones

contact each other along the midline in a parallel and slightly interfingering suture. The length of this suture is shorter than the midline length of the basisphenoid. The posterior two thirds of the pterygoid frame the basisphenoid, parasphenoid, and the basioccipital in a parallel manner. Approximately in the middle of the bone, the pterygoid faintly interfingers with the basisphenoid and ventrally overlaps the laterally extended margins of the parasphenoid in a faintly interfingering suture. The basioccipital contacts the pterygoid at the medioposterior surface of its posterior process in a moderately interfingering suture, by which the basioccipital somewhat clasps the pterygoid. Ventrally, the contact of the two pterygoids forms a fine groove. The pterygoid does not contact the exoccipital or the parietal. Instead, the top of the crista pterygoidea of the left pterygoid is connected to the ventral process of the prootic, in a somewhat vertically transverse, faintly interfingering suture. However, the latter contact does not occur on the right pterygoid. Anteriorly, the pterygoid meets the palatine in a transverse parallel contact. In the medial half of this suture the palatine notably overlaps the pterygoid, whereas in the lateral half the pterygoid faintly overlaps the palatine. Anteromedially, the pterygoid has a small contact with the ventral part of the posterior process of the vomer. Laterally, the pterygoid meets the quadrate's medial surface in a slightly transverse, moderately interfingering suture, by which the quadrate overlaps the pterygoid in a steep angle. Additionally, the processus pterygoideus of the quadrate lies in the fossa cartilaginis epipterygoidei.

Chelydra serpentina—A striking feature is the generally flat ventral plate of the pterygoid of *Chelydra serpentina*. A slight bending of the ventral surface only occurs at the processus pterygoideus externus and the posterior process. This results in the formation of a weak groove that contacts the condylus mandibularis. The anterior margin of the pterygoid medially forms a process, from which it forms a more or less transverse line, following the shape of the fishhook-

1013 like processus pterygoideus externus. The crista pterygoidea is triangular, just like the
 1014 epipterygoid. From the anterolateral part of the crista pterygoidea springs a groove along the
 1015 processus pterygoideus. This groove is an imprint of a presumably cartilaginous extension of the
 1016 anterior process of the epipterygoid (see Discussion). The anterior process lies horizontally on
 1017 the pterygoid and is sutured with it in a moderately interfingering manner. In the rest of the
 1018 contact of these two bones, they meet in a smooth, vertically transverse suture, by which the
 1019 epipterygoid overlaps the lateral side of the pterygoid's crest. The sulcus cavernosus bears the
 1020 foramen nervi vidiani in its anterior part and posteriorly forms a downwards step, which
 1021 constitutes the floor of the fenestra postotica. The two pterygoids meet each other at the midline
 1022 in a parallel, strongly interfingering suture. Anteromedially, the pterygoid meets the vomer in a
 1023 relatively broad and interfingering suture by which the pterygoid clasps the lateral side of the
 1024 vomer's posterior process. In the anteriomedial part of same indentation, the pterygoid clasps the
 1025 palatine. Further laterally, the maxilla sneaks under the palatine into the indentation of the
 1026 pterygoid. At this very point, the contact with the jugal on the dorsal surface begins and
 1027 continuous until the end of the processus. Parallel to that, at the ventral side the maxilla connects
 1028 the pterygoid until the end of the latter process. The type of suture of the pterygoid with the
 1029 maxilla and the jugal is in both cases interfingering. The posterior halve of the pterygoid meets
 1030 the basisphenoid. In the anterior part of this suture, the basisphenoid's rostrum and its base lie on
 1031 the pterygoid in a smooth suture, while ventrally to it, the parasphenoid meets the pterygoid in a
 1032 smooth contact as well. Further posteriorly, the basisphenoid and the pterygoid meet in a parallel
 1033 and moderately interfingering suture, while together they clasp the internal carotid canal.
 1034 Posterodorsally, the pterygoid meets the prootic in a smooth to faintly interfingering suture. In
 1035 the anterior part of the contact, the prootic overlaps the medial rim of the sulcus cavernosus,

while further posteriorly the prootic connects both rims of the sulcus. In the posterior part, the prootic clasps the pterygoid's crest, which separates the canalis cavernosus from the internal carotid canal. The type of the latter suture is rather smooth. Posterolaterally, the pterygoid is overlapped by the quadrate in a steep, faintly interfingering suture. Posteromedially, the pterygoid is clasped by the basioccipital's ventrolaterally protruding parts in a faintly interfingering suture. In its posteriormost part, the pterygoid is overlapped by the exoccipital in a moderately interfingering suture. The pterygoid does not contact the opisthotic. The pterygoid in this specimen does not contribute to the foramen palatinum posterius.

Epipterygoid (Fig. 27)

Desmatochelys lowii—The epipterygoid of *Desmatochelys lowii* is well preserved. It is a parasagittal, flat bone and approximately D-shaped. The epipterygoid participates to a minor part in the anterolateral wall of the sulcus cavernosus. The anterior margin of the epipterygoid is somewhat thicker than the rest of the bone and forms a bulge at the middle. The entire anterior margin is exposed. Posterodorsally, it contacts the processus inferior parietalis in a vertically transverse contact, by which the parietal slightly overlaps the lateral side of the epipterygoid's posterodorsal margin. The posteroventral part of the epipterygoid meets the crista pterygoidea in a vertically transverse, moderately interfingering suture, by which the epipterygoid overlaps the lateral side of the pterygoid's crista. The epipterygoid in this specimen does not participate in the formation of the foramen nervi trigemini.

Eretmochelys imbricata—A distinct epipterygoid is not preserved in the available specimen of *Eretmochelys imbricata*. A slight thickening at the base of the descending process of the

parietal, however, likely represents the fused remnants of this bone. In general, *Eretmochelys imbricata* is known to possess an epipterygoid (Gaffney, 1979).

Dermochelys coriacea—The epipterygoid of *Dermochelys coriacea* is generally known to be absent (Nick, 1912).

Chelydra serpentina—The shape of the thin epipterygoid of *Chelydra serpentina* is subtriangular and, as in *Desmatochelys lowii*, directed parasagittally. The epipterygoid forms three processes that are somewhat curved. The vast majority of the anterior margin of the epipterygoid is in contact with the parietal and is exposed only for a short part at the base of its anterior process. The anterior process constitutes the anterolateral wall of the sulcus cavernosus and a part of it is bent anterolaterally and therefore lays on the dorsal surface of the processus pterygoideus externus. This anterolateral extension has an angular, flat ending. Anterior to this ending, a groove is formed by the pterygoid and jugal that may have held an embryonic precursor of the epipterygoid (see Discussion below). The part between the dorsal processus and the posterior processus of the epipterygoid shows a thickening, which forms a ridge. The posterior margin of the epipterygoid bone in this specimen participates in the formation of the foramen nervi trigemini. Dorsally, the epipterygoid meets the parietal in a slightly transverse suture, by which the processus inferior parietalis contacts the medial side of the epipterygoid. In the posterior part of the latter suture, where the epipterygoid's thickened part is, the two bones strongly interfinger with each other. The epipterygoid connects with the entire dorsal margin of the crista pterygoidea in a transverse suture, by which the pterygoid connects the medial side of the epipterygoid.

Basisphenoid (Figs 26, 28-30, 39-42)

Desmatochelys lowii—In *Desmatochelys lowii* only the anterior part can be discerned. The central and posterior parts were damaged when the skull was drilled for mounting while the ventral limits of this bone are uncertain, as the basicranium is partly crushed and its contacts obscured by the matrix. The rostrum basisphenoidale is 1.5 cm long and consists of a backwards-tilted dorsal plate and a ventrally attached, broad, rod-like structure. The rostrum ascends anteriorly by approximately 30° from the circular sella turcica, forms a sagittal groove, and ends on both sides of the lateral margin in a narrow rod. The left rod is much shorter and was presumably broken off or not fully ossified, whereas the right rod is almost 4 mm long. The two rods are connected by a transverse, rounded crest. From the middle of this crest, a short sagittal crest contacts the anterior end of the rostrum. The anterior end of the rostrum is drop-shaped and concave, with a prominent margin. Further, the surface of the rostrum is porous. The dorsum sellae of the basisphenoid is rather high and narrow. Anteroventrally, the basisphenoid contacts the pterygoids. The lateral side of the basisphenoid constitutes the medial wall of the sulcus cavernosus. Unfortunately, I cannot observe any carotid and nerve canals in this specimen as these internal structures are obscured by matrix.

Eretmochelys imbricata—The rostrum basisphenoidale is rod-like, rounded, and rather thick and has a two-cusped end. On the right side of the rostrum's dorsal surface is a bony peak. The dorsum sellae is rather high and pierced by two rather prominent foramina nervi abducentis. On both sides of the rostrum is a groove that bears the lateral carotid artery and connects the sella turcica through the short canalis caroticus interni. A canalis caroticus lateralis is not present in this specimen. The dorsal surface of the basisphenoid is concave with a crest in the middle. The rostrum basisphenoidale lies on the, along the midline elevated, suture of the two pterygoids. The rest of the basisphenoid meets the pterygoid on both lateral sides in a moderately interfingering,

1104 slightly transverse suture, by which the basisphenoid somewhat overlaps the pterygoid. Between
1105 these two bones the canalis caroticus internus is trapped. In the posterior part of the suture, the
1106 basisphenoid clasps the pterygoid. The ventral surface of the bone forms a prominent Y-shaped
1107 crest. The posteroventrolateral processes underlies the anterior part of the contact between the
1108 pterygoid and basioccipital. Posteriorly, the basisphenoid meets the basioccipital on two levels,
1109 each in a different type of suture. On the upper part, the basisphenoid meets the basioccipital in a
1110 blunt suture. In the lower part, the two bones meet in a strongly interfingering suture. The
1111 basisphenoid does not directly contact the prootic, but those two bones come each other very
1112 near in blunt surfaces, detached from each other by less than 0.5 mm.

1113 *Dermochelys coriacea*—The basisphenoid of the *Dermochelys coriacea* is marked by its
1114 asymmetric morphology in the anterior part. The dorsum sellae is rather low. The right foramen
1115 abducentis is not fully ossified, respectively open. The rostrum basisphenoidale does not seem to
1116 be fully ossified as the bony parts end in the middle of the sella turcica, where basically two
1117 oblique walls descend from the left to the right, forming the canals of the internal carotid artery.
1118 The left oblique wall of the sella turcica is anteriorly elongated by 1.5 cm. This extension is
1119 dorsally covered by the pterygoids, while ventrally it meets the parasphenoid. At the dorsal part
1120 of the basisphenoid, two pits are separated by a crest along the midline, next to which two short
1121 processes ascend vertically. On the lateral sides of the dorsal part, the parallel lateral rims are
1122 bent upwards. On their anterior halves, each of these rims contacts the prootic in a vertically
1123 transverse suture with a hollow center, which during lifetime presumably was filled with
1124 cartilage. Laterally and anteriorly, the basisphenoid contacts the pterygoid in an interfingering
1125 suture. Together the two bones form the canalis caroticus interni. The basisphenoid contacts the
1126 basioccipital posteriorly in a rather loose, parallel, and rough suture. Between the two bones, in

1127 the middle of the suture, a cavity is situated. Ventrally, the basisphenoid meets the parasphenoid
1128 in a concave, faintly interfingering suture.

1129 *Chelydra serpentina*—The basisphenoid of *Chelydra serpentina* is characterized by a rostrum
1130 basisphenoidale that is very flat, oval and remarkably long. In the middle of the rostrum is a
1131 short parasagittal crest, anteriorly to which two very thin canals pass the rostrum vertically. The
1132 two clinoid processes are very pointy and directed anteriorly. A cusp is formed medially to each
1133 clinoid process. The dorsum sellae is rather low. The foramen caroticum laterale is situated
1134 underneath the rostrum basisphenoidale and is smaller than the foramen anterius canalis carotici
1135 interni. The sella turcica is drop-shaped and rather wide. The widely spaced foramina anterius
1136 canalis carotici interni are situated at the posterolateral corners of the sella turcica. The ventral
1137 side of the basisphenoid is flat and shows two slightly concave structures in the posterior part.
1138 The dorsal part of the basisphenoid is rather deep, forming two concavities. Ventrally, the
1139 basisphenoid meets the parasphenoid. Ventrolaterally, it overlaps the pterygoid in a faintly
1140 interfingering suture. These two bones form the canalis caroticus internus. The cerebral carotid
1141 canal is situated within the basisphenoid. The rostrum basisphenoidale fully lies on the suture of
1142 the two pterygoids. Posteriorly, the basisphenoid meets the basioccipital in a mostly blunt, loose
1143 suture, with the exception of the lateroventral area. Laterodorsally, the basisphenoid meets the
1144 prootic in a blunt suture in the posterior two thirds, while in the anterior third the two bones meet
1145 each other in a moderately interfingering suture.

1146

1147 Parasphenoid (Figs 28-30, 41)

1148 *Desmatochelys lowii*—It is not possible to ascertain the presence of a formed or fused
1149 parasphenoid in the available specimen.

1150 *Eretmochelys imbricata*—In this specimen the parasphenoid is absent.

1151 *Dermochelys coriacea*—Among the analyzed specimen, the parasphenoid can only be clearly
1152 distinguished in the available specimens of *Dermochelys coriacea*. The parasphenoid in this
1153 specimen is subtriangular and floors the basisphenoid. The parasphenoid is larger than the
1154 basisphenoid and therefore covers it completely in ventral view. The anterior half of the bone is
1155 flat, whereas the posterior half forms is rounded M-shape in posterior view. Posteriorly, at the
1156 midline, the bone forms a concavity that forms a cone-shaped vacuity together with the overlying
1157 basisphenoid. This vacuity presumably forms a remnant of the notochord (Sheil, 2005). The
1158 lateral margins of the parasphenoid are overlapped by approximately 1 cm by the pterygoid, in a
1159 rather smooth suture. This suture thins out anteriorly, where the lower part of the short rostrum
1160 basisphenoidale lies on the tip of the parasphenoid. Posteriorly, the parasphenoid meets the
1161 basioccipital in a faintly interfingering transverse suture, by which the basioccipital overlaps the
1162 parasphenoid in a steep angle. This contact occurs only at the center part of the two bones, while
1163 the lateral processes of the parasphenoid and the tuberculum of the basioccipital are excluded
1164 from this contact. The posteroventral crest on the parasphenoid continues in the anteroventral
1165 part of the basioccipital.

1166 *Chelydra serpentina*—In *Chelydra serpentina* only the anterior part of what may constitute
1167 remnants of the parasphenoid can be distinguished. The anterior parts of these remnants form a
1168 flat, median slightly elevated, dense bony lamina, which at the front is not fused with the
1169 basisphenoid, but covered by the pterygoids. The contact between the putative parasphenoid and
1170 the pterygoid is smooth. Towards the posterior end of the parasphenoid it is difficult to track the
1171 dorsal outline of the bone, as it seems to be fused with the basisphenoid.

1172

1173

1174 Prootic (Figs 31, 32, 39-42)

1175 *Desmatochelys lowii*—The prootic of the available specimen of *Desmatochelys lowii* is rather
1176 well preserved. However, the limits of this bone are obscured by matrix. The dorsal exposure of
1177 the prootic is rather large. The prootic is situated remarkably elevated relative to the opisthotic.
1178 The foramen stapedio-temporale is situated above the level of the opisthotic. The prootic
1179 participates to about one third to the margin of the foramen stapedio-temporale. Medially, the
1180 prootic meets the parietal in a vertically-transverse and moderately interfingering suture. The
1181 contact between the prootic and the parietal is rather long. Laterally, the prootic meets the
1182 quadrate in a parallel and faintly interfingering suture. Together the two bones form the
1183 processus trochlearis oticum, of which the majority is formed by the quadrate. Posteriorly, the
1184 prootic overlaps the opisthotic. Ventrally, the prootic meets the pterygoid. Posterodorsally, the
1185 prootic meets the supraoccipital in a parallel to vertically transverse suture, by which the prootic
1186 overlaps the lateral side of the supraoccipital's lateral processes. However, no more details about
1187 the contact between the prootic and the opisthotic, pterygoid, and supraoccipital can be observed.
1188 Anteromedially, the prootic constitutes the posterior margin of the foramen nervi trigemini.

1189 *Eretmochelys imbricata*—The dorsal exposure of the prootic is rather large. The lateral
1190 surface of the prootic is convex. The prootic forms half of the processus trochlearis oticum. The
1191 participating part forms a slightly forward leaning bulge with a rugose surface. Laterally, the
1192 prootic meets the quadrate in a moderately interfingering suture. In the anterior part this suture is
1193 parallel while the posterior part quadrate clasps the prootic in a curved suture. With its round
1194 posterodorsal margin, the anterior part the prootic overlaps the supraoccipital anterolateral
1195 margin. In the upper half of the latter contact, the suture is somewhat loose, while the lower half

1196 is marked by a moderate denticulation. In the posterior part of this suture, the two bones are
1197 separated from each other by less than 1 mm, a gap that was likely filled by cartilage.
1198 Posteriorly, the prootic contacts the opisthotic in a few spots in parallel, moderately
1199 interfingering, sutures, but these two bones are otherwise once again separated from each other
1200 by a modest gap.

1201 *Dermochelys coriacea*—The dorsal exposure of the prootic in this specimen is rather large.
1202 With its dorsal margin the prootic connects the supraoccipital in a parallel, partly faintly
1203 interfingering, but mostly loose suture with a hollow center. Posteriorly, the prootic contacts the
1204 opisthotic in a parallel, moderately interfingering but rather loose suture. These two bones
1205 together form approximately 60% of the foramen stapedio-temporale. Laterally, the prootic
1206 meets the quadrate in a slightly interfingering, transverse suture, by which the prootic overlaps
1207 the quadrate's medial margin in an angle of around 45°. The processus trochlearis oticum is not
1208 clearly recognizable in this specimen. With its ventromedial process, the prootic meets the
1209 pterygoid laterally and the basisphenoid medially. The contact between the prootic and the crista
1210 pterygoidea of the pterygoid is interfingering. The prootic and the basisphenoid only contact
1211 each other along their surfaces. A direct contact is absence for the cancellous portions of these
1212 bones. There is no triple junction where the prootic, opisthotic, and supraoccipital meet. Instead,
1213 this area is marked by a gap that was likely filled by cartilage in life. The prootic does not
1214 contact the parietal.

1215 *Chelydra serpentina*—The dorsal exposure of the prootic in this specimen is rather large. The
1216 dorsolateral part of the prootic participates in the processus trochlearis oticum and forms a rather
1217 thin, rod-like process, which borders the anterior part of the foramen stapedio-temporale. From
1218 this foramen, a curved groove crosses the dorsal surface of the prootic towards the midline, with

1219 a bend to the anterodorsal part of the skull. This might be for the cervical artery. The prootic and
 1220 the quadrate meet each other in a parallel, moderately-interfingering suture. The medial wall of
 1221 the prootic has a small vacuity in the posterior part that is pierced by the foramen nervi facialis
 1222 and two foramina nervi acustici. The upper part of the medial wall of the prootic has an oval
 1223 recess that participates in the casing of the cranial cavity. Dorsomedioposteriorly, the prootic
 1224 meets the supraoccipital anteriorly in a transverse suture where the prootic overlaps the
 1225 supraoccipital in a moderately interfingering suture. In the posterior part of this suture, the two
 1226 bones meet in in a parallel, smooth contact. Dorsomedioanteriorly, the prootic meets the parietal.
 1227 In the anterior part of this suture, the prootic underlies the parietal in a faintly interfingering
 1228 suture. In the posterior part of this suture, the prootic is clasped by the parietal in a smooth
 1229 suture. Ventrally, the prootic meets the pterygoid at both borders of the sulcus cavernosus, as
 1230 well as at the lateral and medial borders of the canalis carotici interni. The two bones meet in a
 1231 faintly interfingering suture, by which the prootic overlaps and partly clasps the pterygoid.
 1232 Posterodorsally, the prootic contacts the opisthotic in a parallel, smooth suture, which is rather
 1233 angular along the transverse plane and resembles the letter T.

1234

1235 Opisthotic (Figs 31-33, 39-42)

1236 *Desmatochelys lowii*—The contact of the opisthotic with the pterygoid is obscured. The tip of
 1237 the processus paroccipitalis meets the squamosal in a parallel suture. Posteroventrally, the
 1238 opisthotic lies on the exoccipital in a sub horizontal, parallel suture. Posterodorsally, the
 1239 opisthotic meets the supraoccipital in a, as it seems, parallel suture. Anteriorly, the opisthotic
 1240 underlies the prootic. Laterally, the opisthotic meets the quadrate in an anteriorly parallel suture,
 1241 while in the middle of the contact the opisthotic underlies the quadrate. In the posterior part of

1242 this contact, the two bones again meet each other in a parallel suture. More details about this
1243 contact cannot be observed.

1244 *Eretmochelys imbricata*—The opisthotic in this specimen does not participate in the formation
1245 of the foramen stapedio-temporale. The processus interfenestralis is rather narrow and does not
1246 reach the floor of the cavum acustico-jugulare. The transition part between the processus
1247 interfenestralis and the recessus labyrinthicus opisthoticus is pierced by a rather large foramen
1248 nervi glossopharyngei. The openings of the semicircular canals are rather large, as can be
1249 observed in *Dermochelys coriacea*, while the contrary applies for *Chelydra serpentina*. The
1250 opisthotic meets the prootic anteriorly in an alternating mostly blunt to moderately interfingering
1251 suture. Anterolaterally, the opisthotic is overlapped by the quadrate. In the anterior part of this
1252 suture, the two bones meet in a loose and smooth suture, while in the posterior part, the contact
1253 becomes faintly interfingering and is much tighter and steeper. The opisthotic overlaps the lower
1254 part of the supraoccipital's lateral process in a flat angle and a mostly blunt suture, that is only
1255 serrated a little towards its center. Posteromedially, the opisthotic overlaps the exoccipital in an
1256 alternating smooth to moderately interfingering suture. Posterolaterally, the opisthotic's
1257 processus paroccipitalis meets the squamosal in a remarkably narrow and strongly interfingering
1258 suture. Dorsomedially, the opisthotic in this specimen meets the supraoccipital in a very loose,
1259 blunt suture, while the two bones do not contact each other directly. The opisthotic contributes
1260 posteriorly to the dorsolateral margin of the fenestra postotica, anterolaterally to the fenestra
1261 ovalis, anteromedially to the hiatus acusticus, and to the foramen jugulare anterius. The
1262 opisthotic in this specimen does not contact the pterygoid.

1263 *Dermochelys coriacea*—The opisthotic in this specimen has a remarkably round processus
1264 paroccipitalis. The processus interfenestralis is short and does not reach the floor of the cavum

1265 acustico-jugulare. The foramen internum nervi glossopharyngei is rather small. The openings of
1266 the semicircular canals and the canals themselves are rather large and not fully defined by bone.
1267 Anteriorly, the opisthotic meets the prootic in a parallel, moderately interfingering suture, which
1268 is nearly c-shaped to angular and center-hollowed. Laterally, the opisthotic is clasped by the
1269 quadrate in a slightly transverse suture and slightly interfingering suture. Together with the latter
1270 two bones, the opisthotic contributes to the formation of the foramen stapedio-temporale to
1271 approximately one third. Posteromedially, the opisthotic overlaps the exoccipital in a slightly
1272 interfingering suture and forms the dorsolateral margin of the fenestra postotica. Dorsomedially,
1273 the opisthotic meets the supraoccipital in a parallel, loose, and slightly interfingering suture. The
1274 opisthotic in this specimen neither meets the squamosal nor the pterygoid.

1275 *Chelydra serpentina*—The opisthotic of *Chelydra serpentina* is characterized by its angular
1276 morphology and its kinked processus paroccipitalis. The posterior half of the processus
1277 paroccipitalis is a flat wall, which ascends laterally and meets the squamosal and the posterior
1278 part of the quadrate. The opisthotic overlaps the squamosal in a transverse suture in the anterior
1279 part and faintly interfingers with squamosal in a parallel suture in the posterior part. The
1280 processus interfenestralis in this specimen is proportionally twice as broad as in the other
1281 analyzed specimens. Contrary to the other specimens, the processus interfenestralis of *Chelydra*
1282 *serpentina* does reach the floor of the cavum acustico-jugulare. The foramen jugulare-anterius is
1283 rather wide. The opisthotic contributes to a small part to the foramen jugulare posterius. The
1284 opisthotic meets the supraoccipital dorsomedially in a blunt suture. Anteromedially, the
1285 opisthotic contacts the prootic in a blunt suture. Anterolaterally, the opisthotic is overlapped by
1286 the quadrate in a moderately interfingering suture. Medially, the opisthotic overlaps the

1287 exoccipital in a moderately interfingering suture. The opisthotic of this specimen does not
1288 contribute to the formation of the foramen stapedio-temporale.

1289

1290

1291 Quadrate (Figs 20, 32, 34)

1292 *Desmatochelys lowii*—The contacts between the quadrate and its surrounding bones are
1293 obscured by matrix. The condylus mandibularis is remarkably broad. The medial half of the
1294 condylus is lower than the lateral half, as in *Dermochelys coriacea*. A processus epipterygoideus
1295 is not present in this specimen. The cavum tympani is remarkably shallow and oval. The incisura
1296 columellae auris is posteriorly open. The processus trochlearis oticum is mainly formed by the
1297 quadrate and is very prominent, yet narrow. A deep concavity is present between the processus
1298 trochlearis oticum and the lateral margin of the cavum tympani. The quadrate contributes to a
1299 small part to the foramen stapedio-temporale. The foramen stapedio-temporale is located on the
1300 dorsal side of the otic chamber and points posteriorly. Anteriorly, the quadrate meets the
1301 quadratojugal in a short suture. Dorsolateral, the quadrate meets the squamosal in a varying
1302 suture. In the anteriormost part of the suture, the two bones met each other on a narrow, parallel
1303 suture. In the middle part of the contact, the quadrate overlaps the squamosal's medioventral
1304 part. In the posterior part of this contact, the quadrate is dorsally and ventrally clasped by the
1305 squamosal. Anteromedially, the quadrate meets the prootic in a parallel suture. Posterolaterally,
1306 the quadrate meets the opisthotic. Anteroventrally, the quadrate meets the pterygoid in a
1307 somewhat parallel suture. The quadrate in this specimen does not contact the jugal.

1308 *Eretmochelys imbricata*—The dorsal surface of the quadrate and the posterolateral side of the
1309 processus articularis are remarkably rugose in this specimen. The quadrate constitutes 50% of the

1310 rugose and rather prominent processus trochlearis oticum. The incisura columellae auris is
1311 posteriorly open. The foramina and canal of the chorda tympani are absent in this specimen, as is
1312 typical for *Eretmochelys imbricata* in general (Gaffney, 1979). At about half way up of the
1313 anterior margin of the cavum tympani, a rod-like process of approximately 0.5 cm length ascends
1314 laterally in an angle of approximately 30°. This process contacts the quadratojugal's posterior
1315 rim, which is bent towards the inside of the cavum tympani. At the contact surface, the
1316 quadratojugal forms a ridge that articulates with the quadrate process. The suture is smooth.
1317 Among the herein analyzed specimens, I could observe this feature only in *Eretmochelys*
1318 *imbricata* on both sides of the skull. To my knowledge, this process has neither been described
1319 nor named so far and the functionality of this process is unknown to me. I therefore suggest a
1320 global examination of this feature among other turtles. The quadrate meets the prootic medially,
1321 above the canalis cavernosus. The anterior part of the suture between the two latter bones is
1322 strongly interfingering and transverse, by which the quadrate underlies the prootic in a steep
1323 angle. In the posterior part of this suture, the two bones are separated by the canalis stapedio-
1324 temporalis and shortly meet each other again at the posteriormost part, where they contact each
1325 other in a blunt suture. Posterior to this latter contact, the quadrate meets the opisthotic in a broad
1326 suture, which in the anterior part is parallel and smooth, while in the posterior part opisthotic
1327 underlies the quadrate in a strongly interfingering suture. Finally, at the very posterior end of the
1328 contact between the quadrate and the opisthotic, the two bones meet each other in a blunt
1329 transverse suture. The quadrate meets the squamosal dorsolaterally in a narrow and rather tightly
1330 interfingering suture, which continues onto the opisthotic, while the squamosal's medial wall lies
1331 on the quadrate. Dorsoposteriorly, the quadrate and squamosal are not in direct contact but form
1332 matching surfaces, which are detached from each other by approximately 1 mm. Medially,

1333 beneath the level of the incisura columellae auris, the quadrate meets the pterygoid in a strongly
 1334 interfingering and slightly transverse suture, by which the quadrate faintly overlaps the
 1335 pterygoid. Anteromedially, the processus epipterygoideus of the quadrate lies in the pterygoids
 1336 fossa cartilaginis epipterygoidei. The processus epipterygoideus is approximately four mm long,
 1337 a little porous on its surface, rod like, and has a concave ending with a prominent circular
 1338 margin. The quadrate is sparsely participating in the formation of the floor of the cavum
 1339 acustico-jugulare, as the major part of this floor is formed by the pterygoid. *Dermochelys*
 1340 *coriacea*—The quadrate of *Dermochelys coriacea* is tilted backwards by approximately 30°. As
 1341 in *Eretmochelys imbricata* the incisura columellae auris in this specimen is open posteriorly. A
 1342 processus trochlearis oticum cannot be clearly identified in this specimen. The condylus
 1343 mandibularis has two articular condyles and an additional protrusion at the anterior part of the
 1344 margin. The anterodorsal part of the cavum tympani is flattened. Anterodorsomedially, the
 1345 quadrate contacts the prootic in a strongly interfingering, slightly transverse suture, by which the
 1346 prootic overlaps the quadrate. The quadrate contributes to approximately one half of the margin
 1347 of the foramen stapedio-temporale. Posterodorsally, the quadrate meets the opisthotic in a
 1348 moderately interfingering, transverse suture where the quadrate overlaps the prootic. At the
 1349 lower part of the medial side of the quadrate, the pterygoid connects the quadrate beneath the
 1350 level of the incisura columellae auris in an interfingering, slightly transverse suture, where the
 1351 quadrate overlaps the pterygoid. The processus epipterygoideus is remarkably short and rod like
 1352 and its ending is oval and somewhat concave. Dorsolaterally, the quadrate meets the squamosal
 1353 in a patchy, slightly interfingering suture, which is narrow in the anterior part and broad in the
 1354 posterior part. The quadrate is sparsely participating in the formation of the floor of cavum
 1355 acustico-jugulare, as the major part of this floor is formed by the pterygoid.

1356 *Chelydra serpentina*—The quadrate of *Chelydra serpentina* contributes to the formation of the
1357 cavum tympani and antrum postoticum. The anterior margin of the antrum postoticum is defined
1358 by a loop formed by the quadrate, but the posterior aspects are open, instead being formed by the
1359 squamosal. The posteroventral wall of the antrum postoticum internally forms a small
1360 parasagittal bulge, which continues into a more prominent crest, formed by the squamosal. The
1361 incisura columellae auris is closed posteriorly. The contact of the quadrate with itself forms a
1362 crenulated ridge that runs parallel to the incisura columellae auris and holds the Eustachian tube
1363 below. The small foramen chorda tympani inferius is situated below this ridge. A similar ridge is
1364 formed at the interior side as well. Half way up on the anterior part of the processus articularis, a
1365 1mm large foramen is situated. From this foramen, a canal ascends medially and branches off
1366 into a lower canal and an upper canal. The lower canal connects with the canalis cavernosus,
1367 while the upper canal branches off into two thinner canals, which connect to the canalis stapedio-
1368 temporalis. The foramina to the three corresponding canals can be observed on the medial face of
1369 the quadrate, as marked on the illustration. I am not aware of what these canals contained during
1370 life. Gaffney (1979) described and illustrated the medial face of the *Chelydra serpentina*'s
1371 quadrate, but did not mention any structures like this. On the lateral side, along the anterior
1372 margin of the cavum tympani and on the upper anterior part of the processus articularis, the
1373 quadrate meets the quadratojugal in a strongly interfingering, parallel suture. Medially to the
1374 processus trochlearis oticum, on the anterior wall of the stapedia canal, is a foramen. The
1375 quadrate constitutes approximately 80% to the processus trochlearis oticum. On the dorsal
1376 surface of the quadrate, posterior to the processus trochlearis oticum, a rather deep recess is
1377 situated. The quadrate meets the prootic anteromedially in a moderately interfingering,
1378 transverse suture, where the prootic overlaps the quadrate. Posterior to this suture, the quadrate

meets the opisthotic in a moderately interfingering and transverse suture, where the quadrate overlaps the opisthotic. However, the type of this suture changes at the very posterior end, where the quadrate is clasped by the processus paroccipitalis of the opisthotic. The processus epipterygoideus is rather long and flat and lies orthogonal to the narrow contact surface with the pterygoid. The suture between the quadrate and the pterygoid is moderately interfingering and transverse. The quadrate is sparsely participating in the formation of the floor of cavum acustico-jugulare, as the major part of this floor is formed by the pterygoid.

Columella auris (Figs 35, 36)

The columella auris is not preserved for the available specimens of *Eretmochelys imbricata* and *Dermochelys coriacea*.

Desmatochelys lowii—In KUV 1200, a slightly flattened, partly crushed rod is situated in the incisura columellae auris that protrudes from the fenestra postotica. I conclude that this structure is likely the columella auris from which the basis columellae has broken off. The columella can otherwise only be shown to have an oval cross section.

Chelydra serpentina—The columella of *Chelydra serpentina* consists of a 2 cm long, slightly curved rod and a basis columellae with a diameter of around 4 mm. The basis columellae is a subtriangular hemisphere. In the frontal view, one can observe two pointed corners and a more rounded corner. Both of the pointy corners bear a tiny canal, which can be seen best in the CT scan. In side view, the margin between the two pointy corners is extended backwards and forms a collar-like structure.

Basioccipital (Figs 26, 37, 39-43)

Desmatochelys lowii—I was not able to determine the limits of the basioccipital in the available specimen of *Desmatochelys lowii* due to crushing and a lack of contrast between bone and matrix.

Eretmochelys imbricata—The basioccipital of *Eretmochelys imbricata* consists of a heart shaped dorsal surface, laterally descending processes that end as the tuberculi basalis and a posteriorly descending, subtriangular and rather wide process that forms the ventral third of the condylus occipitalis. The basioccipital in this specimen has a rather prominent crista dorsalis basioccipitalis with an oval, concave basis tuberculi basalis. The lateral margins of the dorsal surface are anteriorly elevated and wide and form the posteroventral margin of the fenestra ovalis. Further, the dorsal surface of the basioccipital is marked posterolaterally by many small concavities, which are part of the partly moderately interfingering and partly loose suture between the exoccipital and the basioccipital. Also, on the dorsal part of the posterolateral descending processes, the basioccipital meets the exoccipital in a strongly interfingering suture. On the posterior process of the basioccipital, the two bones meet in a parallel, smooth suture, while at the lateral edge of the basioccipital process, the two bones are strongly interfingering. Laterally, the basioccipital clasps the pterygoid in a moderately interfingering suture. Ventrally, the basioccipital meets the basisphenoid's ventral crest in a blunt suture. The basioccipital in this specimen does not possess a ventral tubercle.

Dermochelys coriacea—As in *Eretmochelys imbricata*, the ventrolaterally descending processes of *Dermochelys coriacea* are rather prominent and form a c-shaped concavity between each other. Further, on the ventral side of the basioccipital of this specimen, along the midline, is one ventral tubercle. On both sides of the crista dorsalis basioccipitalis is a deep trough each, which laterally end in a rather high wall that contacts the exoccipital. The posterior end of the

basioccipital's process that contributes to the condylus occipitalis, shows a rugose surface as it is not completely ossified. The basioccipital in this specimen is overlapped by the exoccipital posterolaterally in a moderately interfingering suture. The contact between these two latter bones is situated mostly on the dorsal surface of the posterior half of the ventrolateral processes. The dorsal surface of the anterior half of this process floors a part of the cavum acustico-jugulare. The anterior surface of the process contacts the pterygoid in a parallel and strongly interfingering suture. Anteriorly, the basioccipital contacts the basisphenoid in a rather loose, parallel, and moderately interfingering suture. In the middle part of the suture, these two bones do not contact each other, as there is a concave space between the basis tuberculi basalis and the posteromedial part of the basisphenoid. The lowermost part of the basioccipital shortly overlaps the parasphenoid's posterior part in a wavy, moderately interfingering suture.

Chelydra serpentina—The basioccipital of *Chelydra serpentina* differs from the other specimens through its rather flat ventral side. The crista dorsalis basioccipitalis is rather short and the tuberculum high, thereby resembling a knob. The limits of the posterior half of this basioccipital are difficult to determine as this bone is fused with the exoccipital. This condition is common in adult specimens, as those sutures fuse with age (Siebenrock, 1897). However, it can be said that the posterior process of the basioccipital is dorsally covered by the two exoccipitals. Anteriorly the basioccipital meets the basisphenoid in a mostly blunt suture. Exceptions can be observed in the area directly next to the basis tuberculi basalis, where these two bones interfinger moderately with each other in the uppermost part of the contact and in the most lateral part of the basioccipital, where the two bones interfinger moderately with each other in the lowermost part of the contact. Posteroventrally, the basioccipital meets the pterygoid in a transverse suture. In

the posterior part of this moderately interfingering contact, the basioccipital overlaps the pterygoid, while in the anterior part, the pterygoid overlaps the basioccipital.

Exoccipital (Figs 38-43)

Desmatochelys lowii—In *Desmatochelys lowii* I was not able to determine the limits of the exoccipital, as it is nearly impossible to recognize any definite due to crushing and a lack of contrast between bone and matrix. Only the posterolateral part of the exoccipital is rather well preserved and one can clearly observe two foramina nervi hypoglossi. The external limits of the exoccipital are faintly visible in this part of the skull. Dorsally, the exoccipital meets the supraoccipital. Although not certain, it seems that the two exoccipitals do not contact each other dorsally. The foramen jugulare posterius is confluent with the rest of the fenestra postotica. The upper lateral process of the exoccipital is rather long and underlies the opisthotic. This process forms the majority of the dorsal margin of the fenestra postotica.

Eretmochelys imbricata—The exoccipital in this specimen has three foramina nervi hypoglossi on the inside side of the skull that connect to two foramina nervi hypoglossi on the outside of the skull in both sides. The bone between this foramina forms cone-shaped structures. Anteriorly, the exoccipital has a short, forward pointing process, with a backwards oriented distal flange. This process does not reach the opisthotic, therefore the foramen jugulare anterius stays anteroventrally open. The exoccipitals in this specimen do not contact each other dorsally to the foramen magnum. Dorsally, the exoccipital meets the supraoccipital in a vertically transverse, strongly interfingering suture and in the posteriormost part of this suture, the exoccipital is dorsally clasped by the same bone. Ventrally, the exoccipital meets the basioccipital in a strongly interfingering suture, except for at the condylus occipitalis, where the two bones meet each other

1470 in a blunt suture and are only interfingering at the lateral edge of the basioccipital's posterior
1471 process. Laterally, the exoccipital is overlapped by the opisthotic in an alternating blunt to
1472 interfingering suture. Ventrolaterally, the exoccipital overlaps the posterior part of the roof of the
1473 canalis caroticus interni, which is formed by the pterygoid. The suture between those two bones
1474 is strongly interfingering. The exoccipital forms the medial margin of the fenestra postotica. The
1475 posterior process of the exoccipital participates in the formation of the condylus occipitalis. The
1476 foramen jugulare posterius is confluent with the rest of the fenestra postotica.

1477 *Dermochelys coriacea*—The condylus of the exoccipital is not fully ossified. The exoccipitals
1478 do not contact each other dorsally to the foramen magnum. The exoccipital is dorsally
1479 overlapped by the supraoccipital in a moderately interfingering suture. Laterally, the exoccipital
1480 contacts the opisthotic in a moderately interfingering, transverse suture, by which the opisthotic
1481 overlaps the exoccipital. Ventrally, the exoccipital overlaps the basioccipital in a moderately
1482 interfingering suture. On the medial side, two foramen nervi hypoglossi can be observed, from
1483 which the posterior foramen is remarkably wider than the anterior. The anterior process of the
1484 exoccipital does not contact the opisthotic and the foramen jugulare anterius is anteroventrally
1485 open. The exoccipital in this specimen does not contact the pterygoid, as the two bones are
1486 separated by the basioccipital. The foramen jugulare posterius is partly ossified in this specimen.

1487 *Chelydra serpentina*—The exoccipital in this specimen is characterized by its large
1488 anterolateral plate, which is sub horizontal, slightly tilted anteroventrally and floors the recessus
1489 scalae tympani. This process anteriorly connects to the pterygoid in a moderately interfingering
1490 and transverse suture, by which the exoccipital overlaps the pterygoid. The exoccipitals in this
1491 specimen do not contact each other dorsally to the foramen magnum. However, they are fused
1492 with each other ventromedially. The exoccipital is dorsally overlapped by the supraoccipital in a

strongly interfingering suture. The exoccipital is pierced by two foramen nervi hypoglossi which are equal in size. Laterally, the exoccipital meets the opisthotic in a strongly interfingering, transverse suture, where the opisthotic overlaps the exoccipital. The processus interfenestralis is situated at the suture between these two bones. Ventromedially, the exoccipital meets the basioccipital. However, the type of suture cannot be examined between those two bones, as they are fused. This condition is typical in adult specimens (Siebenrock, 1897). The exoccipital forms the majority of the foramen jugulare posterius, with a small contribution of the opisthotic. In contrast to the other species, the anterior process of the exoccipital of *Chelydra serpentina* does contact the opisthotic, which leads to the anteroventral closure of the foramen jugulare anterius.

Supraoccipital (Fig. 32)

Desmatochelys lowii—The supraoccipital of *Desmatochelys lowii* has a broken crest. What remains protrudes 1.5 cm relative to the foramen magnum. The limits of the supraoccipital are mostly obscured by matrix. Dorsally, the supraoccipital meets the parietal. Ventrolaterally the supraoccipital meets the opisthotic in a parallel contact and the prootic in a partly vertically transverse, but mostly parallel contact. The contact between the supraoccipital and the exoccipital is unclear.

Eretmochelys imbricata—The dorsal exposure of the supraoccipital is restricted to the posterior half of its crista. The crista supraoccipitalis is rather long, protruding 3 cm posterior to the foramen magnum. The protrusion of the crista relative to the foramen magnum is longer than the rest of the supraoccipital bone. At the point where the crista appears in the dorsal view, it forms a horizontal, rhomboidal expansion of 1,5 cm. From the crista, the supraoccipital bone widens continuously. Dorsolaterally, three quarters of the supraoccipital are covered by the

parietal in a rather strongly interfingering suture. Posteroventrally, the supraoccipital overlaps the exoccipital in a strongly interfingering suture. At the very posterior end of this suture, the supraoccipital clasps the dorsal crest of the exoccipital. Posterolaterally, the supraoccipital meets the opisthotic in a remarkably blunt and rounded suture. Anteroventrally, the supraoccipital contacts the prootic in a transverse suture where the prootic overlaps the supraoccipital's anterolateral margin. In the anterior part of this suture, the upper half of the contact is somewhat loose, while the lower half shows strong denticulations. The two flat lateral processes of the supraoccipital are ventrally wider, form the recessus labyrinthicus supraoccipitalis, as they participate in the formation of the anterior and posterior semicircular canals of the inner ear. Ventromedially, these processes each form the upper margin of the hiatus acusticus. In the middle of the upper margin is a notch, the foramen aqueducti vestibuli. The supraoccipital constitutes the uppermost part of the foramen magnum.

Dermochelys coriacea—The crista supraoccipitalis in this specimen is rather short and massive and the dorsal exposure of the crista reaches only 0.5 cm. The shape of the crista is somewhat asymmetric, but it does not form any horizontal crests. The protrusion of the crista relative to the foramen magnum is slightly shorter than the rest of the supraoccipital bone. The anteriormost upper part of the supraoccipital forms a slightly backwards tilted, arched end. Dorsally, the supraoccipital is overlapped by the parietal in a slightly transverse and moderately interfingering suture. Posteroventrally, the supraoccipital overlaps the exoccipital in an interfingering and rather tight suture. Anteroventrally, the supraoccipital's lateral processes each contact a prootic in a transverse and slightly interfingering suture, by which the prootic overlaps the supraoccipital's lateroventral margins. Much of the bones surrounding the inner ear and poorly ossified and the recessus labyrinthicus supraoccipitalis is therefore poorly defined. Due to

many cavities, the contact between the supraoccipital and the opisthotic is rather fragmentary but can be classified as moderately interfingering and transverse, as the supraoccipital overlaps the opisthotic. The supraoccipital forms the upper margin of the hiatus acusticus and a notch, the foramen aqueducti vestibuli, in the middle of this very margin.

Chelydra serpentina—The supraoccipital in this specimen is more prominent than in the other herein analyzed specimens due to its fully exposed crest. However, except for the crest, the supraoccipital bone itself is not exposed on the dorsal skull roof. The protrusion of the crista relative to the foramen magnum is longer than the rest of the supraoccipital bone. The bone in the center of the crista supraoccipitalis is remarkably thin, as well as the ventromedial walls of the lateral processes, which are even partly broken. Anterodorsally, the supraoccipital contacts the parietal in a strongly interfingering and transverse suture, where the parietal overlaps the supraoccipital. The anteriormost upper part of the supraoccipital forms a vertically cut, arched end. Posteroventrally, the supraoccipital overlaps the exoccipital in a strongly interfingering suture. Posterolateroventrally, the supraoccipital meets the opisthotic in a blunt suture. Anteroventrally, the supraoccipital contacts the prootic in a transverse suture, where the posterior half of the two bones contact each other in a blunt suture, which changes in the anterior half into an interfingering suture. As in the other specimens, the supraoccipital forms the upper margin of the hiatus acusticus and a notch, the foramen aqueducti vestibuli, in the middle of this margin.

Carotid circulation and vidian nerve

Desmatochelys lowii—Unfortunately, due to the bad condition of the basicranium in the available specimen, the course of the carotid canals cannot be examined. Although the sella turcica is rather well preserved, no foramina can be observed in its vicinity. Nevertheless, a foramen is present in the center of the dorsal side of the processus pterygoideus externus, which most probably represents an exit of the vidian canal.

Eretmochelys imbricata—The internal carotid artery enters the skull through the posterior foramen of the internal carotid canal, which is fully surrounded by the pterygoid. The posterior half of the canal is formed by the pterygoid, while the basisphenoid medially participates in the formation of the anterior half of the canal. At the level of the basioccipital-basisphenoid contact, the internal carotid canal shortly opens to the floor of the fenestra ovalis. Further anteriorly, the internal carotid canal gives off a canal, the ‘foramen’ pro ramo nervi vidiani, which connects to the sulcus cavernosus and at least transmits the vidian nerve (palatine branch of the facial nerve VII) (Albrecht, 1967). Finally, the large internal carotid canal opens into the anterior, lower situated part of the sulcus cavernosus, where it branches into the thick palatine artery and the thin cerebral artery, which enters the sella turcica medially through the canalis carotici cerebialis. A developed palatine carotid canal is not present in this specimen. Ventrally, each internal carotid canal is connected to two carotico-pharyngeal canals, which may have contained small branches of the vidian nerve.

Dermochelys coriacea—The vast majority of the internal carotid canal is not ossified in this specimen. The canal is briefly enclosed between the basisphenoid and the pterygoid on the right side of the basisphenoid only. However, on the anterior half of the basisphenoid, two deep, asymmetric grooves give indication for the further path of the internal carotid artery. The carotid

artery most probably enters the skull through the fenestra postotica. The course of the cerebral carotid artery and the vidian nerve cannot be observed in this specimen.

Chelydra serpentina—The internal carotid artery enters the skull through the fenestra postotica and only later enters a defined internal carotid canal. The posterior part of this canal is formed by the prootic and the pterygoid. Further anteriorly, where the canal comes closer to the midline, the basisphenoid participates in the formation of the canal as well. The canal gives off a branch that connects to the sulcus cavernosus, the ‘foramen’ pro ramo nervi vidiani. Shortly afterward, the canal of the vidian nerve splits off the internal carotid canal, crosses the pterygoid, and ends in the foramen nervi vidiani at the level of the anterior part of the basisphenoid’s rostrum. Anteriorly to the latter split, the internal carotid canal splits into the thin palatine canal, that crosses the pterygoid and exists in the sulcus cavernosus, and the cerebral canal, which crosses the basisphenoid and exists at the sella turcica.

1595

RESULTS

New Characters

I herein expand the character/taxon matrix of Cadena & Parham (2015) through the addition of the seven characters listed in Table 3. Character 62 pertains to the participation of the epipterygoid to the foramen nervi trigemini. This character had first been developed by Meylan (1987) to investigate trionychian relationships, but has not yet been applied to a global matrix. Character 88 addresses the participation of the opisthotic in the formation of the foramen stapedio-temporale. This character had first been utilized by Brinkman & Nicholls (1991) to reconstruct relationships among baenids, but also has not yet been applied to more global questions. As far as I am aware, characters 32, 33, 64, 87 and 92 are new and are therefore explained in greater detail. Character 32 addresses the presence of a hemispherical depression in the middle of the ventral side of the skull roof typically formed by varying contributions from the postorbital, frontal, and parietal (Fig. 17). This recess can be observed in *Desmatochelys lowii*, where it is situated in the middle of the anterior half of the postorbital's ventral side and in *Chelydra serpentina*, where the recess is more strongly pronounced than in *Desmatochelys lowii* and situated at the triple junction of the postorbital, frontal, and parietal. Such a recess is not present in the other two analyzed specimens. Character 33 describes the notch in the posterior rim of the orbit (Fig. 18). When present, this notch is either located at the top of the posterior margin of the orbit (as in *Eretmochelys imbricata* and *Dermochelys coriacea*) or in the middle of the posterior margin of the orbit (as in *Chelydra serpentina* and *Desmatochelys lowii*). Character 64 pertains to the length of the suture between the prootic and the parietal (Fig. 32). In the examined specimen, this contact is either long, constituting almost half of the dorsomedial

margin of the prootic, or remarkably short, less than 5% of the dorsomedial margin of the prootic, to absent. Character 87 addresses variation to the morphology of the dorsomedial process of the prootic in medial view (Figs 39-42). Two states are observed: the prootic either lacks a dorsomedial extension while having a similar height as the opisthotic or the prootic forms a dorsal medial process that ascends far beyond the level of the opisthotic. This character cannot be applied to the available specimen of *Desmatochelys lowii*, because the limits of the two corresponding bones are not clear. Finally, character 92 pertains to the presence of the processus epipterygoideus, which is absent in *Desmatochelys lowii*, but present in the other specimens. The newly included characters were only scored for the four taxa studied herein, because internal views are not yet available for the taxa included in the matrix of Cadena & Parham (2015).

Update of the coding of *Desmatochelys lowii* of Cadena & Parham (2015)

The scoring of the following list of characters was updated relative to that of Cadena & Parham (2015) based on new observations obtained as part of this study. As Cadena & Parham (2015) relied on previously available literature that only imperfectly documented KU VP1200, all noted differences can be viewed as improvements, not observations of polymorphism.

Character 7, dorsal exposure of prefrontal: previous coding: 0; new: 1

Comment: The interorbital space in the skull of *Desmatochelys lowii* is formed to an equal degree by the nasals, prefrontals, and frontals. The dorsal exposure of the prefrontal should therefore be viewed as “reduced” (character state 1), not “large” (character state 0) (see Fig. 6).

Character 8, development of prefrontal scutes: previous coding: 0; new: ?

Comment: No cranial scutes can be observed in the available specimen of *Desmatochelys lowii*. This therefore cannot be scored.

1642 Character 18, presence of pineal foramen: previous coding: 1; new: 0

1643 Comment: A pineal foramen is not present in the available specimen of *Desmatochelys lowii*.

1644 Instead, the relevant part of the skull is damaged, as can be seen by reference to historic literature
1645 (see Discussion) (see Figs 45, 46).

1646 Character 21, jugal-quadrato contact: previous coding: 1; new: 0

1647 Comment: The jugal of *Desmatochelys lowii* is rather short and separated from the quadrato
1648 by the quadratojugal (see Figs 5, 18).

1649 Character 57, presence and development of antrum postoticum:

1650 previous coding: 2; new: 1

1651 Comment: The antrum postoticum is present in *Desmatochelys lowii*, but it does not fully
1652 enclose the anterior perimeter of the antrum, as the lower and upper margin of the antrum formed
1653 by the quadrato do not touch each other to form a loop.

1654 Character 78, presence of median pterygoid ridge: previous coding: 1; new: 0

1655 Comment: A median pterygoid ridge cannot be observed in *Desmatochelys lowii*. The
1656 relevant area instead is flat.

1657 Character 84, development of basioccipital tubercles: previous coding: 1; new: ?

1658 Comment: As the basicranium is badly damaged in the relevant part of the skull of the
1659 available specimen of *Desmatochelys lowii*, the morphology of this aspect of the basioccipital
1660 cannot be discerned.

1661 Character 90, morphology of rostrum basisphenoidale: previous coding: 0; new: 1

1662 Comment: The rostrum basisphenoidale of *Desmatochelys lowii* is rod-like, and drop-shaped
1663 in cross-section. It is more than twice as high as wide at its maximum height.

1664 Character 96, high of dorsum sellae: previous coding: 0; new: 1

Comment: The dorsum sellae of *Desmatochelys lowii* is notably high, about four times higher than the vertical protrusion of the sella turcica relative to the floor of the sulcus cavernosus.

Character 102, location of foramen stapedio-temporale: previous coding: 0; new: -

Comment: The foramen stapedio-temporale of *Desmatochelys lowii* is located on the dorsal part of the otic chamber but is not oriented dorsally, but rather posteriorly. As neither character state is developed, it is scored as inapplicable.

Character 105, ventral covering of foramen nervi hypoglossi: previous coding: 0; new: 2

Comment: The foramen nervi hypoglossi are not visible on the ventral view, as they are fully covered by the basioccipital.

Character 107, formation of foramen posterius canalis carotici interni: previous coding: 1; new: ?

Comment: The foramen posterius canalis carotici interni, if present, is not visible in the available specimen of *Desmatochelys lowii*.

Character 109, size of the fenestra perilymphatica: previous coding: 0; new: ?

Comment: The fenestra perilymphatica cannot be identified in the available specimen of *Desmatochelys lowii*.

Phenetic study

The results of the phenetic study are provided in Table 4 in the form of a similarity matrix. The greatest similarity with 51% is observed between the extant marine turtles *Dermochelys coriacea* and *Eretmochelys imbricata*. The smallest among of similarity, by contrast, is observed between *Desmatochelys lowii* and *Chelydra serpentina*. In all cases, *Desmatochelys lowii* shows the least amount of similarity relative to the other three species.

1688

1689 **Phylogenetic analysis**

1690 The phylogenetic analysis resulted in 10 most parsimonious trees with 932 steps. A time
1691 calibrated extract of the strict consensus tree is provided in Figure 44. The full strict consensus
1692 tree including node numbers is provided in the Supplementary Material (Appendix S7, Figs
1693 S7.1-7.3). Protostegidae is universally recovered as monophyletic, but is placed as the immediate
1694 sister of crown Chelonioidea.

1695

DISCUSSION

Morphology

Processus epipterygoideus of *Desmatochelys lowii*

The processus epipterygoideus was defined by Gaffney (1972) to be an anterior extension of the quadrate that either ascends towards the epipterygoid or the descending process of the parietal and normally is situated ventral to the foramen nervi trigemini. This structure does not exist in *Desmatochelys lowii*. Instead, the contact between the quadrate and the pterygoid is rather straight and no process-like structure can be observed on the anterior part of the quadrate. A lack of the processus epipterygoideus has previously only been noted in pleurodires (Gaffney, 1979), but the structure is rarely addressed in the description of fossils. It is therefore unclear to me if the absence of this structure in *Desmatochelys lowii* is an autapomorphy or has phylogenetic significance.

‘Pineal foramen’ of *Desmatochelys lowii*

The skull roof of KU VP1200, the holotype of *Desmatochelys lowii*, is currently characterized by a median hole located between the parietals, just posterior to the frontals (Fig. 45). Elliott et al. (1997) and Cadena & Parham (2015) interpreted this hole to be a pineal foramen, but I here conclude it to be an artifact, as neither Williston (1894, Fig. 45c) nor Zangerl & Sloan (1960, Fig. 45b, Fig. 46) illustrate or mention the presence of a pineal foramen in this specimen. The description of Williston (1894) is relatively brief, but he explicitly mentions damage to the basicranium, while illustrating an intact dorsal skull roof. Zangerl & Sloan (1960) similarly draw attention to the broken crista supraoccipitalis and the crushed basicranium of the skull, but once

again do not highlight any damages to the skull's roof. As all of these authors certainly were aware of the significance that a pineal foramen would have in a fossil turtle, it seems all but certain that the hole was not yet present when they studied this skull. Detailed observation of the margins surrounding the hole reveal radiating fractures, which further suggests that this part of the skull was damaged post-burial, likely in the last decades. It is nevertheless clear that the parietals are unusually thin in the damaged part of the skull.

The hole in the skull of *Desmatochelys lowii* is located on top and slightly anterior to an elevation on top of the skull roof, just above the highest point of the braincase, as can be observed in the medial view of the 3D models. In *Dermochelys coriacea* a similar arrangement can be observed, but the parietal bone is only thinned instead of showing a hole. Davenport et al. (2014) conducted a study on the so called 'pink spot' on the head of *Dermochelys coriacea*, an unpigmented spot in living individuals located just above the thin bone roofing the top of the braincase. At the uppermost part of the brain, the pineal gland (epiphysis) is situated (Wyneken, 2001). Davenport et al. (2014) suggested that this translucent spot (Fig. 47) helps stimulate the pineal gland by allowing light to pass through the skull roof as a way to sense seasons. The skull of *Desmatochelys lowii* appears to be equivalent to that of *Dermochelys coriacea* and it seems reasonable to infer that it may have served a similar function. Only a sister group relationship, however, will be able to confirm if these structures are truly homologous (i.e., synapomorphic).

Basicranium of *Desmatochelys lowii*

Unfortunately, it is nearly impossible to discern characters from the basicranium of the available specimen of *Desmatochelys lowii* that may yield phylogenetically relevant information. The basicranium is badly crushed, partially missing, and the contrast between the bone and the

1743 matrix low. As a result, it is nearly impossible to observe any sutures, even in the scans. In
1744 addition to that, in the area of the posterior part of the basisphenoid and the anterior part of the
1745 basioccipital, a hole of 1 cm diameter was drilled for public installation. Neither Williston (1894)
1746 nor Zangerl & Sloan (1960) illustrate the posteroventral part of this specimen, but instead note its
1747 poor preservation.

1748 Everhart & Pearson (2009) recently reported a fossil marine turtle (FHSM VP17470), which
1749 they preliminarily identified as *Desmatochelys lowii* (Everhart & Pearson, 2009). The fossil
1750 consists of a fragmented shell, limb bones, paddles, and a skull from the Turonian Fairport Chalk
1751 of Mitchell County, Kansas, USA. The skull is crushed, but the basicranium seems to be intact.
1752 A detailed analysis of this specimen will first need to clarify if it is indeed referable to
1753 *Desmatochelys lowii* and I therefore here refrain from describe the morphology of its
1754 basicranium.

1755

1756 Parasphenoid

1757 The parasphenoid is a dermal bone that is located below the endochondral basisphenoid and
1758 that occurs in most vertebrates (e.g., de Beer, 1937; Pehrson, 1945; Jollie, 1957; Bellairs &
1759 Kamal, 1981; Klembara, 1993; Rieppel, 1993; Sheil, 2013). However, the two bones often fuse
1760 during ontogeny, making it difficult to distinguish them from one another in adult specimens
1761 (Sterli et al., 2010). Pehrson (1945) conducted an embryological study and summarized the
1762 available literature on the development and presence of the parasphenoid in reptiles concluded
1763 that cheloniids do not posses a parasphenoid, as the corresponding blastemas do not ossify
1764 during ontogeny of *Lepidochelys olivacea*. By contrast, all other turtles, including *Dermochelys*

1765 *coriacea*, at some point of their ontogeny shows signs of an ossified parasphenoid, a conclusion
1766 recently confirmed by observations from fossil turtles (Sterli et al., 2010; Rabi et al., 2013).

1767 As it is difficult to discern the parasphenoid in extant turtles externally, the use of CT scans
1768 provides novel access to this structure. The available adult specimen of *Chelydra serpentina*
1769 allows discerning the parasphenoid from the basisphenoid towards the anterior, but both bone
1770 become indistinguishable towards the posterior. On the other hand, the parasphenoid can be fully
1771 distinguished from the basisphenoid in the available adult specimen of *Dermochelys coriacea*.
1772 Although high quality scans are available for *Eretmochelys imbricata*, there is no trace of a
1773 distinct, dense bone that underlies the fully spongiose basisphenoid therefore confirming the
1774 absence of this structure in this species of marine turtle (Fig. 48). Finally, the parasphenoid could
1775 also not be observed in the available specimen of *Desmatochelys lowii*, but as internal structures
1776 cannot be resolved with any confidence in the basicranium of this specimen, this should not be
1777 taken as evidence of absence.

1778

1779 Sulcus pro-epipterygoidei in *Chelydra serpentina*

1780 In *Chelydra serpentina* a groove is present on the dorsal side of the external pterygoid process
1781 (Fig. 49). Gaffney (1972) illustrated and briefly noted (Gaffney, 1979) that there is an unnamed
1782 “anterior space” that holds the unossified anterior extension of the anterior process of the
1783 epipterygoid. This extension is ossified, among others, in various emydids (Gaffney & Meylan,
1784 1988; Joyce & Bell, 2004). To aid communication, I propose the term *sulcus pro-epipterygoidei*,
1785 which highlights the anatomical position of this groove in the anterior prolongation of the
1786 epipterygoid. As this structure has not yet been reported for many turtles, its phylogenetic
1787 relevance is unclear to me.

1788

1789 Phenetic analysis of bone contacts

1790 The use of CT scanning technology not only provides novel insights into the internal
1791 morphology of the skull (i.e., brain endocast, nerve and circulation canal systems), but also the
1792 nature of the bony contacts. I here document the detailed nature of all available bony contacts for
1793 four turtle taxa in the form of tables (Supplementary Material, Appendix S3, Tables S3.1-3.4).
1794 Although the information encoded in these tables may contain phylogenetic information, it is
1795 impractical to integrate it into an explicit phylogenetic matrix for the moment, as only four taxa
1796 would be scored for all newly developed characters.

1797 As an alternative I here present a phenetic study that quantifies the amount of similarity in
1798 regards to the contacts developed between two taxa. The results of this study (Table 4) show that
1799 *Eretmochelys imbricata* and *Dermochelys coriacea* show the greatest amount of bone contact
1800 similarity with 51%. *Chelydra serpentina* shares more similar bone contacts with *Eretmochelys*
1801 *imbricata* (45%) than with *Dermochelys coriacea* (38%). *Desmatochelys lowii* has more
1802 similarities in bone contacts with *Eretmochelys imbricata* (44%) than with *Dermochelys*
1803 *coriacea* (35%) and the fewest with *Chelydra serpentina* (33%). Among extant species, the
1804 strong similarity between *Eretmochelys imbricata* and *Dermochelys coriacea* and their lower
1805 degree of similarity with *Chelydra serpentina* correspond with the currently hypothesized
1806 phylogenetic relations of these species (Crawford et al., 2015). If similarity is used as a tentative
1807 phylogenetic tool, the high dissimilarity between *Desmatochelys lowii* and all extant taxa might
1808 be used to suggest that it is perhaps situated outside the clade formed by the extant taxa (i.e.,
1809 Americhelydia). This result is consistent with protostegids not being situated within or near
1810 Chelonioida. Nevertheless, it has to be mentioned that there is a certain bias in the data of
1811 *Desmatochelys lowii* due to the fact that some contacts are obscured by matrix and not

completely identifiable. It would be interesting to further test this method by exploring if additional recent turtle species are ‘correctly’ placed in currently accepted phylogenies as well, as this method might provide independent data for the assessment of phylogenetic relationships of fossil taxa. The more elaborate, but methodological more sound method would be to include this data into an explicit phylogenetic matrix. As presented, each bony contact exhibits four different spatial relationships in combination with four suture depths. Although characters could be developed that utilize 16 character states, it may be more prudent to utilize both aspects separately, as this would allow ordering character states.

Phylogeny

As part of this study, I expanded the phylogenetic analysis of Cadena & Parham (2015) by updating the scoring of *Desmatochelys lowii* based on the new observations obtained herein and by adding seven new characters. Two analyses were performed that differ in the including of the new characters. The tree that only utilizes the updated coding of *Desmatochelys lowii* does not show any major differences to the one in Cadena & Parham (2015) by recognizing a monophyletic Protostegidae within Dermochelyidae. The tree that including the new character as well, however, places Protostegidae basal to Chelonioidae in all of the ten most parsimonious trees. The resulting strict consensus tree (see Fig. 44 and Supplementary Material, Appendix S5, Fig. S5.1) has weak resolution within Protostegidae. Only *Archelon ischyros* and *Protostega gigas* are shown to be monophyletic, but not *Desmatochelys padillai* and *Desmatochelys lowii*. There is no reason to name a new genus for *padillai* for the moment, as the tree is too poorly resolved to contradict the sister group relationship previously hypothesized for the two currently accepted species of *Desmatochelys* (Cadena & Parham, 2015). The analyses highlight that the

1834 improved scoring of *Desmatochelys lowii* had no impact on the tree, in contrast to the newly
1835 developed characters.

1836 Placement of protostegids along the stem lineage of Chelonioidea is a novel result for a global
1837 phylogenetic analysis of turtle relationships. Joyce (2007) had shown ‘protostegids’ to be
1838 situated outside crown Cryptodira, but sampling was limited to *Santanachelys gaffneyi*. Using a
1839 large sample of marine turtles in a global context, Cadena & Parham (2015) on the other side
1840 recently retrieved Protostegidae within Dermochelyidae. This result mirrors previous analyses of
1841 marine turtle relationships (e.g., Hirayama, 1998; Kear & Lee, 2015), but is contradicted by
1842 molecular calibration analyses, that suggest a divergence data for crown Chelonioidea near the
1843 K-T boundary, not the Barremian, as suggested by the oldest known protostegids (Joyce et al.,
1844 2013). The herein proposed placement of protostegids partially resolves this conflict, as
1845 Barremian protostegids are still within the maximum proposed divergence date for
1846 Americhelyidia, the next more inclusive clade (Joyce et al., 2013).

1847

CONCLUSIONS

The type skull of *Desmatochelys lowii* from the Late Cretaceous (middle Cenomanian to early Turonian) Greenhorn Limestone of Jefferson County, Nebraska, is herein redescribed in detail using μ CT scans to provide new data that may help resolve the conundrum surrounding the phylogenetic placement of the Cretaceous marine turtle group Protostegidae and the origin of extant marine turtles. The detailed external and internal morphology of this specimen are compared bone by bone with the extant marine turtles *Dermochelys coriacea* and *Eretmochelys imbricata* and the snapping turtle *Chelydra serpentina*. Novel insights include the realization that the pineal gland may have approached the surface of the skull of *Desmatochelys lowii*, but that a true foramen is not developed, as in the extant *Dermochelys coriacea*. A parasphenoid, or at least remnants of the parasphenoid, are present in *Chelydra serpentina* and *Dermochelys coriacea*, but confirmed to be absent in *Eretmochelys imbricata*. The available skull of *Desmatochelys lowii* is too poorly preserved to allow discerning the presence of this bone. A sulcus is found in the anterior prolongation of the epipterygoid in *Chelydra serpentina*, which is herein named the sulcus pro-epipterygoidei. A phenetic analysis that utilizes newly obtained bone contact data suggests that *Desmatochelys lowii* is least similar of the four turtles included, which would be concordant with a phylogenetic placement outside Americhelydia. The recent global phylogeny of turtle relationships of Cadena and Parham (2015) was expanded through the inclusion of seven new characters and updated in regards to the coding of *Desmatochelys lowii*. The resulting phylogenetic analysis is in broad agreement with that of Cadena and Parham (2015), but inclusion of the new characters results in the placement of Protostegidae in the stem of Chelonioidae.

Additional insights into the basicranial anatomy of *Desmatochelys lowii* might be gained in the future by obtained μ CT scans of FHSM VP17470 and MNA V4516, two crushed skulls from the Late Cretaceous of Kansas and Arizona, respectively, which have preliminarily been referred to that taxon, but still lack detailed description (Elliott et al., 1997; Everhart & Pearson, 2009). As the phenetic study herein obtained results that are broadly congruent with some recent phylogenetic analyses, it may be of interest to expand the dataset obtained herein through the addition of more taxa.

INSTITUTIONAL ABBREVIATIONS

KU University of Kansas, Lawrence, Kansas, USA
FHSM Fort Hays State Museum, Fort Hays, Kansas, USA
MNA Museum of Northern Arizona, Flagstaff, Arizona, USA
NMB Naturhistorisches Museum Basel, Basel, Switzerland
UFR Université de Fribourg, Fribourg, Switzerland
SMF Senckenberg Naturmuseum, Frankfurt, Germany

ACKNOWLEDGEMENTS

I wish to thank my friends and family for endless support. I would like to thank Walter G. Joyce, my MS thesis supervisor, for proposing this topic, for supervision, and for helping me bring this manuscript to fruition. I am grateful to Virginie Volpato and Christoph Neururer (both University of Fribourg) for training me with the use of the software Amira and the micro CT scanner at the University of Fribourg, respectively. I wish to thank Chris Beard (KU) for loaning the holotype of *Desmatochelys lowii*, and David Burnham (KU) for transport and April Isch (University of Chicago) for the CT scanning of this important specimen. I similarly thank Gunther Köhler (SMF) for loan of the herein used specimen of *Dermochelys coriacea* and Krister Smith (SMF) for its transport and Nicole Schwendener (University of Bern) for its CT scanning. Additional specimens were provided by Loïc Costeur (NMB). Silvia Bonizzoni (Dolphin Biology and Conservation) generously provided permission to use a picture of a living individual of *Dermochelys coriacea*. This study was financially supported by funds from the Department of Geosciences of the University of Fribourg.

1904 REFERENCES

1905

1906 **Albrecht PW. 1967.** The cranial arteries and cranial arterial foramina of the turtle genera
1907 *Chrysemys*, *Sternotherus* and *Trionyx*: a comparative study of analysis with possible
1908 evolutionary implications. *Tulane Studies in Zoology* **14**:81–99.

1909 **Albrecht PW. 1976.** The cranial arteries of turtles and their evolutionary significance. *Journal of*
1910 *Morphology* **149**:159–182.

1911 **Anquetin J. 2012.** Reassessment of the phylogenetic interrelationships of basal turtles
1912 (Testudinata). *Journal of Systematic Palaeontology* **10**:3–45.

1913 **Anquetin J, Püntener C, Joyce WG. 2017.** A review of the fossil record of turtles of the clade
1914 Thalassocheyleia. *Bulletin of the Peabody Museum of Natural History* **58**:317–369.

1915 **Baur G. 1888a.** Osteologische Notizen über Reptilien (Fortsetzung III). *Zoologischer Anzeiger*
1916 **11**:417–424.

1917 **Baur G. 1888b.** Osteologische Notizen über Reptilien (Fortsetzung V). *Zoologischer Anzeiger*
1918 **11**:736–737.

1919 **Baur G. 1891.** The very peculiar tortoise, *Carettochelys* Ramsay, from New Guinea. *Science*
1920 **17**:190.

1921 **Baur G. 1893.** Notes on the classification of the Cryptodira. *American Naturalist* **27**:672–675.

1922 **Bonaparte CL. 1832.** Saggio d'una distribuzione metodica degli animali vertebrati a sangue
1923 freddo. Roma: Antonio Boulzaler.

1924 **Bardet N, Jalil N-E, de Lapparent de Broin F, Germain D, Lambert O. 2013.** A giant
1925 chelonoid turtle from the Late Cretaceous of Morocco with a suction feeding apparatus
1926 unique among tetrapods. *PLoS ONE* **8**:e63586.

- 1927 **Bellairs ADA, Kamal AM. 1981.** The chondrocranium and the development of the skull in
1928 recent reptiles. *Biology of the Reptilia*, **11**:1–264.
- 1929 **Brinkman DB, Nicholls EL. 1991.** Anatomy and relationships of the turtle *Boremys pulchra*
1930 (Testudines: Baenidae). *Journal of Vertebrate Paleontology* **11**:302–315
- 1931 **Cadena EA. 2015.** The first South American sandownid turtle from the Lower Cretaceous of
1932 Colombia. *PeerJ* **3**:e1431 DOI 10.7717/peerj.1431
- 1933 **Cadena EA, Parham JF. 2015.** Oldest known marine turtle? A new protostegid from the Lower
1934 Cretaceous of Colombia. *PaleoBios* **32**:1–42.
- 1935 **Cope ED. 1872.** A description of the genus *Protostega*, a form of extinct Testudinata.
1936 *Proceedings of the American Philosophical Society* **12**:422–433.
- 1937 **Cope ED. 1873.** [Description of *Toxochelys latiremis*]. *Proceedings of the Academy of Natural*
1938 *Sciences of Philadelphia* **1873**:10.
- 1939 **Crawford NG, Parham JF, Sellas AB, Faircloth BC, Glenn TC, Papenfuss TJ, Henderson**
1940 **JB, Hansen MH, Simison WB. 2014.** A phylogenomic analysis of turtles. *Molecular*
1941 *Phylogenetics and Evolution* **83**:250–257.
- 1942 **Davenport J, Jones TT, Work TM, Balazs GH. 2014.** Pink spot, white spot: the pineal
1943 skylight of the leatherback turtle (*Dermochelys coriacea* Vandelli 1761) skull and its possible
1944 role in the phenology of feeding migrations. *Journal of Experimental Marine Biology and*
1945 *Ecology* **461**:1–6 DOI 10.1016/j.jembe.2014.07.008
- 1946 **Dollo ML. 1886.** Premiere note sur les Cheloniens du Bruxellien (Éocène moyen) de la
1947 Belgique. *Bulletin Musée Royale d'Histoire Naturelle de Belgique* **4**:75–91.

- 1948 **Everhart MJ, Pearson G. 2009.** First report on a marine turtle from the Fairport Chalk member
1949 of the Carlile Shale of Mitchell County, Kansas. *Transactions of the Kansas Academy of Science*
1950 **112**:138–139.
- 1951 **Elliot DK, Irby GV, Hutchison JH. 1997.** *Desmatochelys lowi*, a marine turtle from the Upper
1952 Cretaceous. In: Callaway JM, Nicholls EL, eds. *Ancient Marine Reptiles*. Academic Press,
1953 243–258.
- 1954 **Gaffney ES. 1972.** An illustrated glossary of turtle skull nomenclature. *American Museum*
1955 *Novitates*, 2486:1–33.
- 1956 **Gaffney E S, Tong H, Meylan PA. 2006.** Evolution of the side-necked turtles: the Families
1957 Bothremydidae, Euraxemydidae, and Araripemydidae. *Bulletin of the American Museum of*
1958 *Natural History* **300**:1–698.
- 1959 **Gaffney ES, Meylan PA, Wood RC, Simons E, De Almeida Campos D. 2011.** Evolution of
1960 the side-necked turtles: the family Podocnemididae. *American Museum Novitates* **350**:1–237.
- 1961 **Gaffney ES, Meylan PA. 1988.** A phylogeny of turtles. In: Benton MJ, ed. *The phylogeny and*
1962 *classification of the tetrapods, Volume 1: amphibians, reptiles, birds*. Systematic Association
1963 Special Volume 35A. Oxford: Clarendon Press. 157–219.
- 1964 **Goloboff PA, Farris JS, Nixon K. 2008.** TNT: a free program for phylogenetic analysis.
1965 *Cladistics* **24**:774–786.
- 1966 **Hattin DE. 1975.** Stratigraphy and depositional environments o Greenhorn. Limestone (Upper
1967 Cretaceous) of Kansas. *Bulletin of the Kansas Geological Survey* 209:1–128.
- 1968 **Hirayama R. 1994.** Phylogenetic systematics of chelonoid sea turtles. *Island Arc* **3**:270–284.
- 1969 **Hirayama R. 1998.** Oldest known sea turtle. *Nature* **392**:705–708.

- 1970 **Joyce WG, Parham JF. 2004.** Developing a protocol for the conversion of rank-based taxa
1971 named to phylogenetically defined clade names, as exemplified by turtles. *Journal of*
1972 *Paleontology* **78**:989–1013.
- 1973 **Joyce WG. 2007.** Phylogenetic relationships of Mesozoic turtles. *Bulletin of Peabody Museum*
1974 *of Natural History* **48**:3–102.
- 1975 **Joyce WG, Chapman SD, Moody RTJ, Walker CA. 2011.** The skull of the solemydid turtle
1976 *Helochelydra nopcsai* from the Early Cretaceous of the Isle of Wight (UK) and a review of
1977 Solemydidae. *Special Papers in Palaeontology* **86**:75–97.
- 1978 **Joyce WG, Parham JF, Lyson TR, Warnock RCM, Donoghue PCJ. 2013.** A divergence
1979 dating analysis of turtles using fossil calibrations: an example of best practices. *Journal of*
1980 *Paleontology* **87**:612–634.
- 1981 **Kear BP, Lee MSY. 2006.** A primitive protostegid from Australia and early sea turtle evolution.
1982 *Biology Letters* **2**:116–119.
- 1983 **Lapparent de Broin F, Bardet N, Amaghazaz M, Meslouh S. 2014.** A strange new chelonoid
1984 turtle from the Latest Cretaceous phosphates of Morocco. *Comptes Rendus Palevol* **13**:87–95.
- 1985 **Lehman TM, Tomlinson SL. 2004.** *Terlinguachelys fischbecki*, a new genus and species of sea
1986 turtle (Chelonioidea: Protostegidae) from the Upper Cretaceous of Texas. *Journal of*
1987 *Paleontology* **78**:1163–1178.
- 1988 **Linnaeus C. 1766.** *Systema naturæ per regna tria naturæ, secundum classes, ordines, genera,*
1989 *species, cum characteribus, differentiis, synonymis, locis. Tomus I. Editio duodecima,*
1990 *reformata.* Holmiæ: Salvius.
- 1991 **Longman HA. 1915.** On a giant turtle from the Queensland Lower Cretaceous. *Memoirs of the*
1992 *Queensland Museum* **3**:24–29.

- 1993 **Lydekker R. 1889.** Note on some points in the nomenclature of fossil reptiles and amphibians,
1994 with preliminary notices of two new species. *Geological Magazine* **6**:325–326.
- 1995 **Meylan PA. 1987.** The phylogenetic relationships of soft-shelled turtles (family Trionychidae).
1996 *Bulletin of the American Museum of Natural History* **186**:1–110
- 1997 **Nick L. 1913.** Das Kopfskelet von *Dermochelys coriacea* L. *Zoologische Jahrbücher, Abteilung*
1998 *für Anatomie und Ontogenie der Tiere* **33**:1-283.
- 1999 **Oppel M. 1811.** *Die Ordnungen, Familien und Gattungen der Reptilien als Prodrom einer*
2000 *Naturgeschichte derselben.* München: Lindauer.
- 2001 **Paulina-Carabajal A, Sterli J, Georgi J, Poropat SF, Kear BP. 2017.** Comparative
2002 neuroanatomy of extinct horned turtles (Meiolaniidae) and extant terrestrial turtles
2003 (Testudinidae), with comments on the palaeobiological implications of selected endocranial
2004 features. *Zoological Journal of the Linnean Society* **180**:930–950 DOI
2005 10.1093/zoolinlean/zlw024
- 2006 **Parham JF, Pyenson ND. 2010.** New sea turtle from the Miocene of Peru and the iterative
2007 evolution of feeding ecomorphologies since the Cretaceous. *Journal of Paleontology* **84**:231–
2008 247.
- 2009 **Parham JF, Donoghue PCJ, Bell CJ, Calway TD, Head JJ, Holroyd PA, Inoue JG, Irmis**
2010 **RB, Joyce WG, Ksepka DT, Patané JSL, Smith ND, Traver JE, Van Tuinen M, Yang Z,**
2011 **Angielczyk KD, Greenwood JM, Hipsley CA, Jacobs L, Makovicky PJ, Müller J, Smith**
2012 **KT, Theodor JM, Warnock RCM, Benton MJ. 2012.** Best practise for justifying fossil
2013 calibrations. *Systematic Biology* **61**:346–359.
- 2014 **Pehrson T. 1945.** Some problems concerning the development of skulls in turtles. *Acta*
2015 *Zoologica* **26**:1–28.

- 2016 **Pereira AG, Sterli J, Moreira FRR, Schrago CG. 2017.** Multilocus phylogeny and statistical
- 2017 biogeography clarify the evolutionary history of major lineages of turtles. *Molecular*
- 2018 *Phylogenetics and Evolution* **113**:59–66.
- 2019 **Rabi M, Zhou C-F, Wings O, Ge S, Joyce WG. 2013.** A new xinjiangchelyid turtle from the
- 2020 Middle Jurassic of Xinjiang, China and the evolution of the basipterygoid process in
- 2021 Mesozoic turtles. *BMC Evolutionary Biology* **13**:203.
- 2022 **Rütimeyer L. 1873.** Die fossilen Schildkröten von Solothurn. *Neue Denkschrift der Allgemeinen*
- 2023 *Schweizerischen Naturforschenden Gesellschaft* **25**:1–185.
- 2024 **Seeley HG. 1869.** *Index to the fossil remains of Aves, Ornithosauria, and Reptilia, from the*
- 2025 *Secondary System of Strata, arranged in the Woodwardian Museum of the University of*
- 2026 *Cambridge.* Cambridge: Deighton, Bell, & Co, 1–143
- 2027 **Sheil CA. 2005.** Skeletal development of *Macrochelys temminckii* (Reptilia: Testudines:
- 2028 Chelydridae). *Journal of Morphology* **263**: 71–106.
- 2029 **Sheil CA. 2013.** Development of the skull of the hawksbill sea turtle, *Eretmochelys imbricata*.
- 2030 *Journal of Morphology* **274**:1124–1142.
- 2031 **Siebenrock F. 1897.** Das Kopfskelet der Schildkröten. *Sitzungsberichte der Kaiserlichen*
- 2032 *Akademie der Wissenschaften* **106**:245–328.
- 2033 **Sterli J. 2008.** A new, nearly complete stem turtle from the Jurassic of South America with
- 2034 implications for turtle evolution. *Biology Letters* **4**:286–289.
- 2035 **Sterli J, Müller J, Aquentin J, Hiliger A. 2010.** The parabasisphenoid complex in Mesozoic
- 2036 turtles and the evolution of the testudinate basicranium. *Canadian Journal of Earth Sciences*
- 2037 **47**:1337–1346.

- 2038 **Sterli J, de la Fuente MS. 2013.** New evidence from the Palaeocene of Patagonia (Argentina)
2039 on the evolution and palaeo-biogeography of Meiolaniformes (Testudinata, new taxon name).
2040 *Journal of Systematic Palaeontology* **11**:835–852.
- 2041 **Tong H, Meylan P. 2012.** Morphology and relationships of *Brachyopsemys tingitana* gen. et sp.
2042 nov. from the Early Paleocene of Morocco and recognition of the new eucryptodiran turtle
2043 family: Sandownidae. In: Brinkman DB, Holroyd PA, Gardner JD, eds. *Morphology and*
2044 *Evolution of Turtles* Dordrecht: Springer Verlag 187-212
- 2045 **[TTWG] Turtle Taxonomy Working Group [Rhodin AGJ, Iverson JB, Bour R, Fritz U,**
2046 **Georges A, Shaffer HB, van Dijk PP]. 2017.** Turtles of the World: Annotated checklist and
2047 atlas of taxonomy, synonymy, distribution, and conservation status (8th Ed.). *Chelonian*
2048 *Research Monographs* **7**:1–292 DOI 10.3854/crm.7.checklist.
- 2049 **Vandellii D. 1761.** Epistola de holothurio, et testudine coriacea ad celeberrimum Carolum
2050 Linneum equitem. Padua: Conzetti.
- 2051 **Williston SW. 1894.** A new turtle from the Benton Cretaceous. *Kansas Quarterly* **3**:5–18.
- 2052 **Zangerl R. 1953.** The vertebrate fauna of the Selma Formation of Alabama. Part IV. The turtles
2053 of the family Toxochelyidae. *Fieldiana: Geology Memoirs* **3**:145–277.
- 2054 **Zangerl, R. and R. E. Sloan. 1960.** A new specimen of *Desmatochelys lowi* Williston, a
2055 primitive cheloniid sea turtle from the Cretaceous of South Dakota. *Fieldiana, Geology*
2056 **14**:7–40.
- 2057 **Zhou C-F, Rabi M, Joyce WG. 2014.** A new specimen of *Manchurochelys manchoukuoensis*
2058 from the Early Cretaceous Jehol Biota of Chifeng, Inner Mongolia, China and the phylogeny
2059 of Cretaceous basal eucryptodiran turtles. *BMC Evolutionary Biology* **14**:77.

2060 **Zittel KA. 1889.** *Handbuch der Paläontologie. Section 1: Paläozoologie, 3: Vertebrata,*
2061 *Shipment 3: Reptilia.* München: R. Oldenburg.
2062

Table 1(on next page)

Scan settings for the specimens used herein.

<i>Specimen</i>	<i>Scanner</i>	<i>Institution</i>	<i>Voltage (kV)</i>	<i>Current (μA)</i>	<i>Voxel size (μm)</i>	<i>Filter</i>
<i>Desmatochelys lowii</i>	Phoenix v tome x μ CT	University of Chicago, Department of Organismal Biology and Anatomy	210	190	79,8	Cu 0,15mm Sn 0,50mm
<i>Eretmochelys imbricata</i>	Bruker SkyScan μ CT	University of Fribourg, Department of Geosciences	125	63	43,0	0,50 Al mm
<i>Dermochelys coriacea</i>	Siemens Medical CT	University of Bern, Institute of Forensic Medicine	120	210	98,6	-
<i>Chelydra serpentina</i>	Bruker SkyScan μ CT	University of Fribourg, Department of Geosciences	80	550	35,0	Ti 0,50 mm Al 0,125 mm

Table 2 (on next page)

Settings used in the conversion of scan data to slice data.

<i>Specimen</i>	<i>Software</i>	<i>Smoothing</i>	<i>Ring artifact correction</i>	<i>Beam hardening correction</i>
<i>Desmatochelys lowii</i>	-	-	-	-
<i>Eretmochelys imbricata</i>	NRecon	1	0	70%
<i>Dermochelys coriacea</i>	-	-	-	-
<i>Chelydra serpentina</i>	NRecon	0	16	13%

1

Table 3(on next page)

Description and scoring of characters 32, 33, 62, 64, 87, 88 and 92.

character	bone	character description	<i>Desmatochelys lowii</i>	<i>Eretmochelys imbricata</i>	<i>Dermochelys coriacea</i>	<i>Chelydra serpentina</i>
32	postorbital	Recess on the ventral side of the dorsal part of the postorbital. 0= absent; 1=present	1	0	0	1
33		Position of notch in the posterior margin of the orbit. 0=at the top of the orbit; 1=at the mid level	1	0	0	1
62	epipterygoid	Participation of the epipterygoid to the foramen nervi trigemini. 0= absent; 1=present	0	-	-	1
64	prootic	Extent of the suture with the parietal. 0=very short or absent; 1=long	1	0	0	1
87		Dorsomedial process of the prootic in medial view. 0=absent, prootic has a similar height to the opisthotic; 1=present, prootic process significantly higher than opisthotic	-	0	0	1
88	opisthotic	Participation of the opisthotic to the formation of the foramen stapedio-temporale. 0=absent; 1=present	1	0	1	0
92	quadrate	Processus epipterygoideus. 0=absent; 1=present	0	1	1	1

Table 4(on next page)

Similarity Matrix.

The similarity between taxa is shown in %.

	<i>Desmatochelys lowii</i>	<i>Eretmochelys imbricata</i>	<i>Dermochelys coriacea</i>	<i>Chelydra serpentina</i>
<i>Desmatochelys lowii</i>	-	44%	34%	33%
<i>Eretmochelys imbricata</i>	44%	-	51%	45%
<i>Dermochelys coriacea</i>	34%	51%	-	38%
<i>Chelydra serpentina</i>	33%	45%	38%	-

1

Figure 1

The skull of *Eretmochelys imbricata* in four types of digital representation.

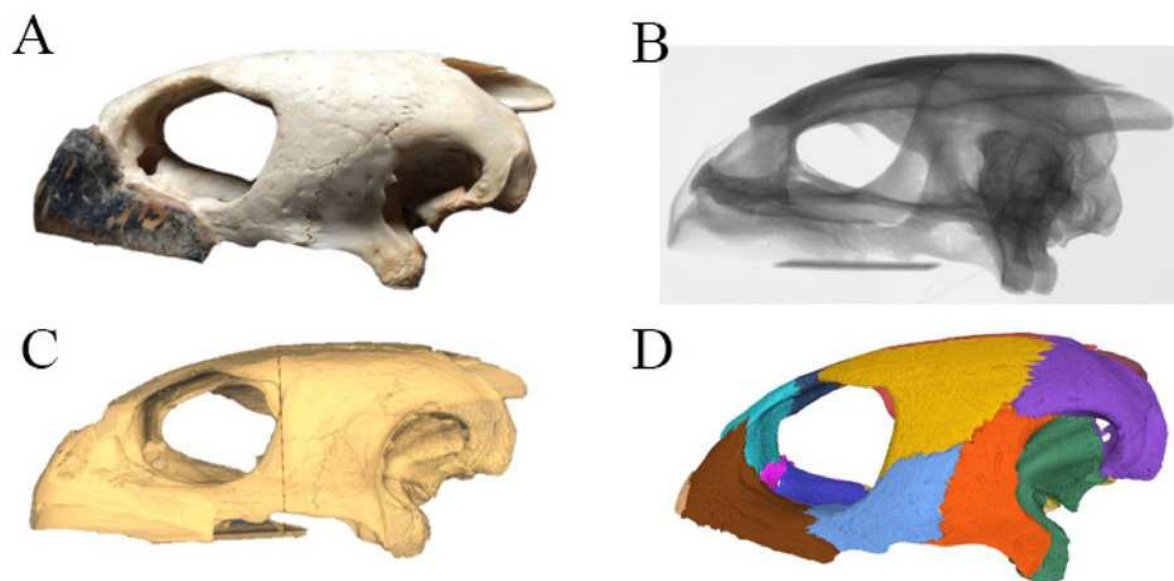


Figure 2(on next page)

Sketches illustrating the categories of observed spatial relations between bones (left) and the depth of sutures (right).

The spatial relations between bones can be classified into: parallel, overlapping or underlying, clasping, and vertically transverse. The depth of suture can range from smooth to strongly interfingering.



p: parallel

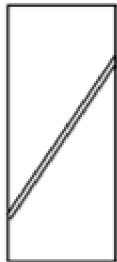


o: overlapping

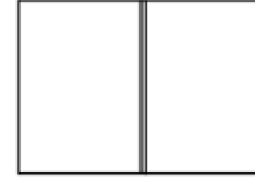
u: underlying



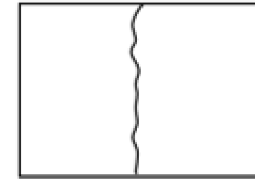
c: clasps cb: clasped by



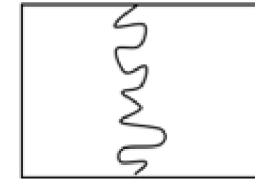
t: vertically transverse



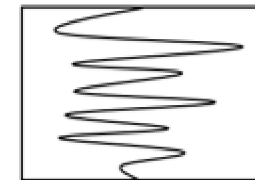
s: smooth



if: faintly interfingering



im: moderately
interfingering



is: strongly interfingering

Figure 3

Examples of bone contacts based on cross – section images in *Eretmochelys imbricata*.

(A) parallel and moderately interfingering; (B) underlying / overlapping and faintly interfingering; (C); clasping and faintly interfingering. The width of each image is about 1 cm.

**Note: Auto Gamma Correction was used for the image. This only affects the reviewing manuscript. See original source image if needed for review.*

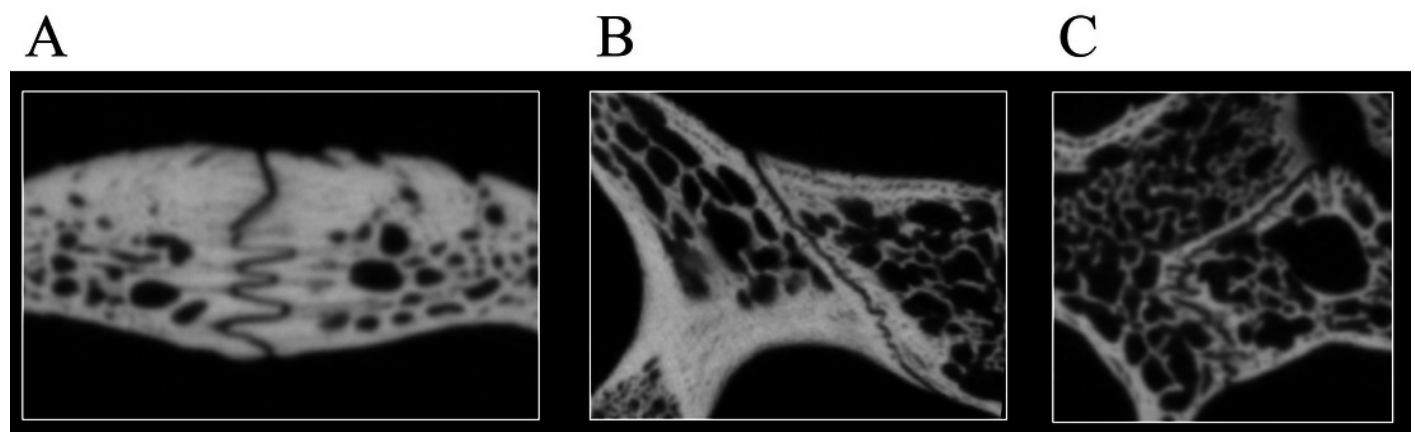


Figure 4

Cross section image of *Desmatochelys lowii* along the coronal plane.

In the lower half, one can observe damage to the skull that is additionally obscured by matrix.

**Note: Auto Gamma Correction was used for the image. This only affects the reviewing manuscript. See original source image if needed for review.*



Figure 5

The segmented skull of *Desmatochelys lowii*.

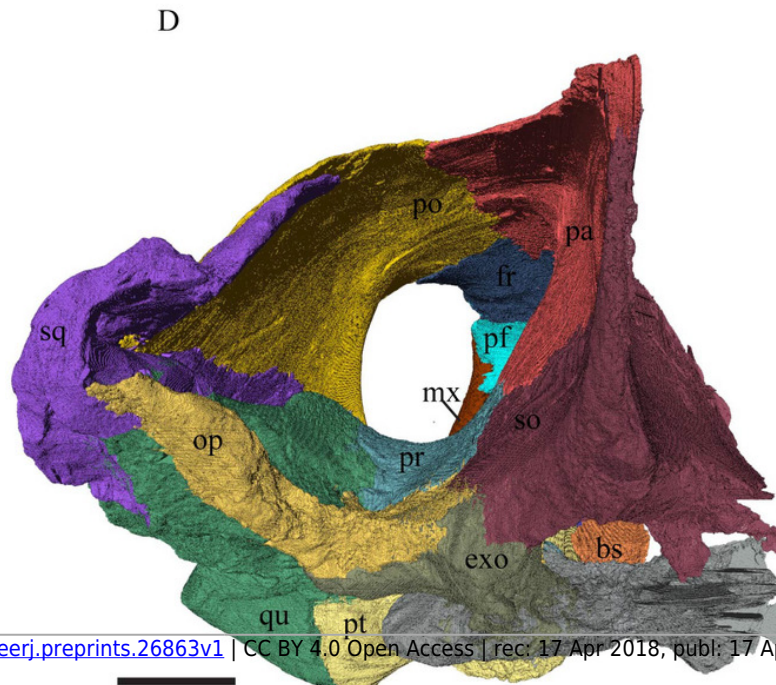
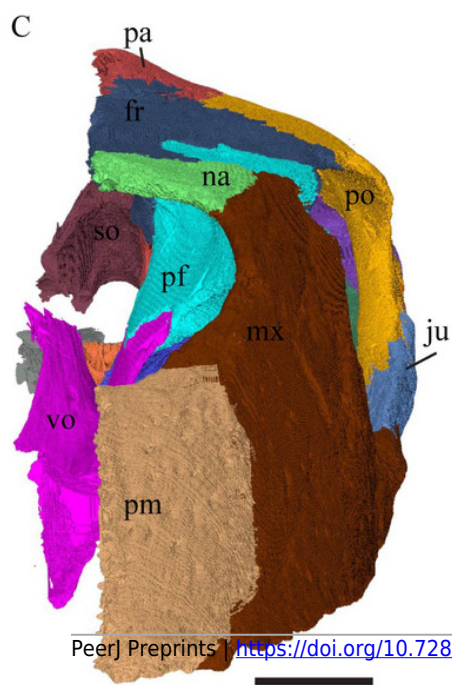
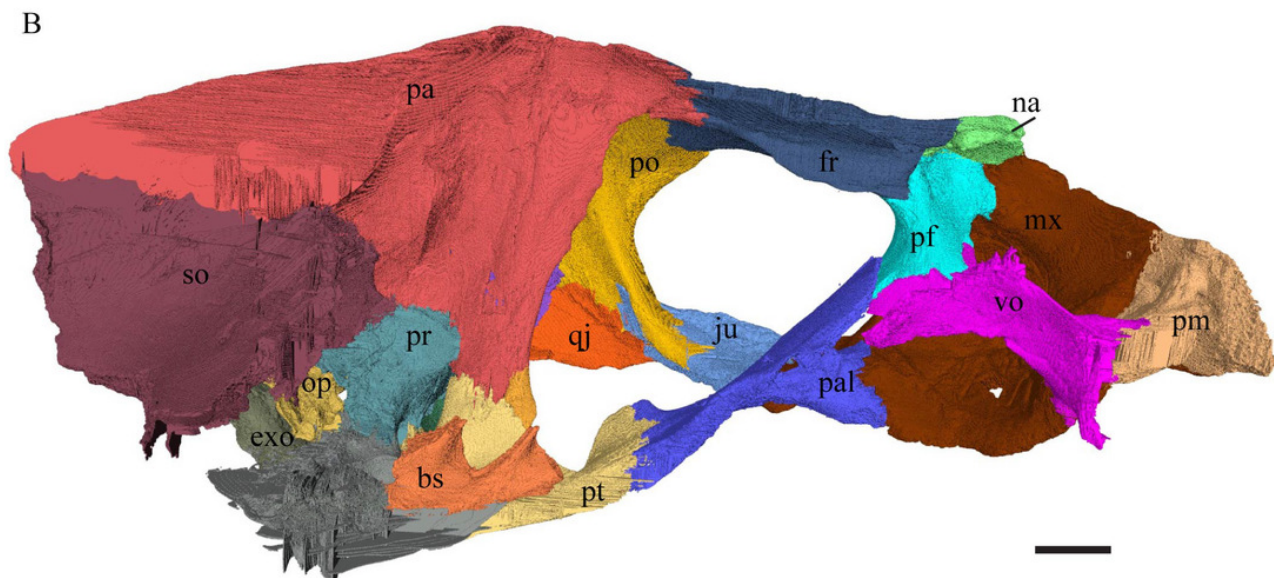
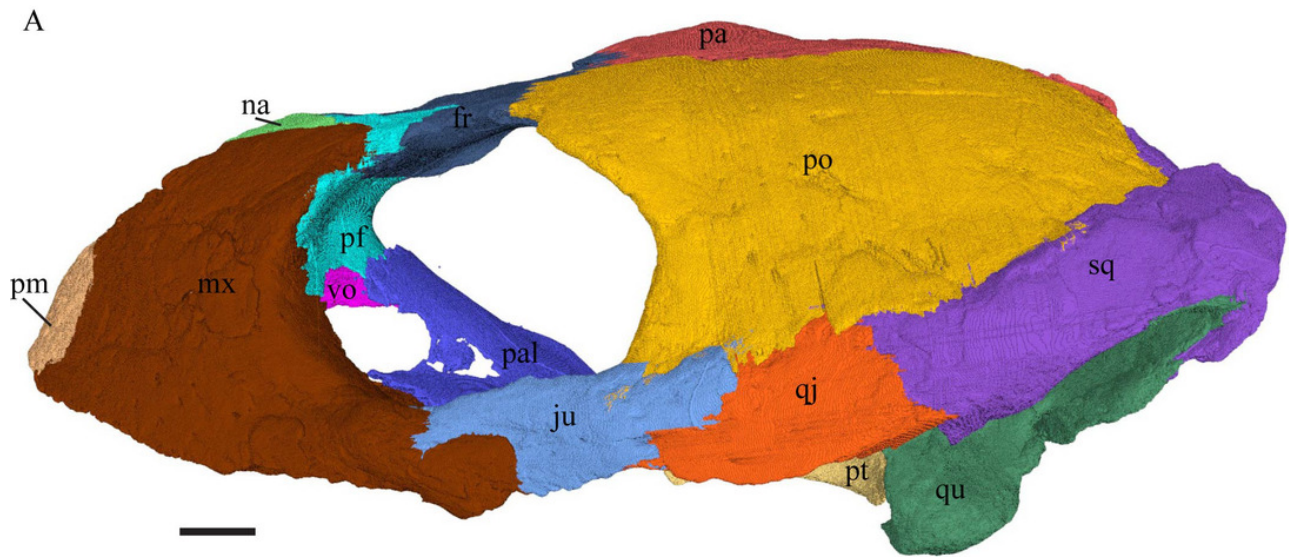


Figure 6

The segmented skull of *Desmatochelys lowii*.

(A) dorsal; (B) ventral views. The bar marks 10mm.

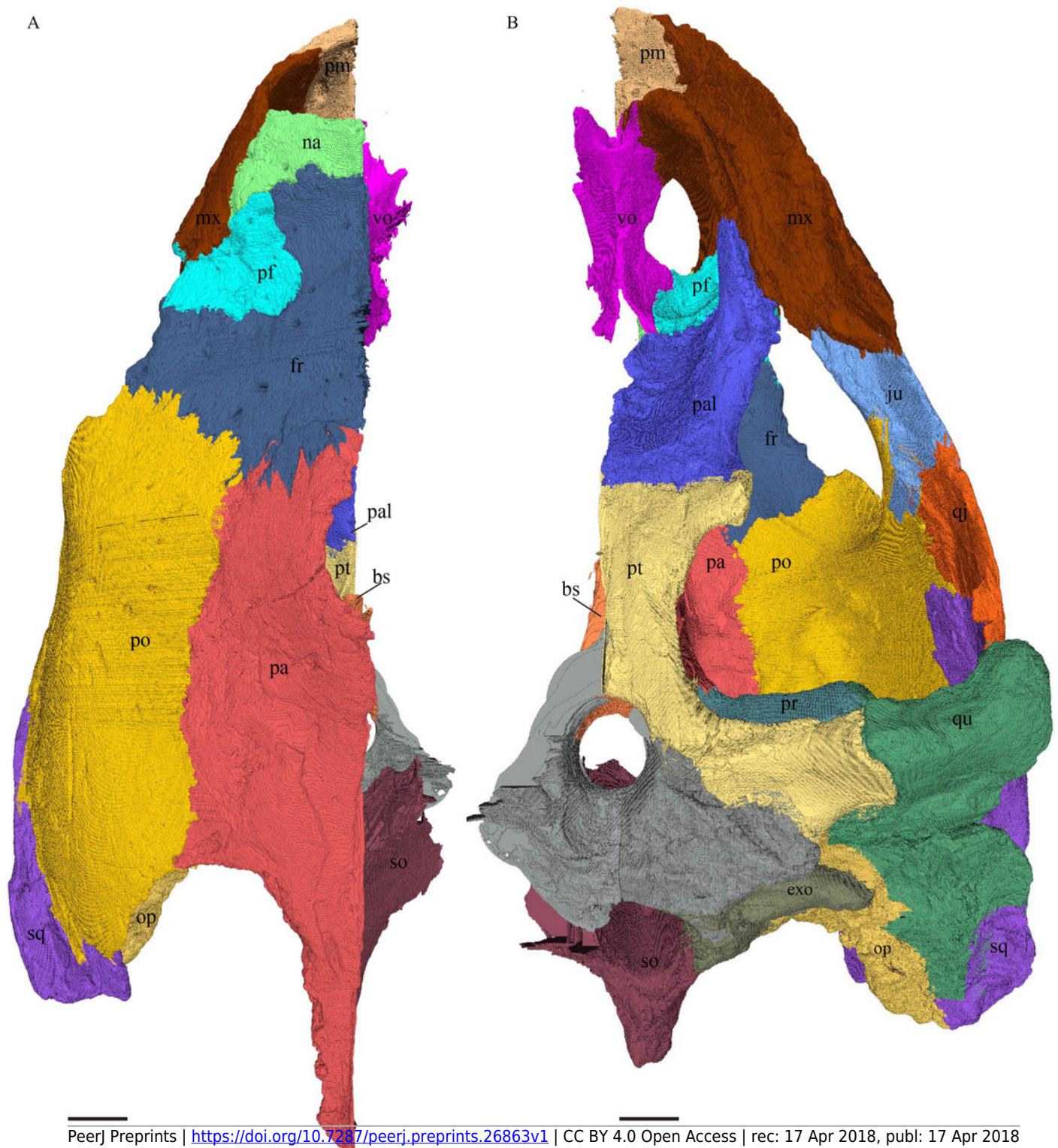


Figure 7

The segmented skull of *Eretmochelys imbricata*.

(A) lateral; (B) medial; (C) anterior; (D) posterior views. The bar marks 10mm.

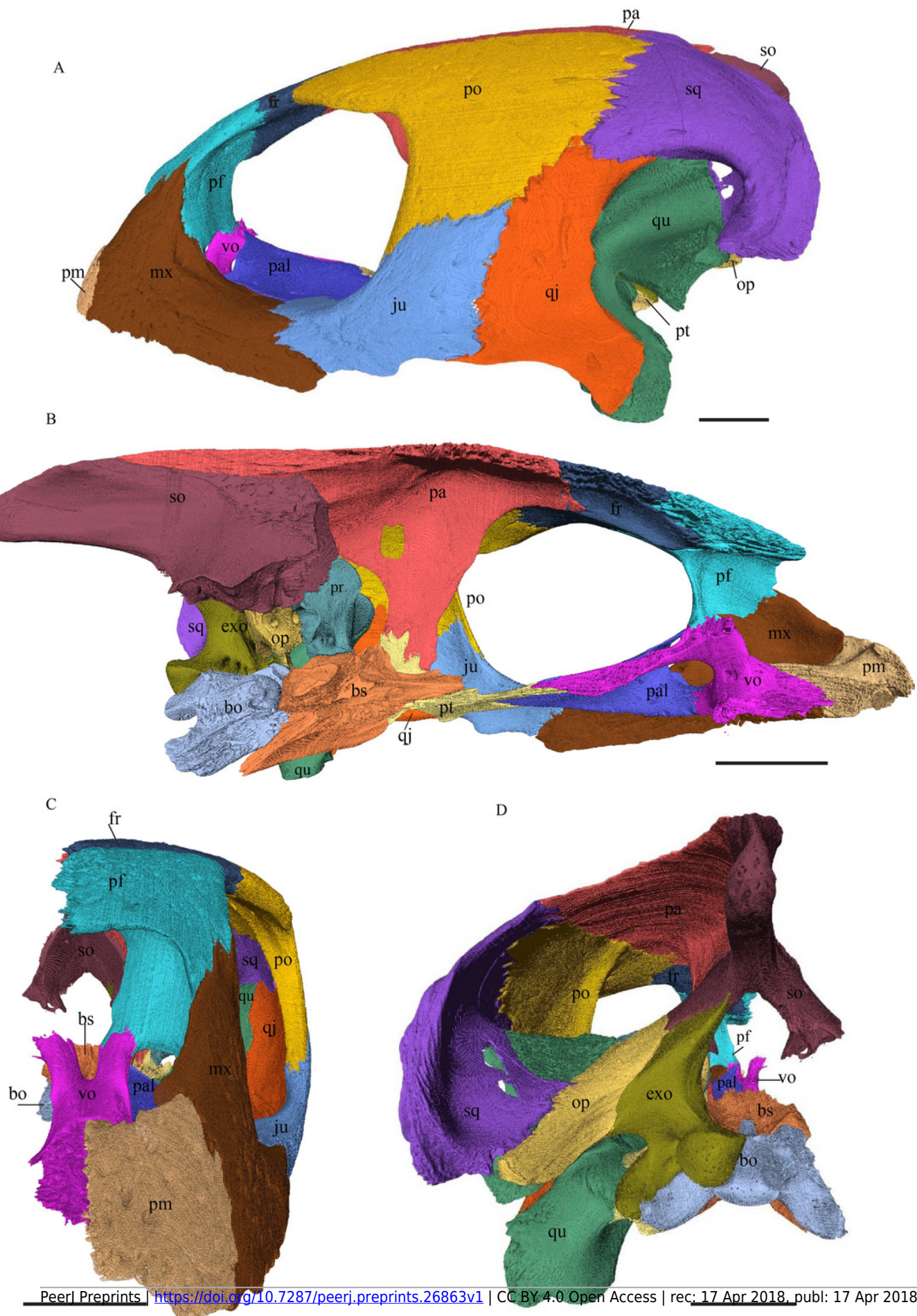


Figure 8

The segmented skull of *Eretmochelys imbricata*.

(A) dorsal; (B) ventral views. The bar marks 10mm.

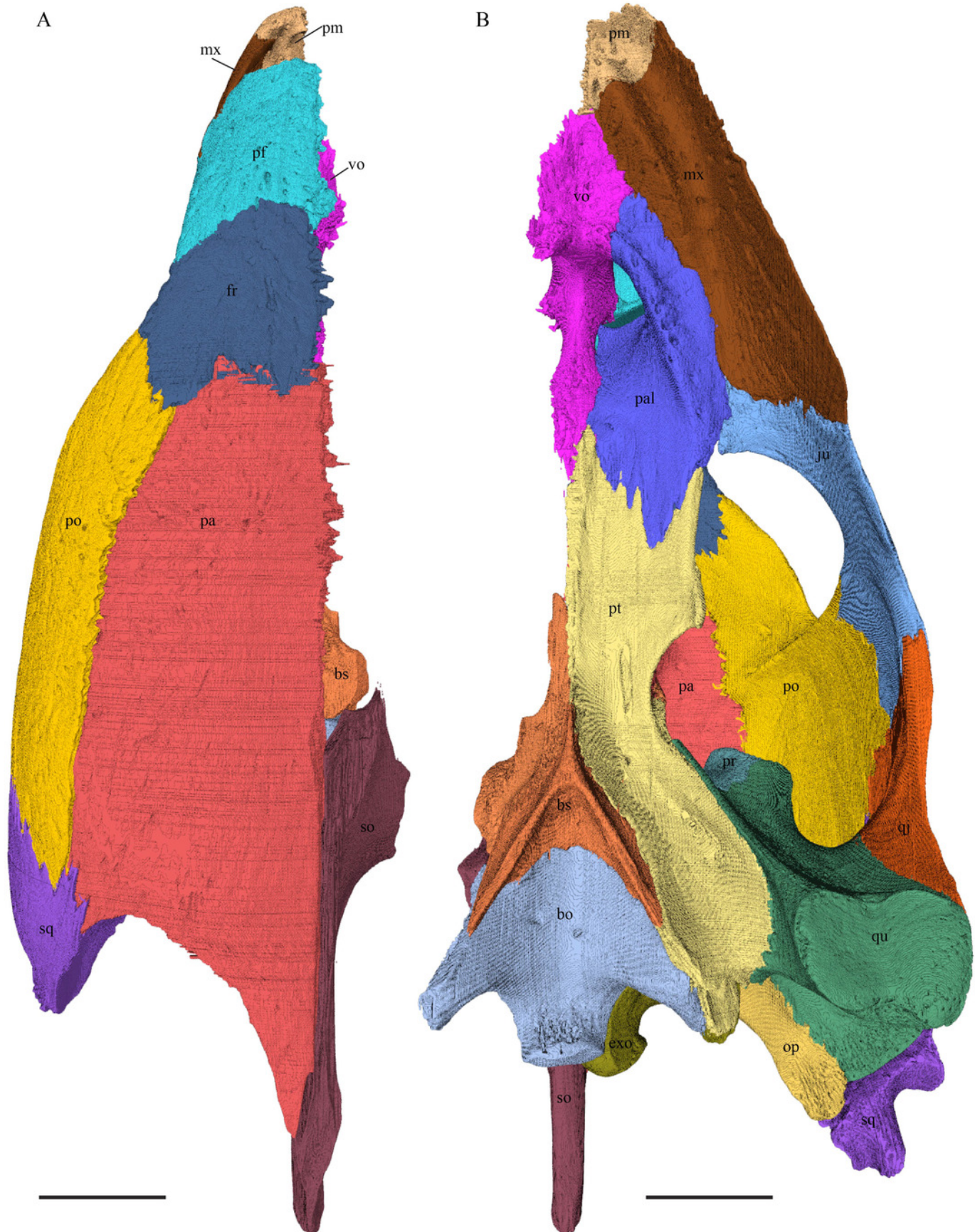
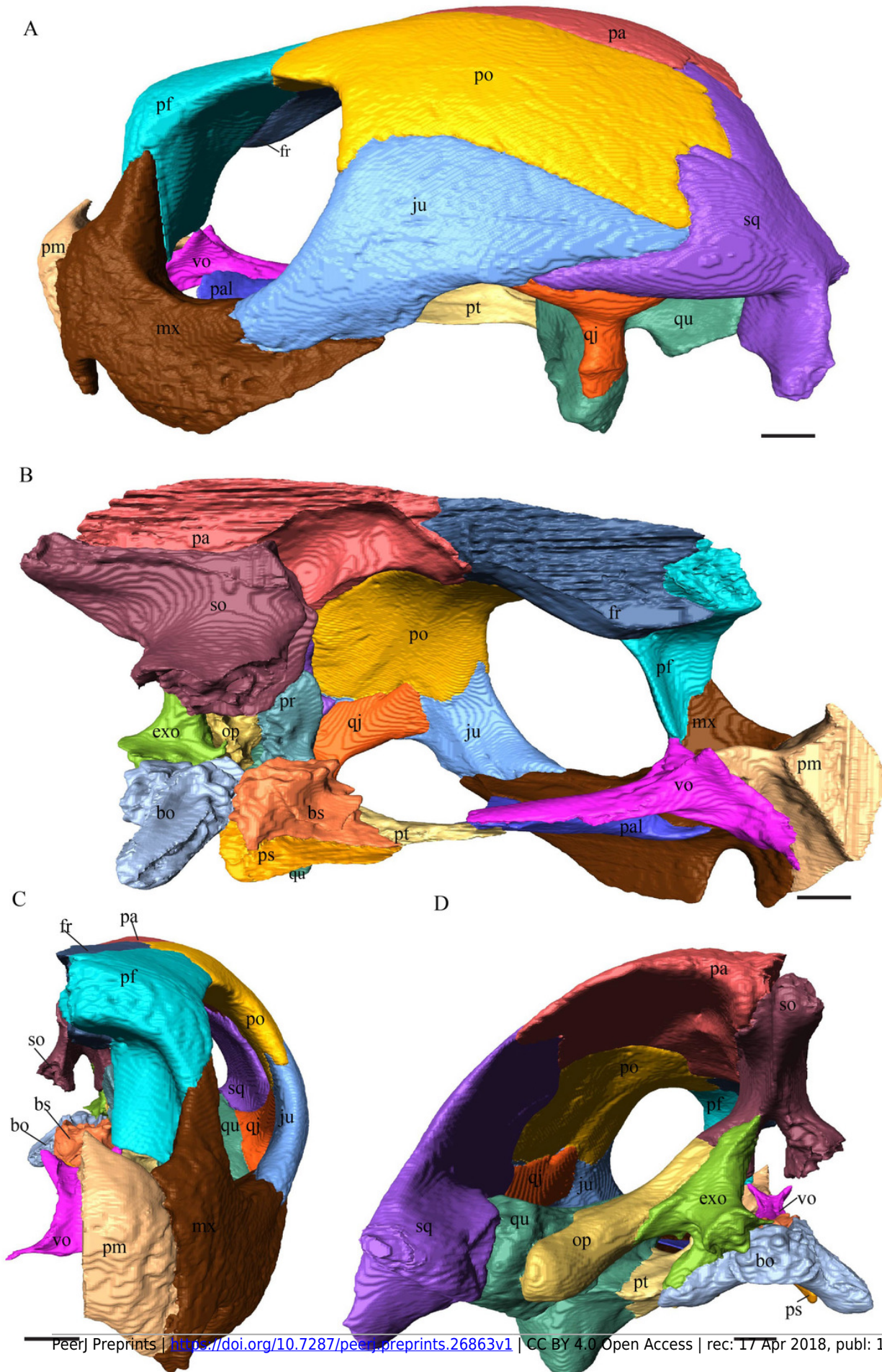


Figure 9

The segmented skull of *Dermochelys coriacea*.

(A) lateral; (B) medial; (C) anterior; (D) posterior views. The bar marks 10mm.



The segmented skull of *Dermochelys coriacea*.

Figure 11

The segmented skull of *Chelydra serpentina*.

(A) lateral; (B) medial; (C) anterior; (D) posterior views. The bar marks 10mm.

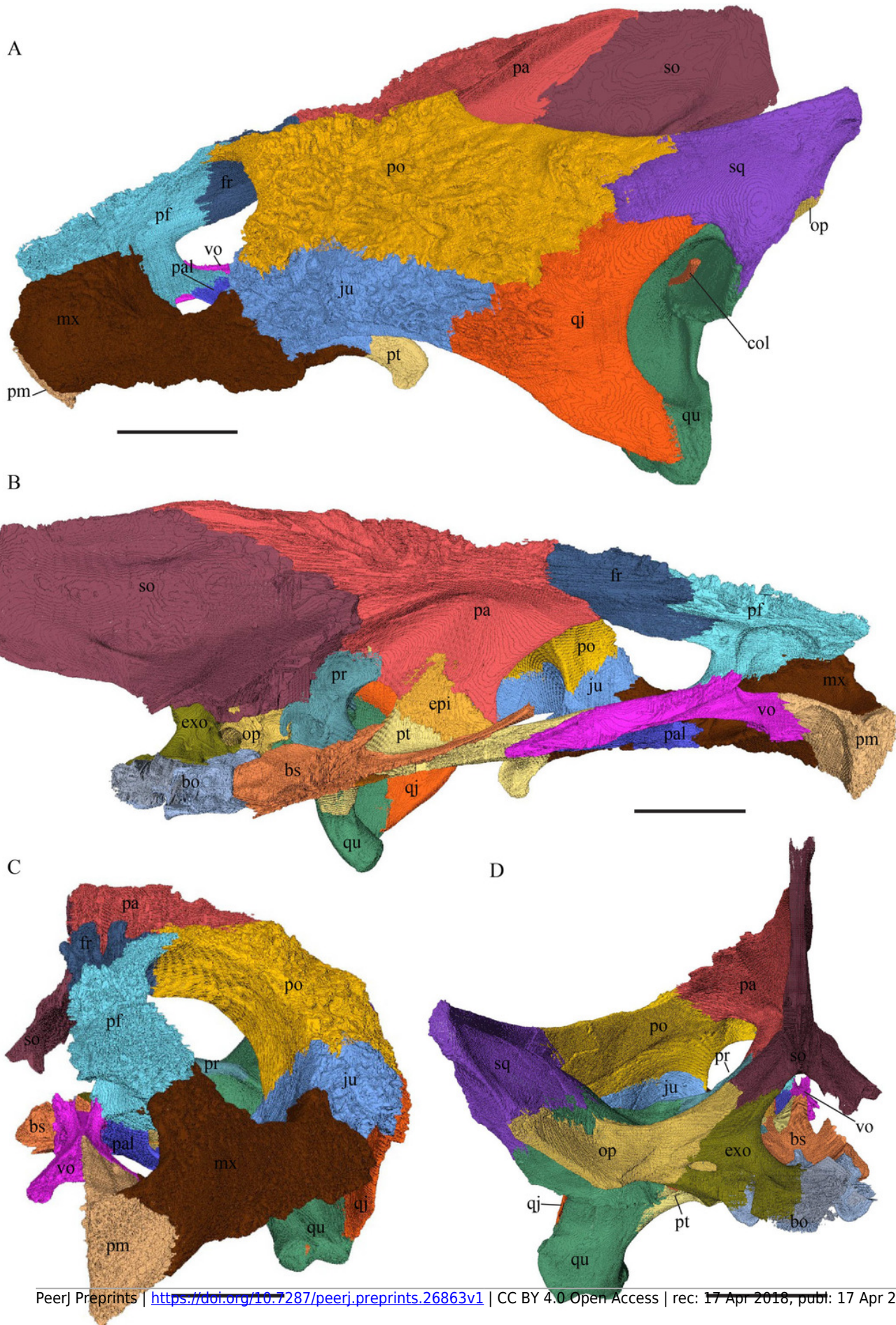


Figure 12

The segmented skull of *Chelydra serpentina*.

(A) dorsal; (B) ventral views. The bar marks 10mm.

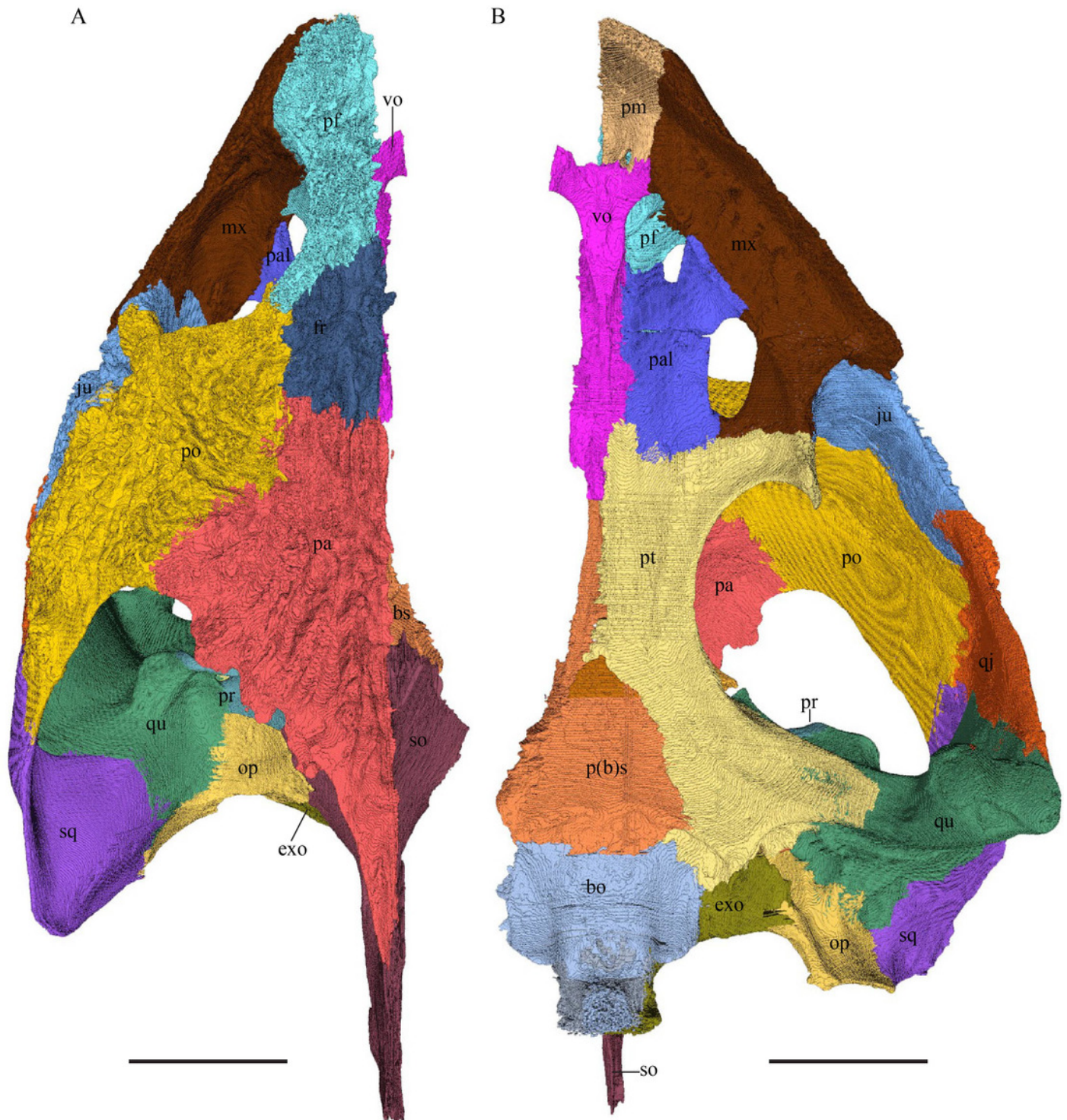


Figure 13

The nasal of *Desmatochelys lowii*.

(A) 3D model in dorsal view; (B) 3D model in anteroventral view; (C) illustration in anteromedial view, highlighting the parasagittal processes. The scale marks 10mm.

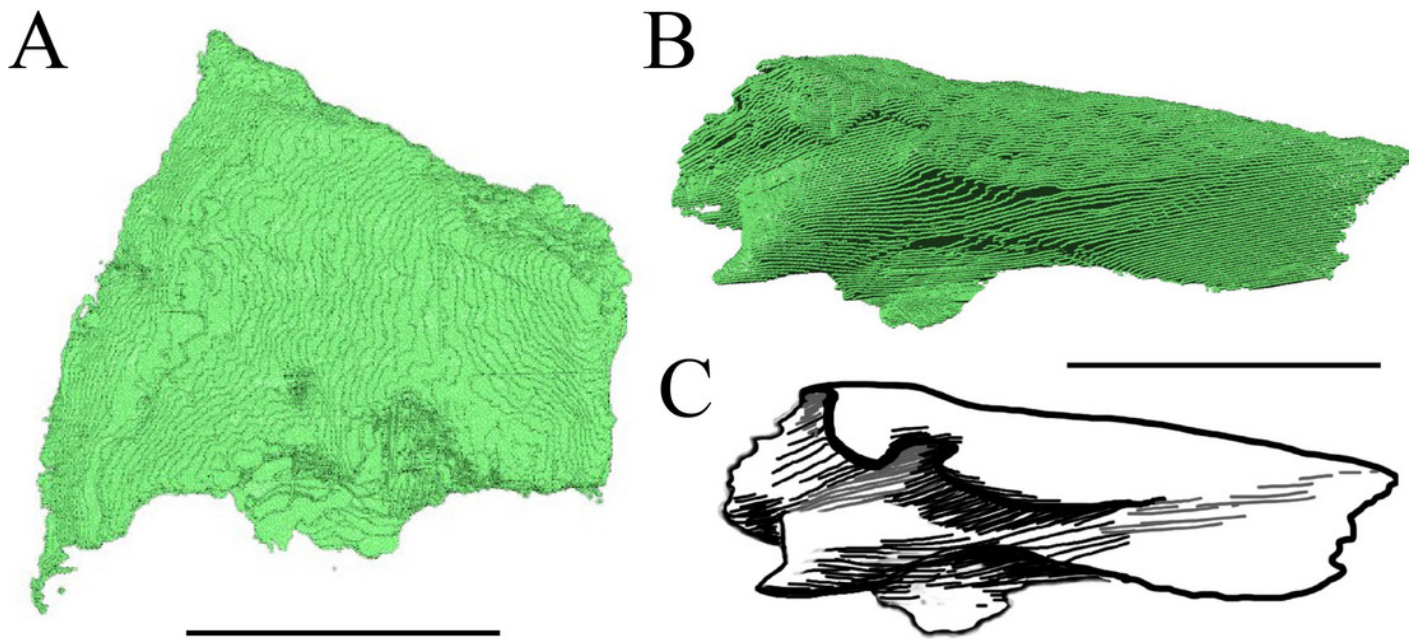


Figure 14

The prefrontal and frontal in dorsal (left), anterior (middle), and posterior (right) views.

(A) *Desmatochelys lowii*; (B) *Eretmochelys imbricata*; (C) *Dermochelys coriacea*; and (D) *Chelydra serpentina*. Orange dots indicate the positions of foramina. The bar marks 10mm.

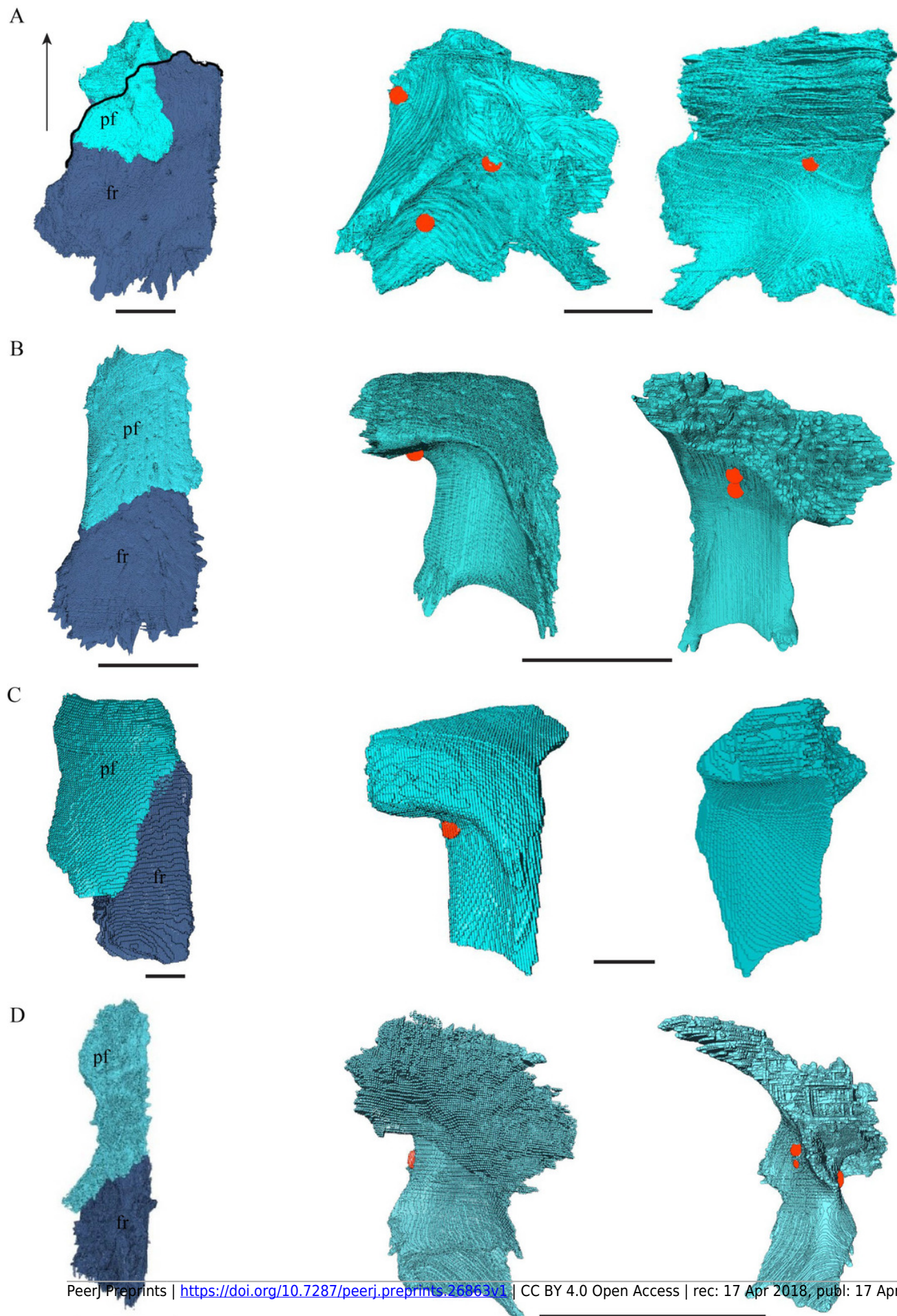


Figure 15

The frontal in anterolateral view of the 3D model (left) and illustration (right).

(A) *Desmatochelys lowii*; (B) *Eretmochelys imbricata*; (C) *Dermochelys coriacea*; and (D) *Chelydra serpentina*. Light blue surface indicates the suture area with the prefrontal. The bar marks 10mm.

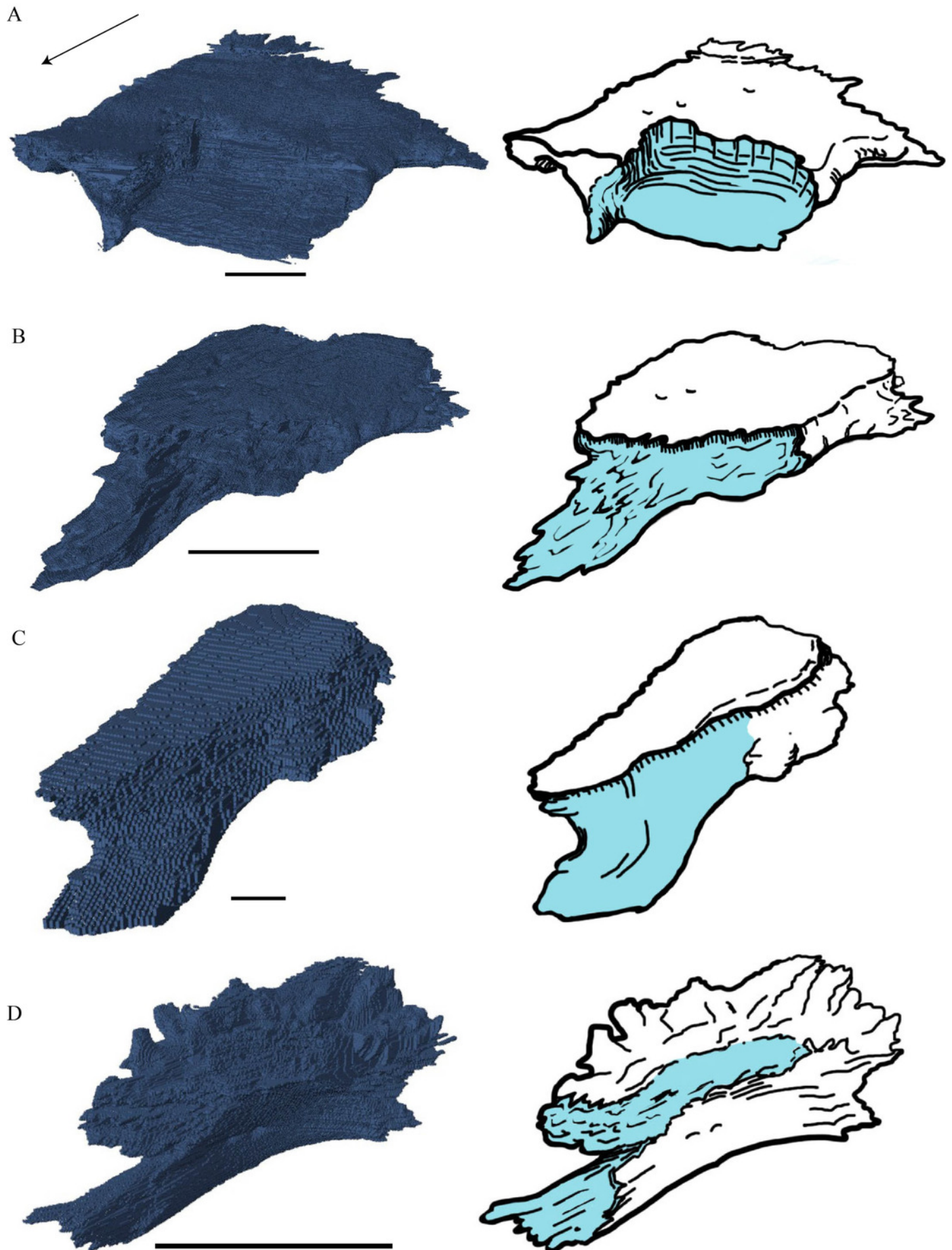


Figure 16

Medial view of the parietal.

(A) *Desmatochelys lowii*; (B) *Eretmochelys imbricata*; (C) *Dermochelys coriacea*; and (D) *Chelydra serpentina*. The bar marks 10mm.

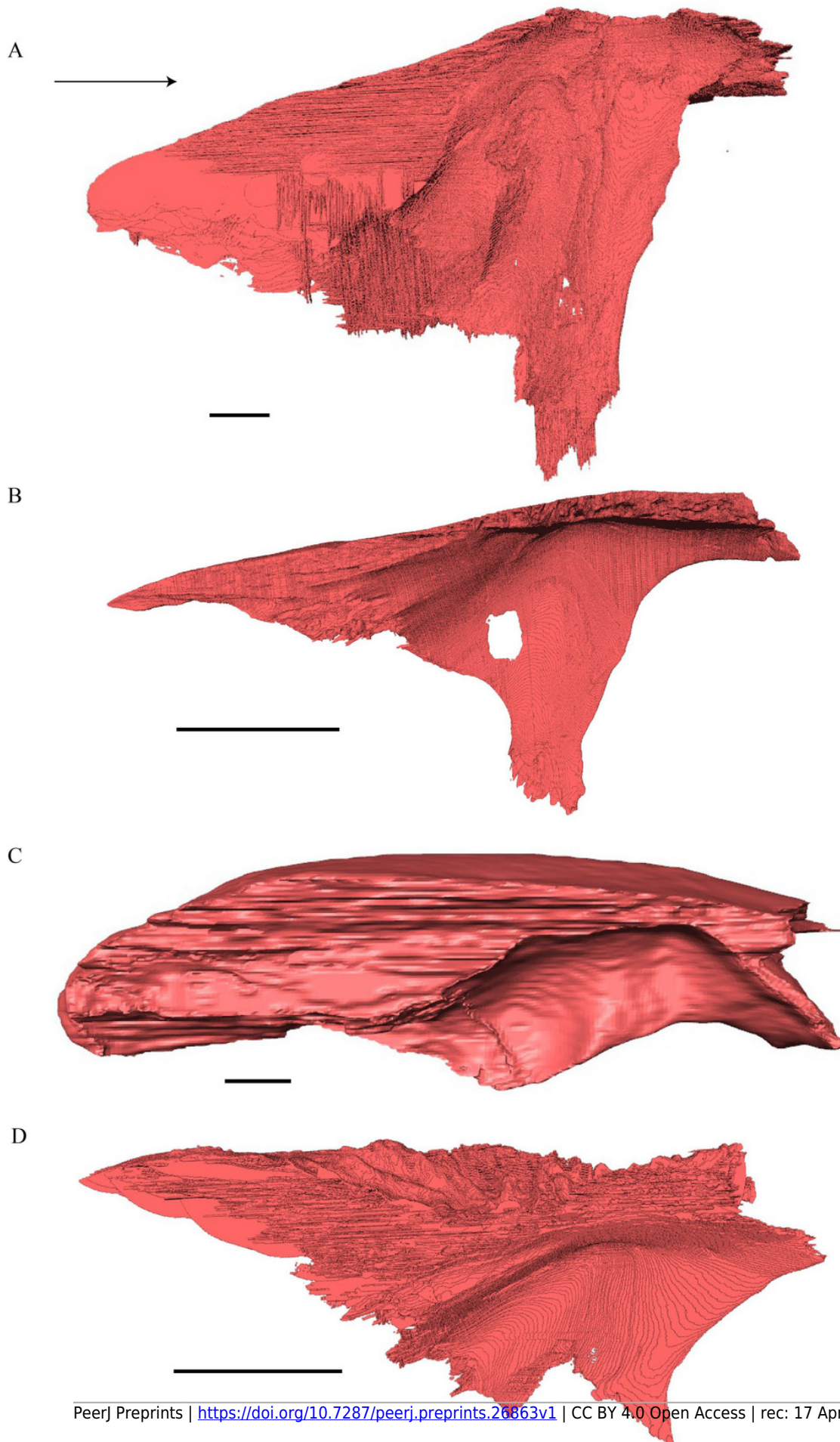


Figure 17

Ventral view the prefrontal, frontal, parietal, and postorbital.

(A) *Desmatochelys lowii*; (B) *Eretmochelys imbricata*; (C) *Dermochelys coriacea*; and (D) *Chelydra serpentina*. The bar marks 10mm.

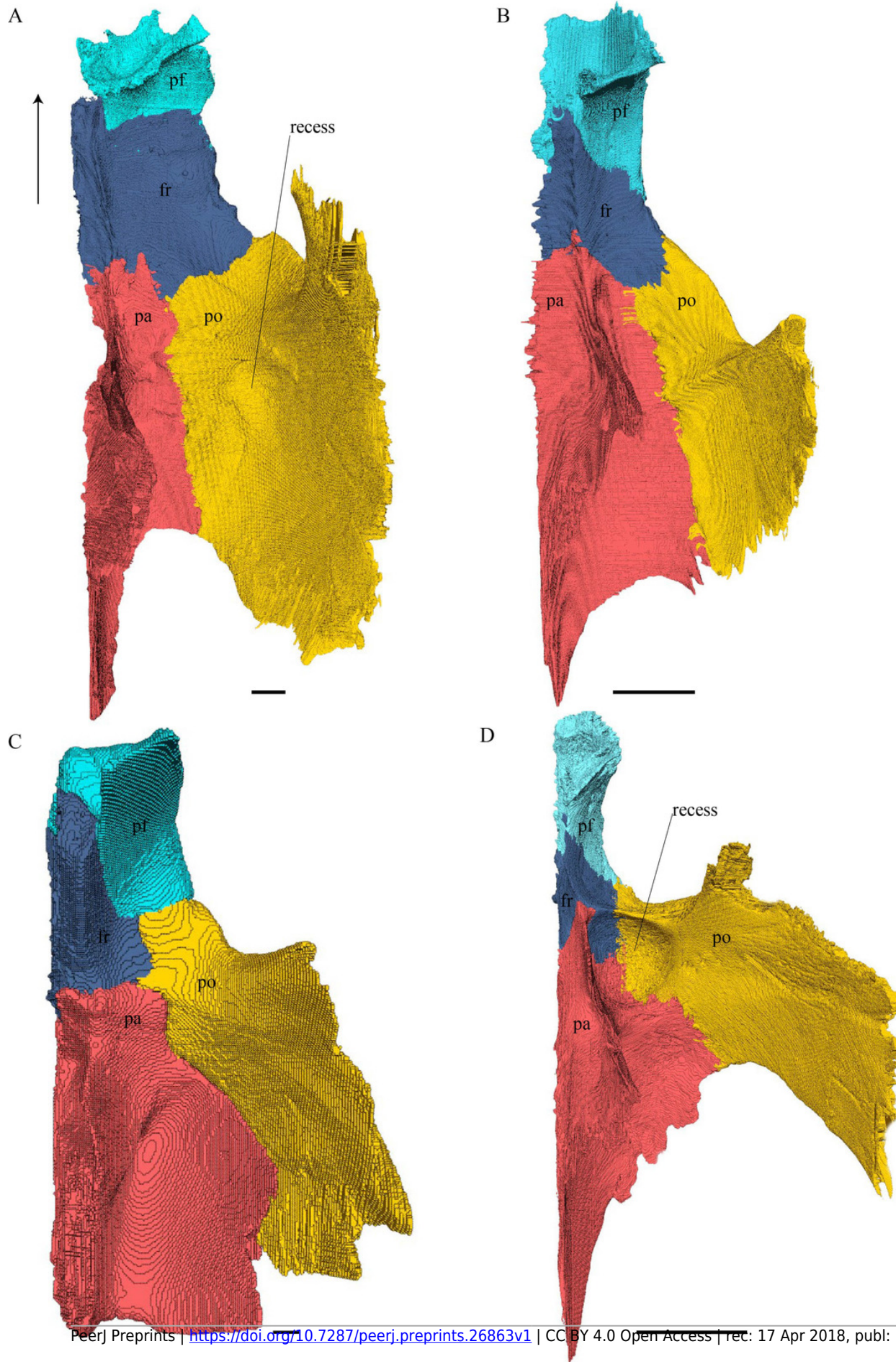


Figure 18

Lateral view the postorbital, squamosal, quadratojugal and jugal.

(A) *Desmatochelys lowii*; (B) *Eretmochelys imbricata*; (C) *Dermochelys coriacea*; and (D) *Chelydra serpentina*. The bar marks 10mm.

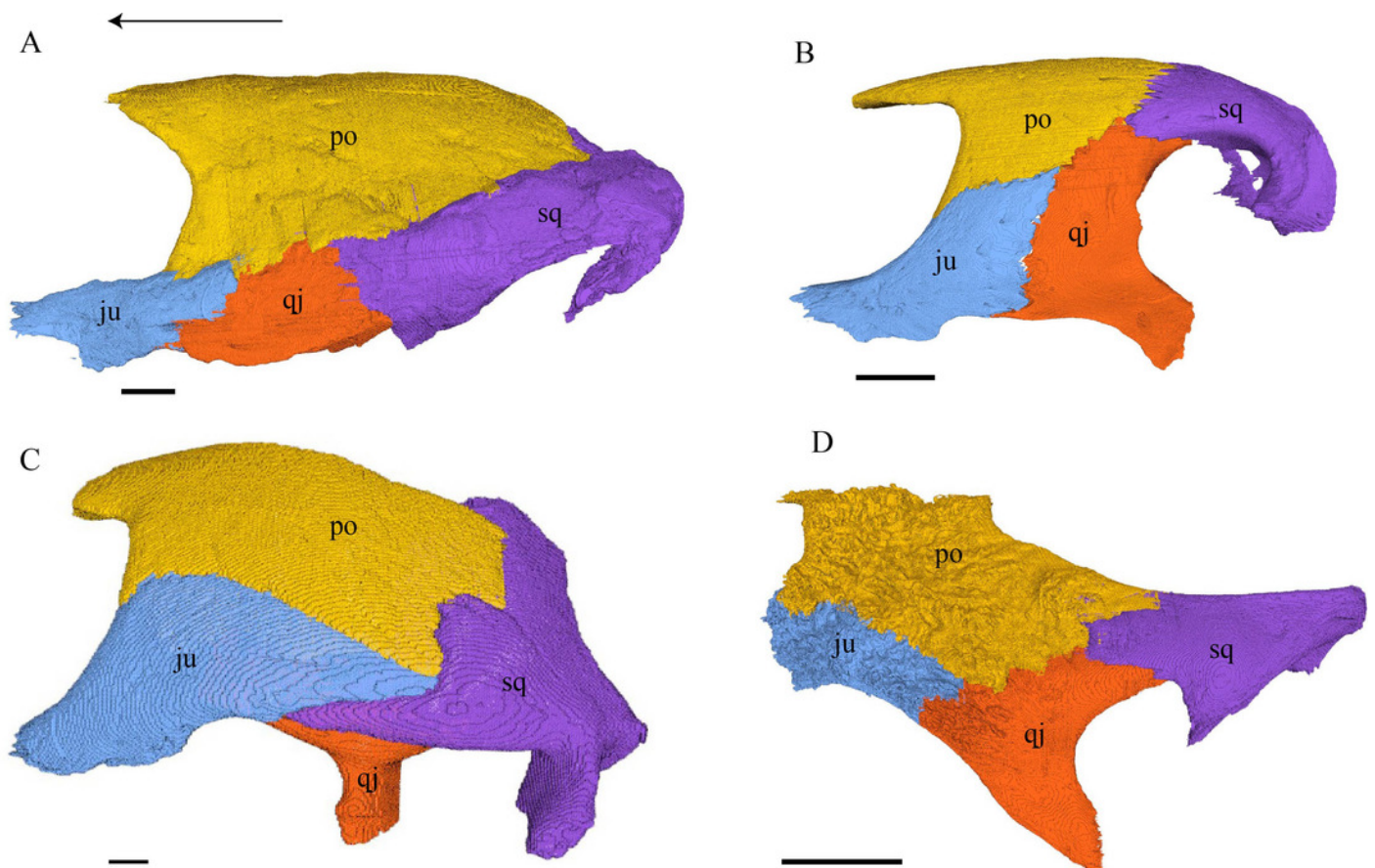


Figure 19

Frontal view of the jugal.

(A) *Desmatochelys lowii*; (B) *Eretmochelys imbricata*; (C) *Dermochelys coriacea*; and (D) *Chelydra serpentina*. The bar marks 10mm.

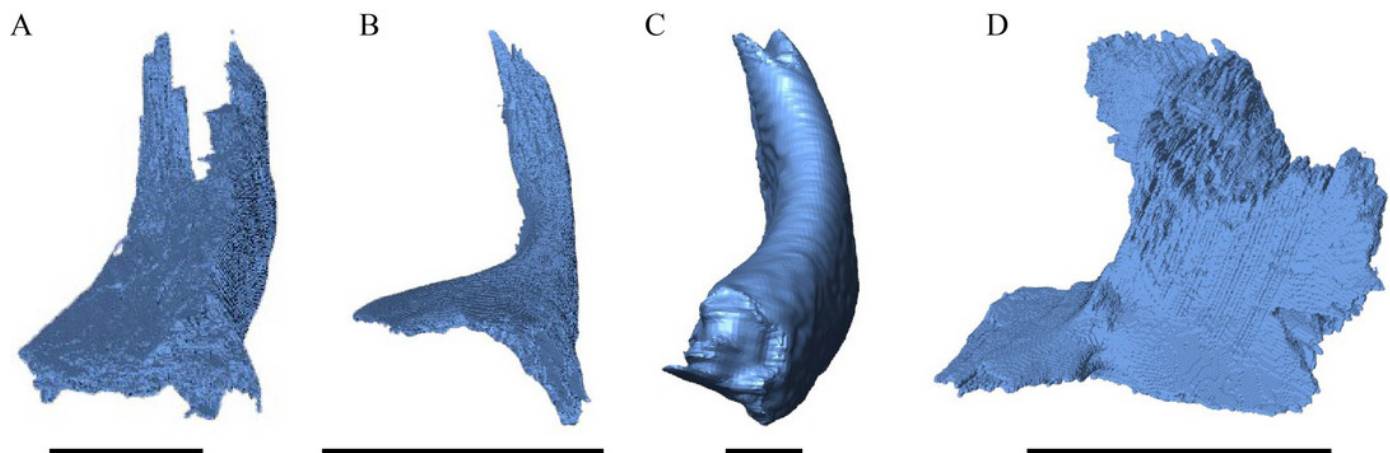


Figure 20

Quadrate and quadratojugal in posterolateral view.

(A) *Desmatochelys lowii*; (B) *Eretmochelys imbricata*; (C) *Dermochelys coriacea*; and (D) *Chelydra serpentina*. The bar marks 10mm.

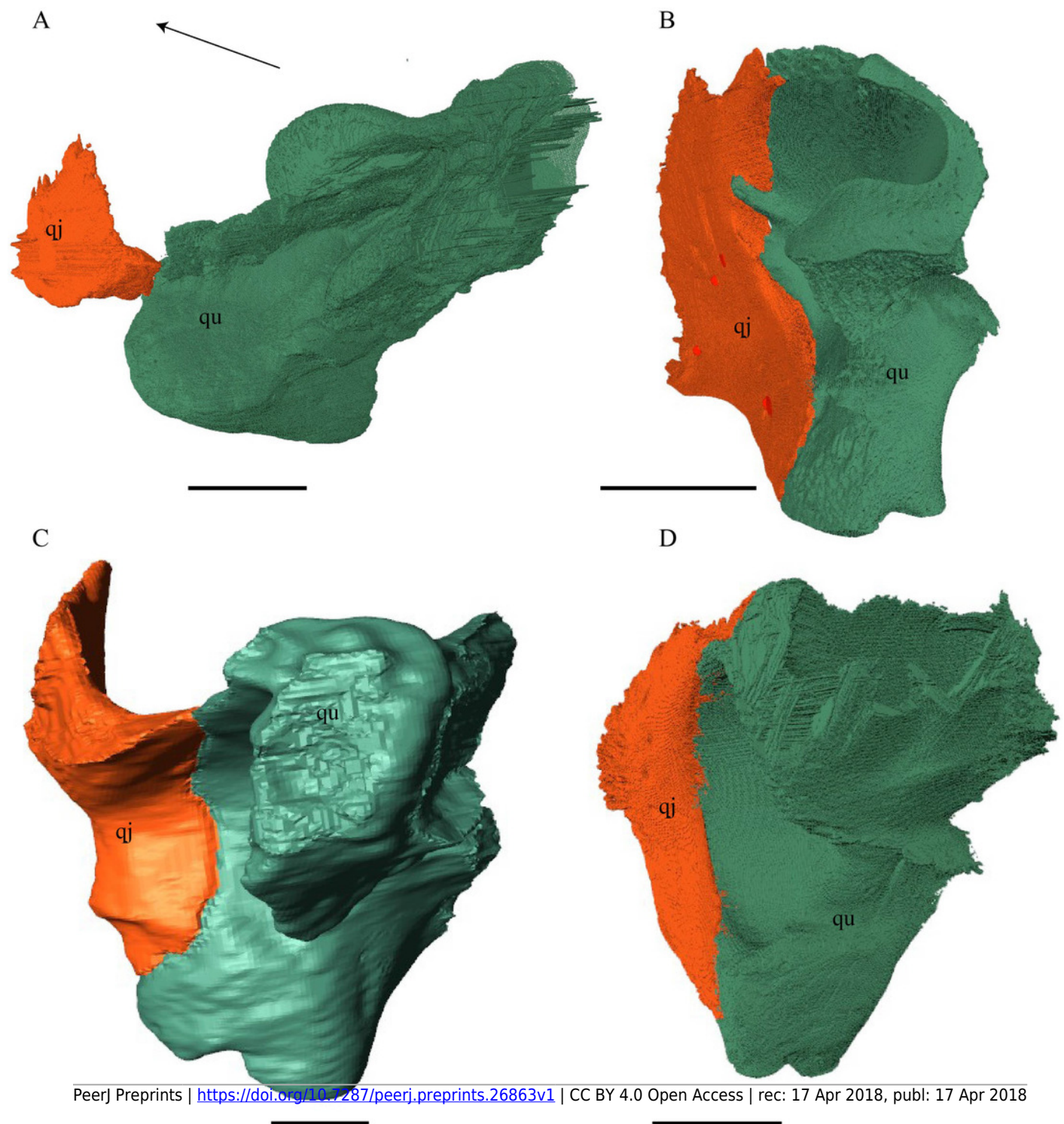


Figure 21

Posterior (left) and ventral (right) view of the squamosal.

(A) *Desmatochelys lowii*; (B) *Eretmochelys imbricata*; (C) *Dermochelys coriacea*; and (D) *Chelydra serpentina*. The bar marks 10mm.

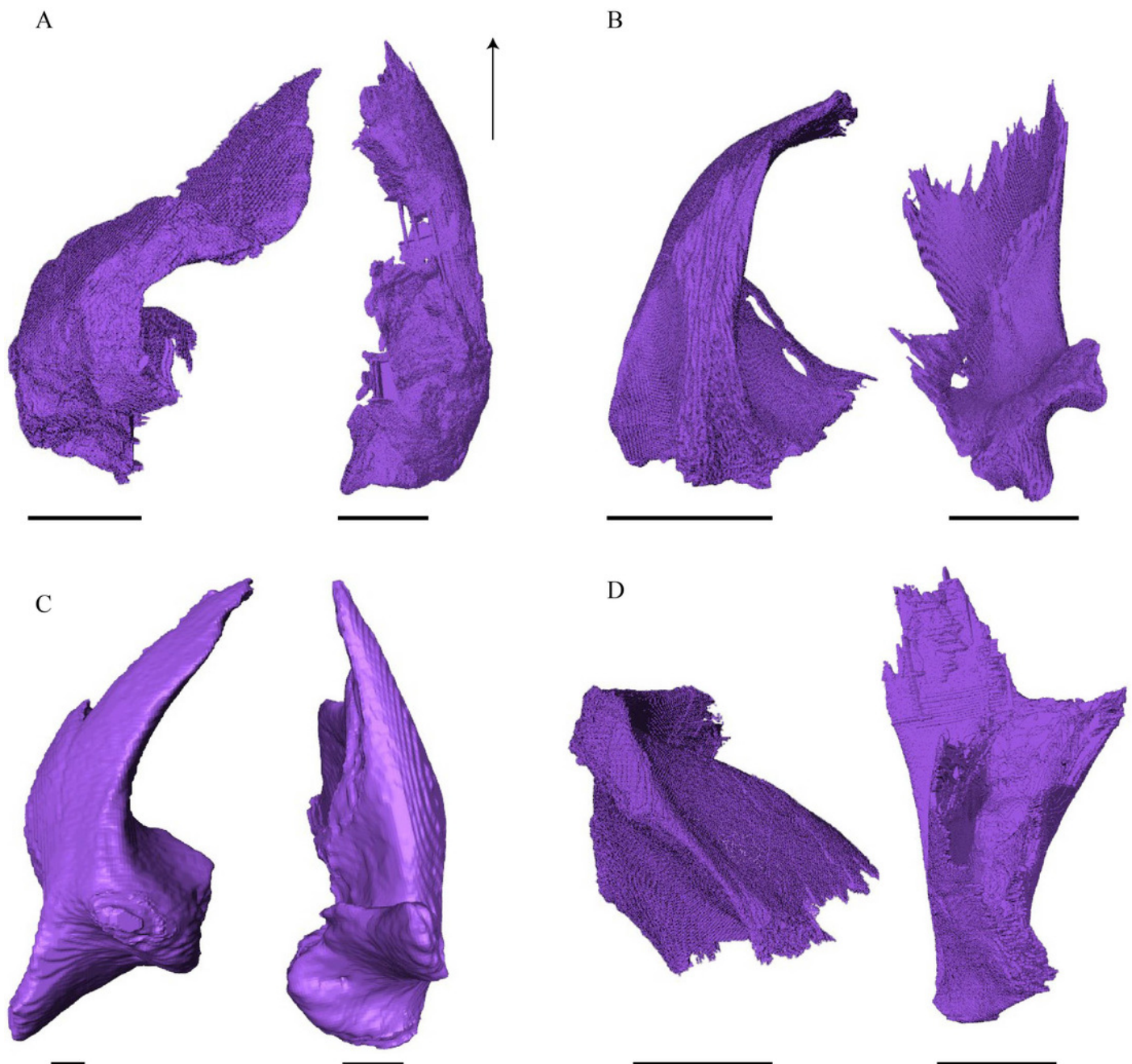


Figure 22

Lateral (left) and anterior (right) view of the premaxilla.

(A) *Desmatochelys lowii*; (B) *Eretmochelys imbricata*; (C) *Dermochelys coriacea*; and (D) *Chelydra serpentina*. The bar marks 10mm.

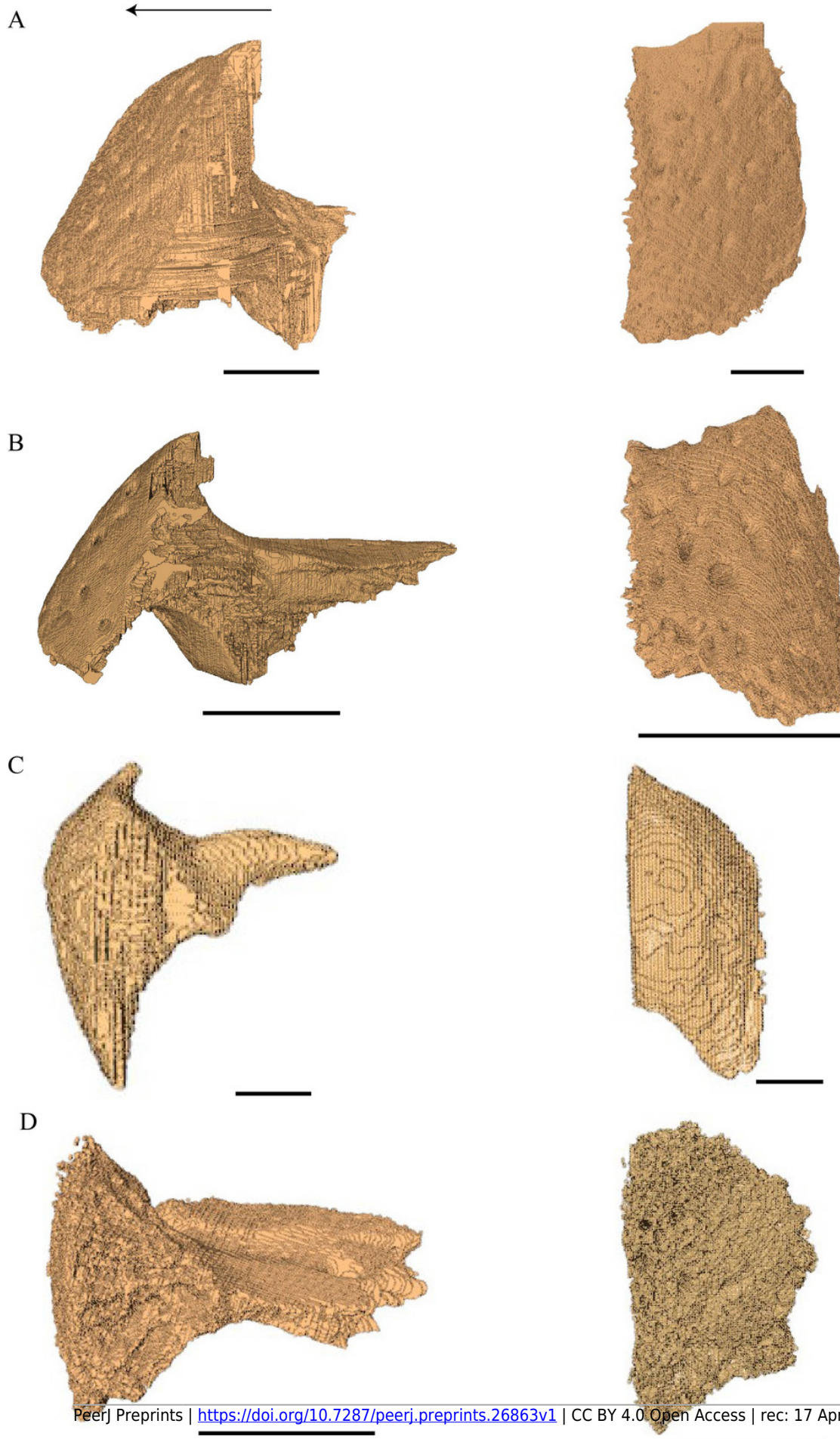


Figure 23

Premaxilla, maxilla, vomer, palatine, and jugal in dorsal view.

(A) *Desmatochelys lowii*; (B) *Eretmochelys imbricata*; (C) *Dermochelys coriacea*; and (D) *Chelydra serpentina*. The bar marks 10mm.

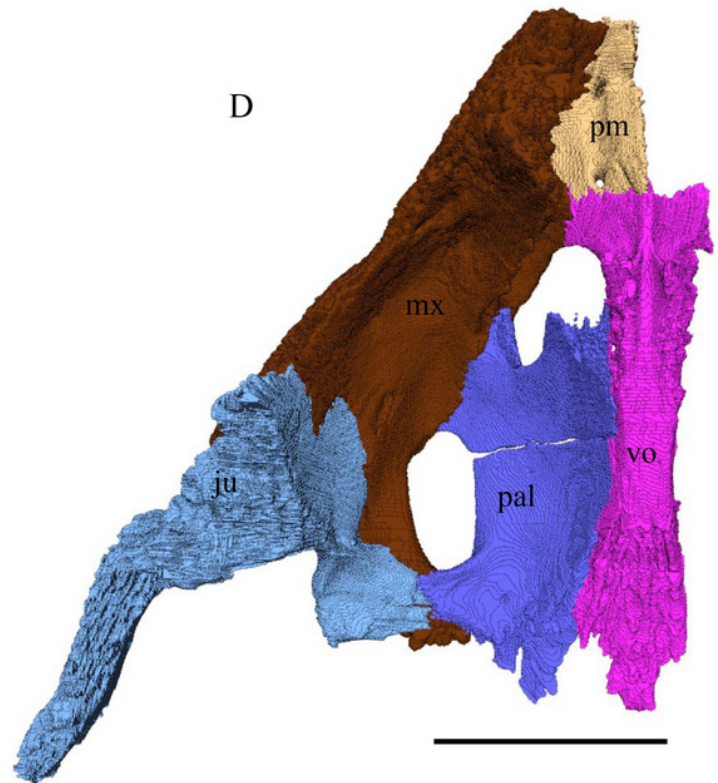
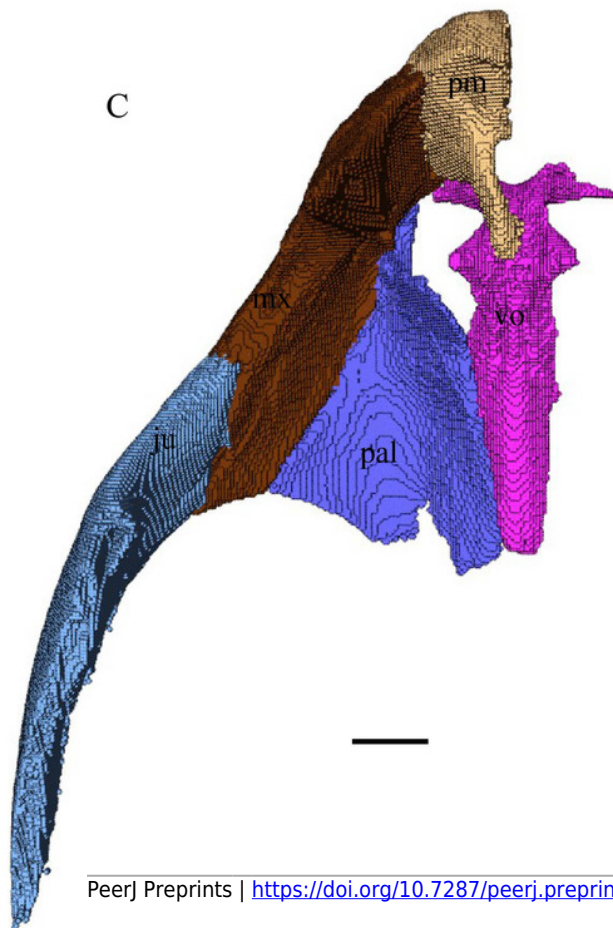
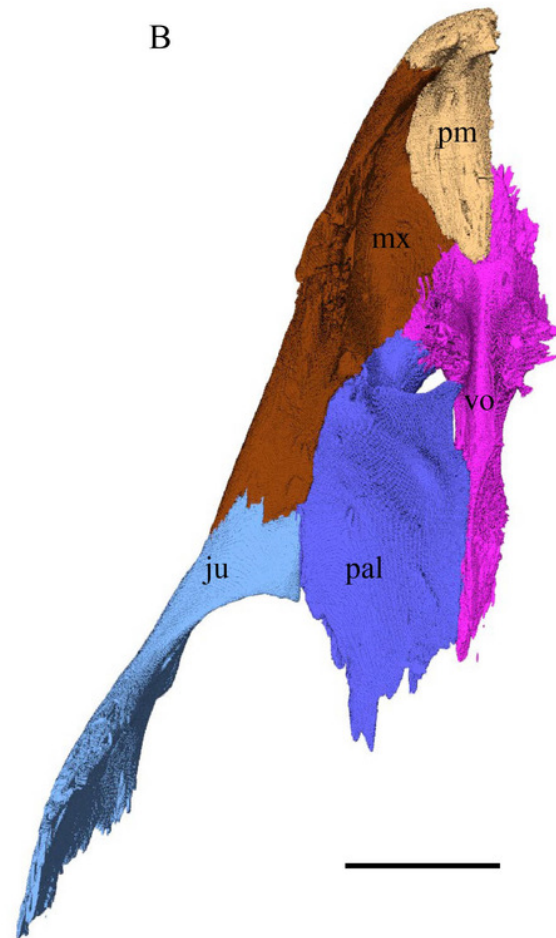
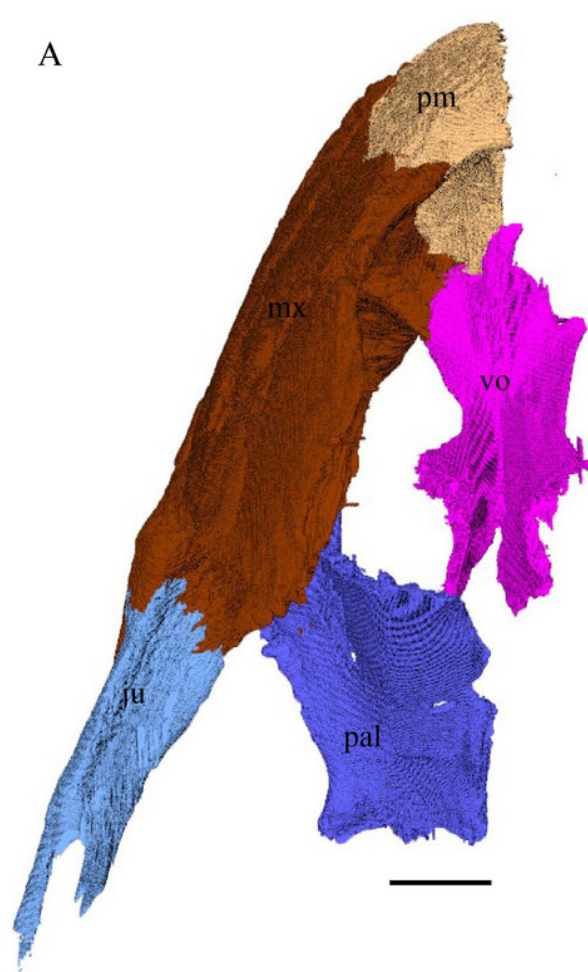


Figure 24

Vomer (left) and vomer with palatine (right) in lateral view.

(A) *Desmatochelys lowii*; (B) *Eretmochelys imbricata*; (C) *Dermochelys coriacea*; and (D) *Chelydra serpentina*. The bar marks 10mm.

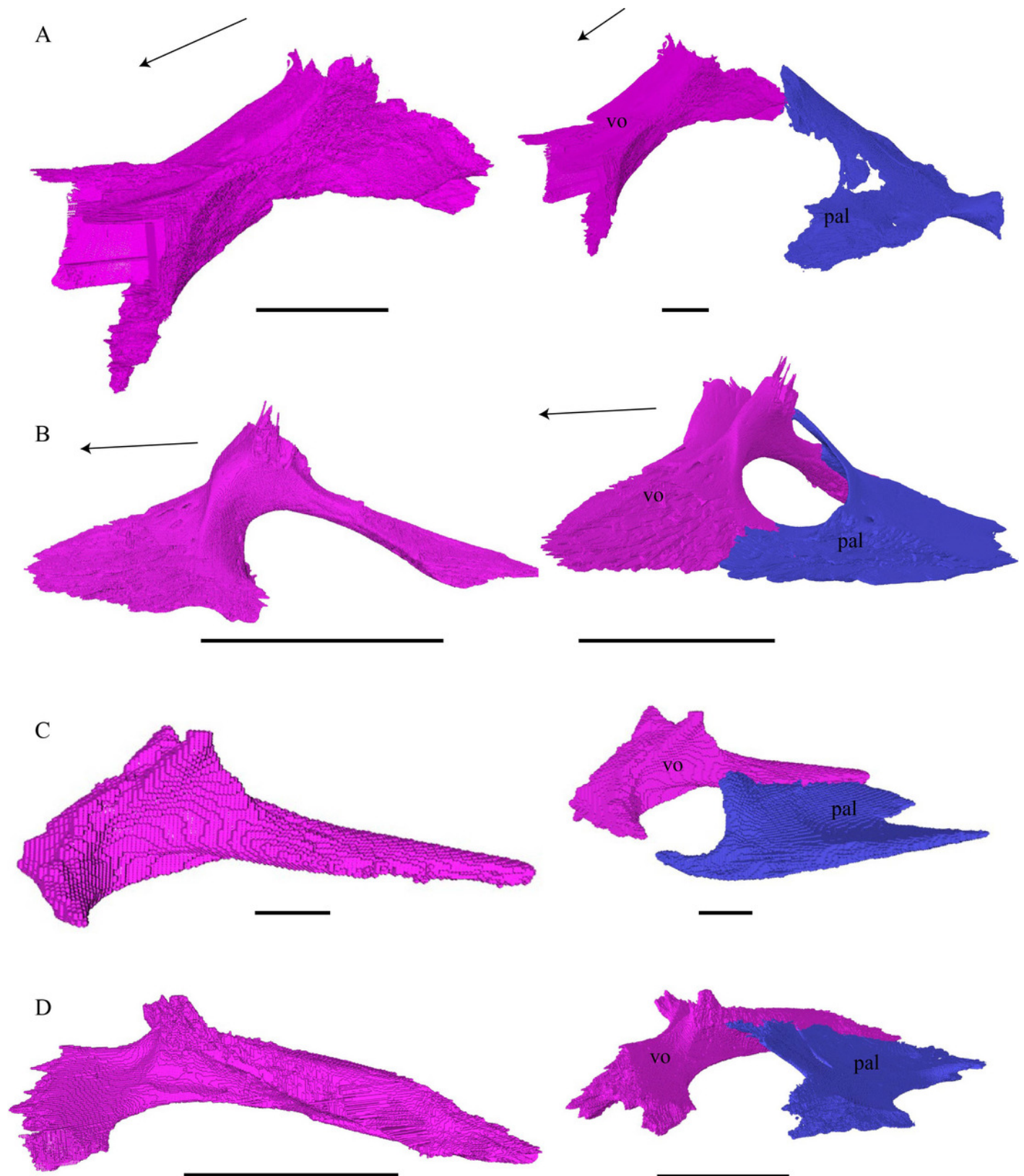


Figure 25

Palatine in dorsolateral view.

(A) *Desmatochelys lowii*; (B) *Eretmochelys imbricata*; (C) *Dermochelys coriacea*; and (D) *Chelydra serpentina*. The bar marks 10mm.

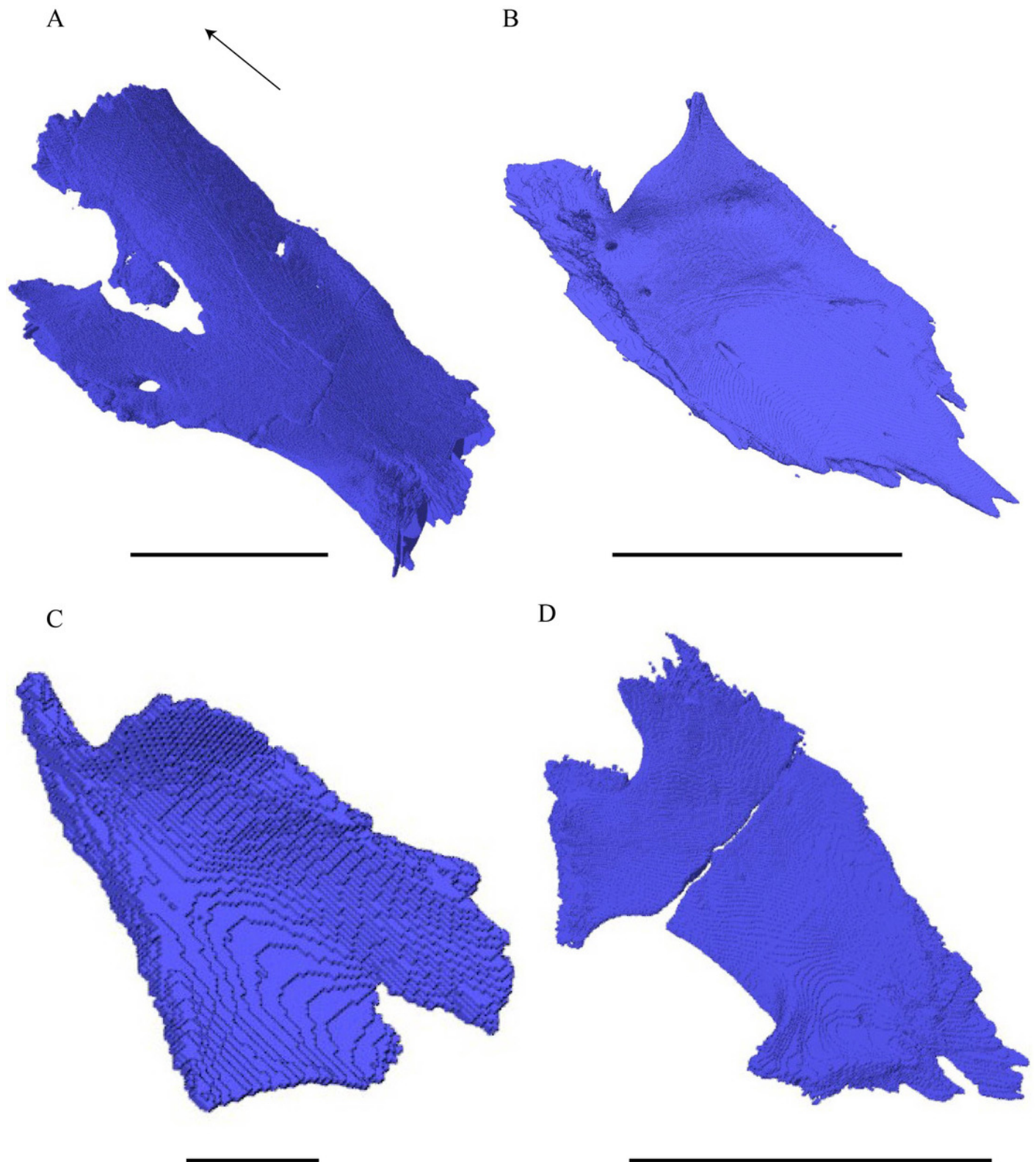


Figure 26

Pterygoid (A-D) and pterygoid, basisphenoid, and basioccipital (E-H) in dorsal view.

(A) *Desmatochelys lowii*; (B) *Eretmochelys imbricata*; (C) *Dermochelys coriacea*; and (D) *Chelydra serpentina*. The bar marks 10mm.

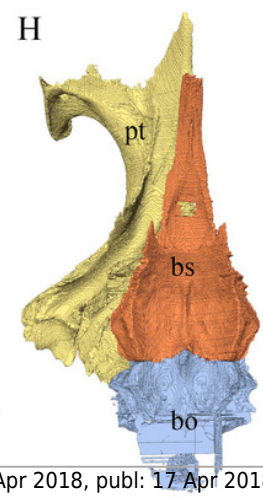
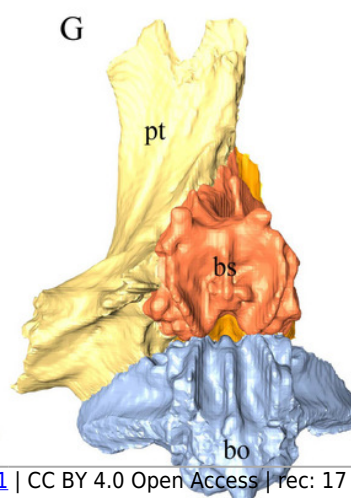
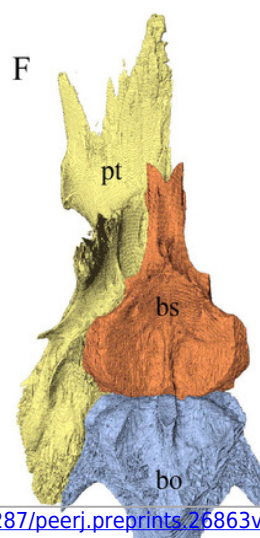
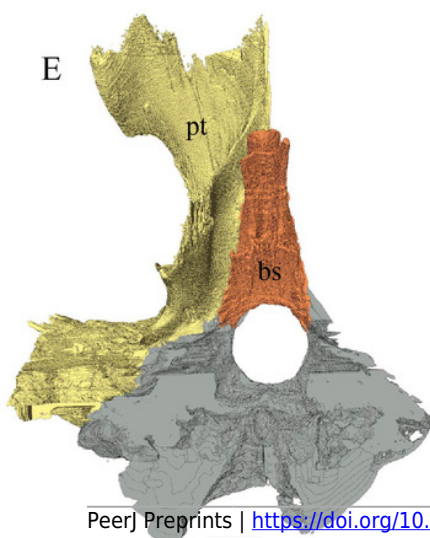
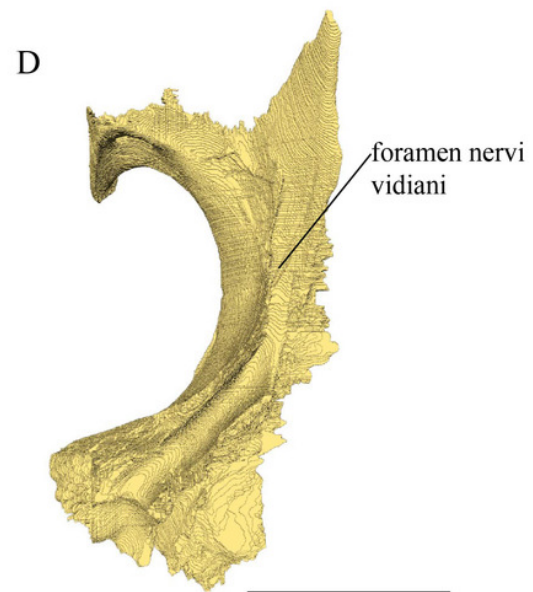
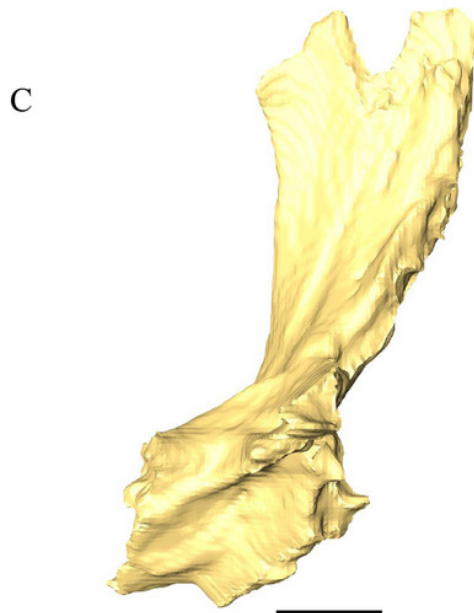
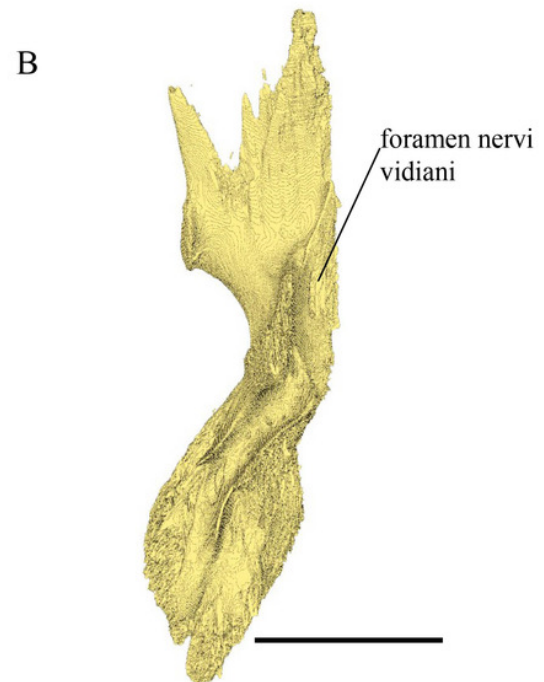
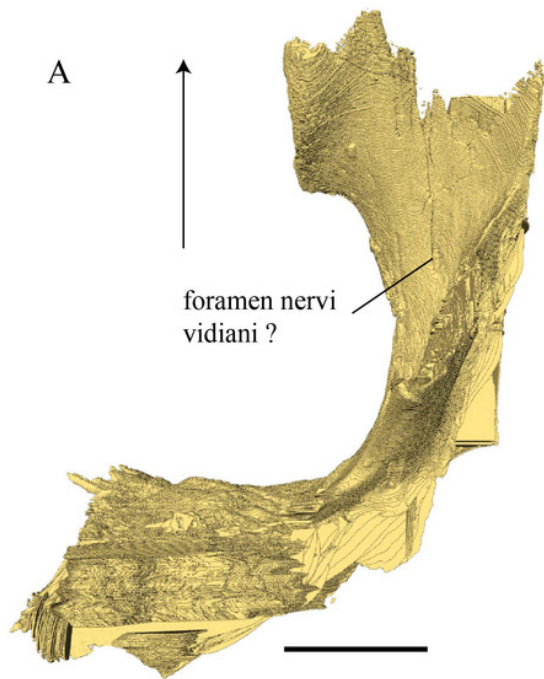


Figure 27

Epipterygoid, parietal, and pterygoid.

(A) *Desmatochelys lowii*; and (B) *Chelydra serpentina*. The bar marks 10mm.

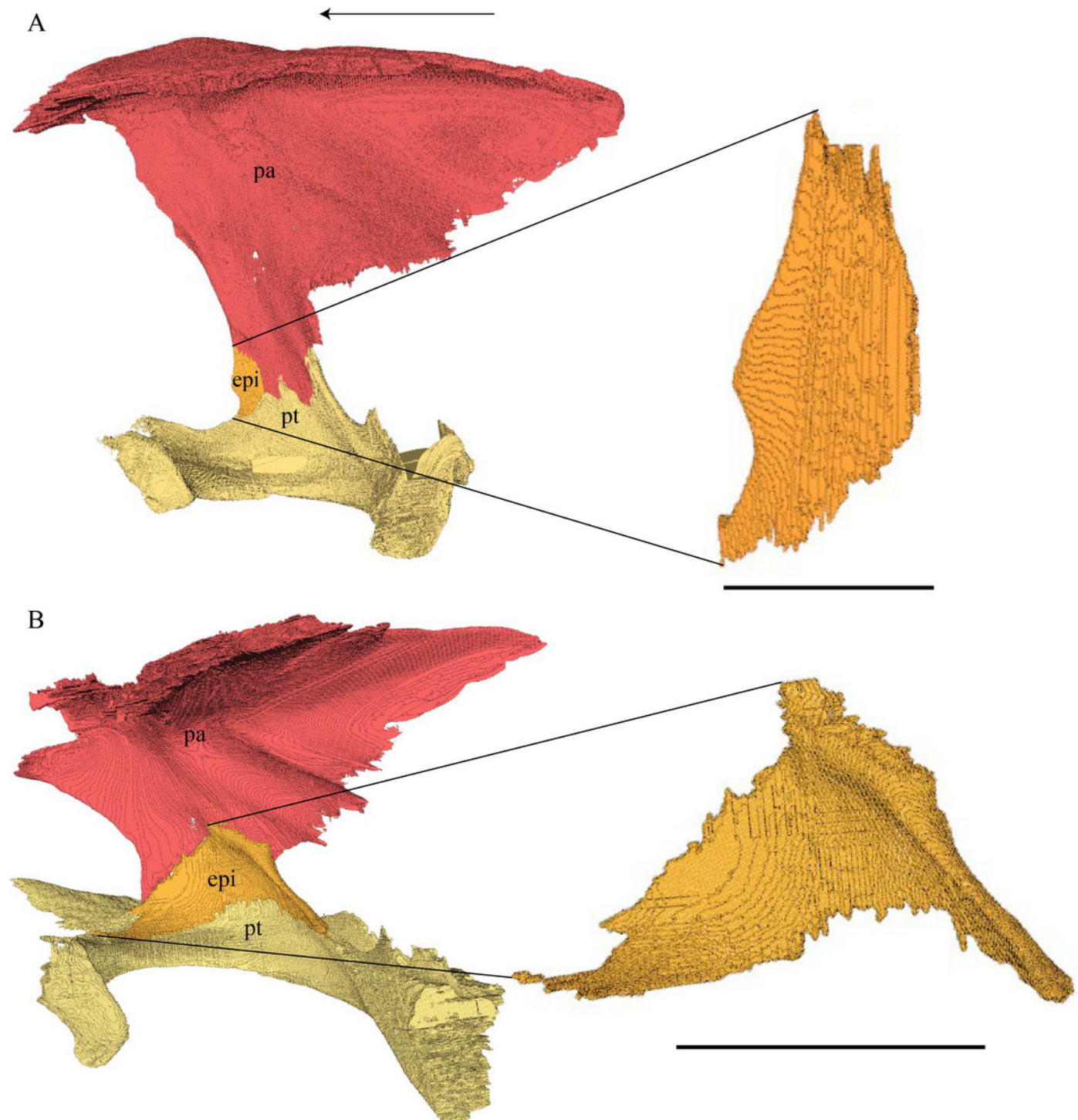


Figure 28

Basisphenoid and parasphenoid in anterolateral view.

(A) *Desmatochelys lowii*; (B) *Eretmochelys imbricata*; (C) *Dermochelys coriacea*; and (D) *Chelydra serpentina*. The bar marks 10mm.

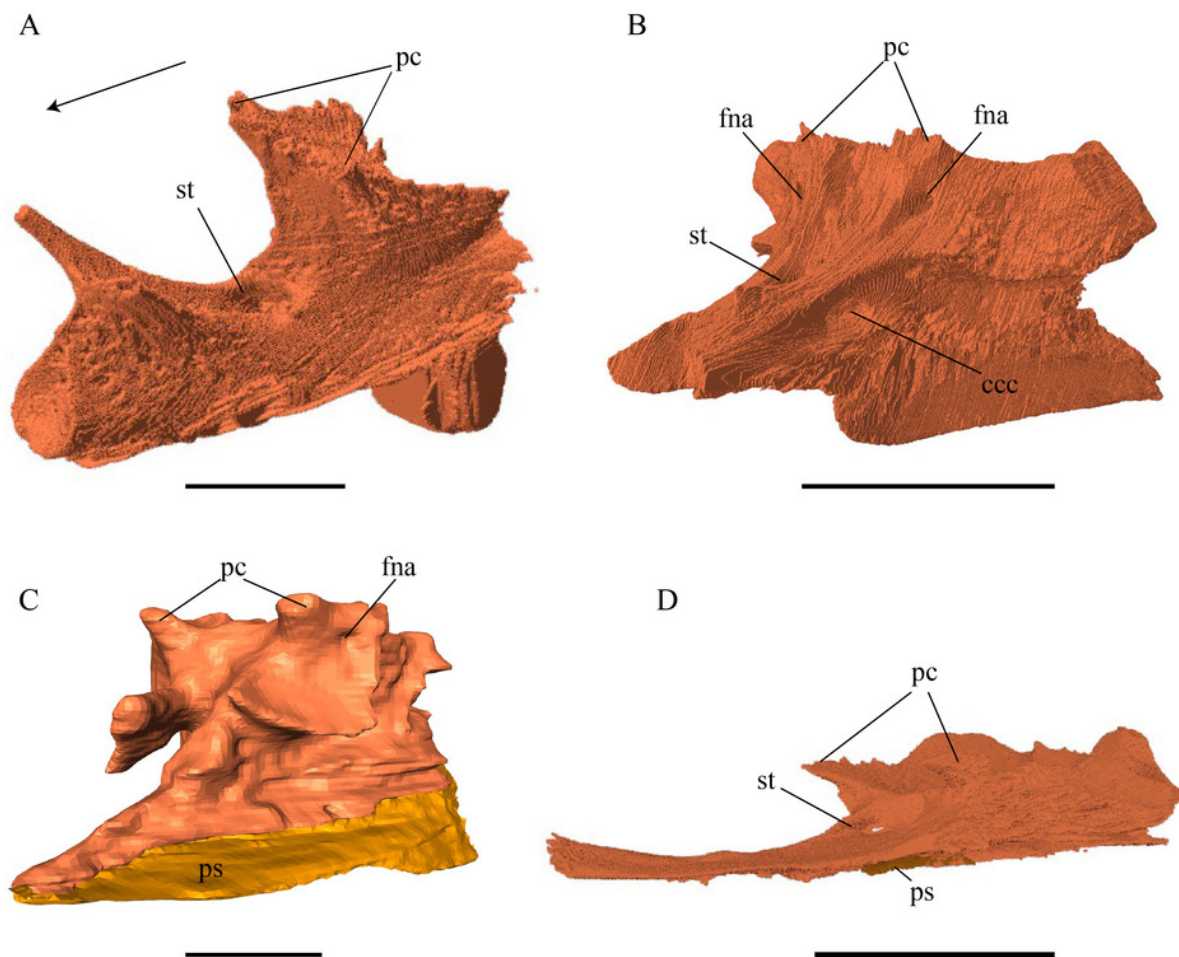


Figure 29

Parasphenoid of *Dermochelys coriacea*.

(A) lateral; (B) posterior; and (C) dorsal view. The bar marks 10mm.

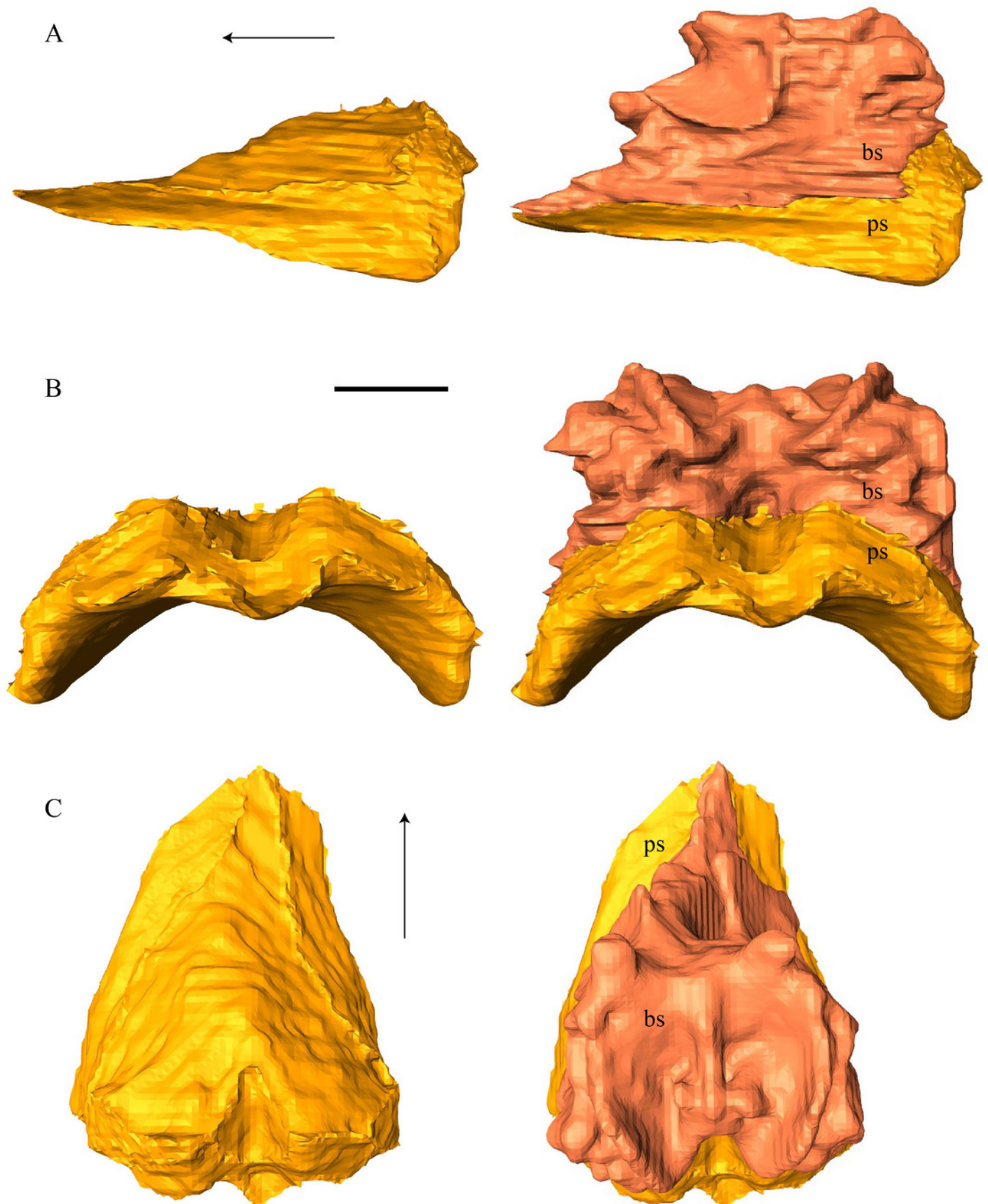


Figure 30

Parasphenoid of *Chelydra serpentina*.

(A) Ventral view on the pterygoid, basisphenoid and parasphenoid; (B) cross-section image highlighting the parasphenoid in red. The bar marks 10mm.

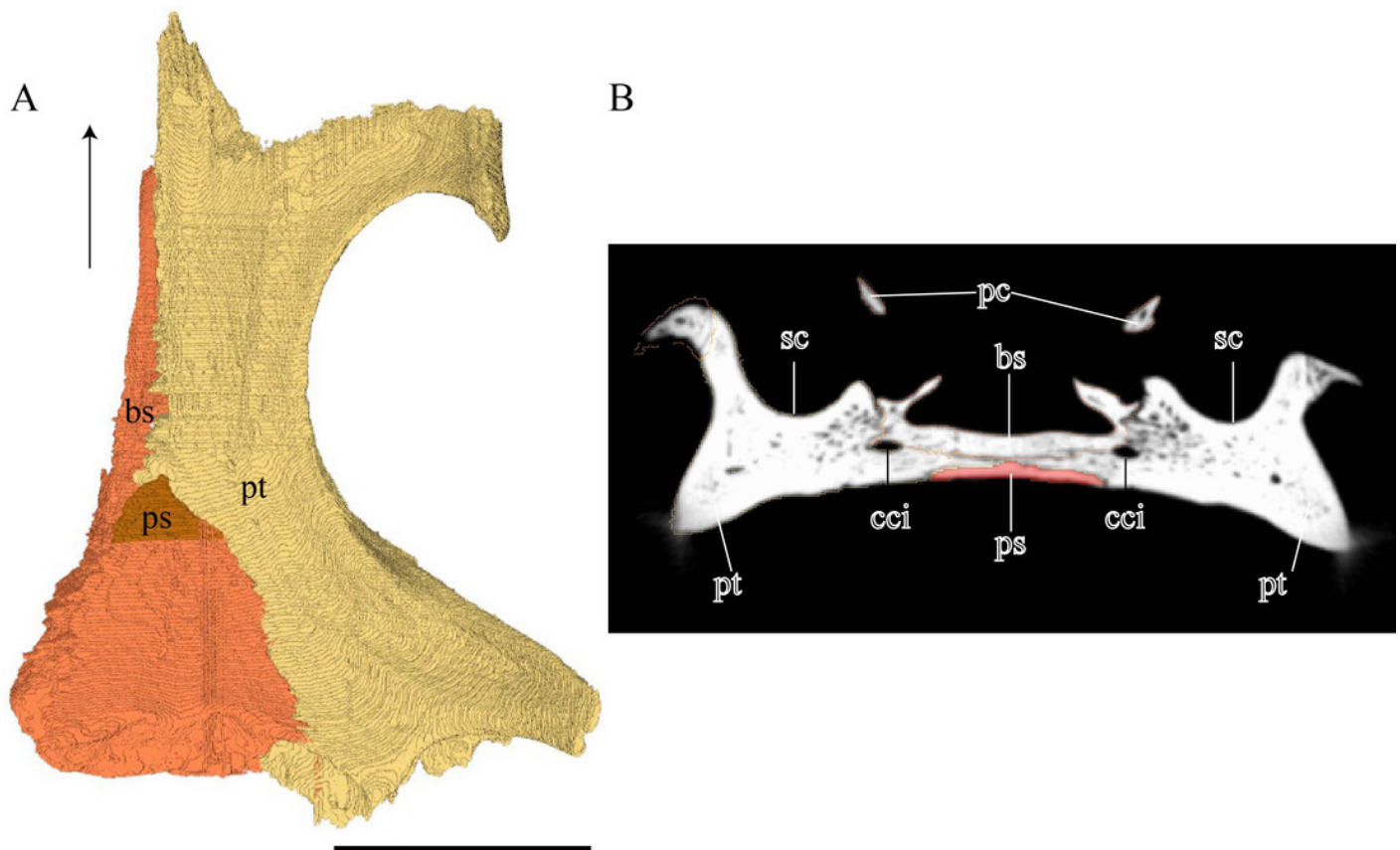


Figure 31

Medial (left) and lateral (right) view of the opisthotic and prootic.

(A) *Desmatochelys lowii*; (B) *Eretmochelys imbricata*; (C) *Dermochelys coriacea*; and (D) *Chelydra serpentina*. The bar marks 10mm.

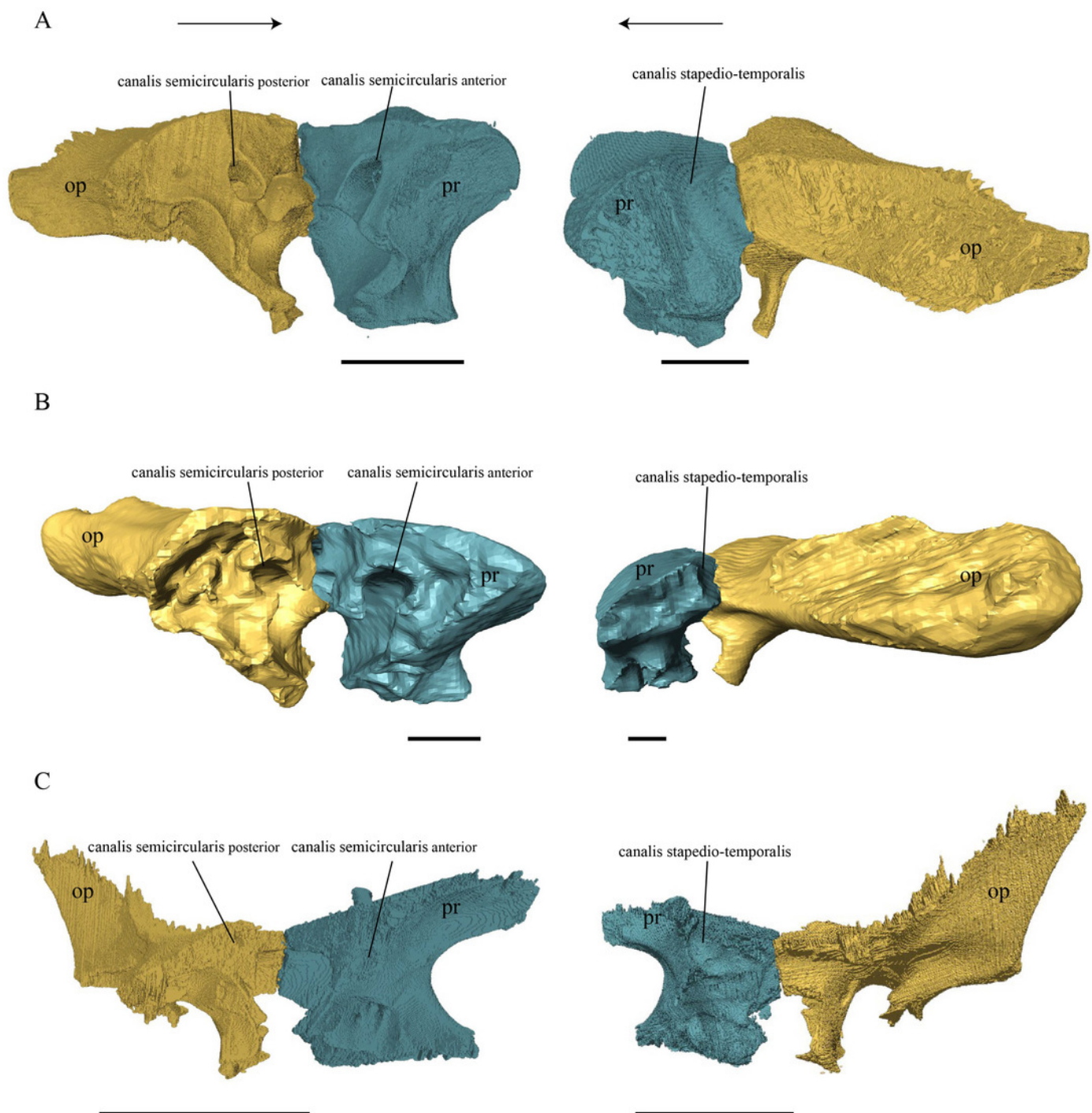


Figure 32

Quadrate, prootic, opisthotic, and supraoccipital in dorsal view.

(A) *Desmatochelys lowii*; (B) *Eretmochelys imbricata*; (C) *Dermochelys coriacea*; and (D) *Chelydra serpentina*. The bar marks 10mm.

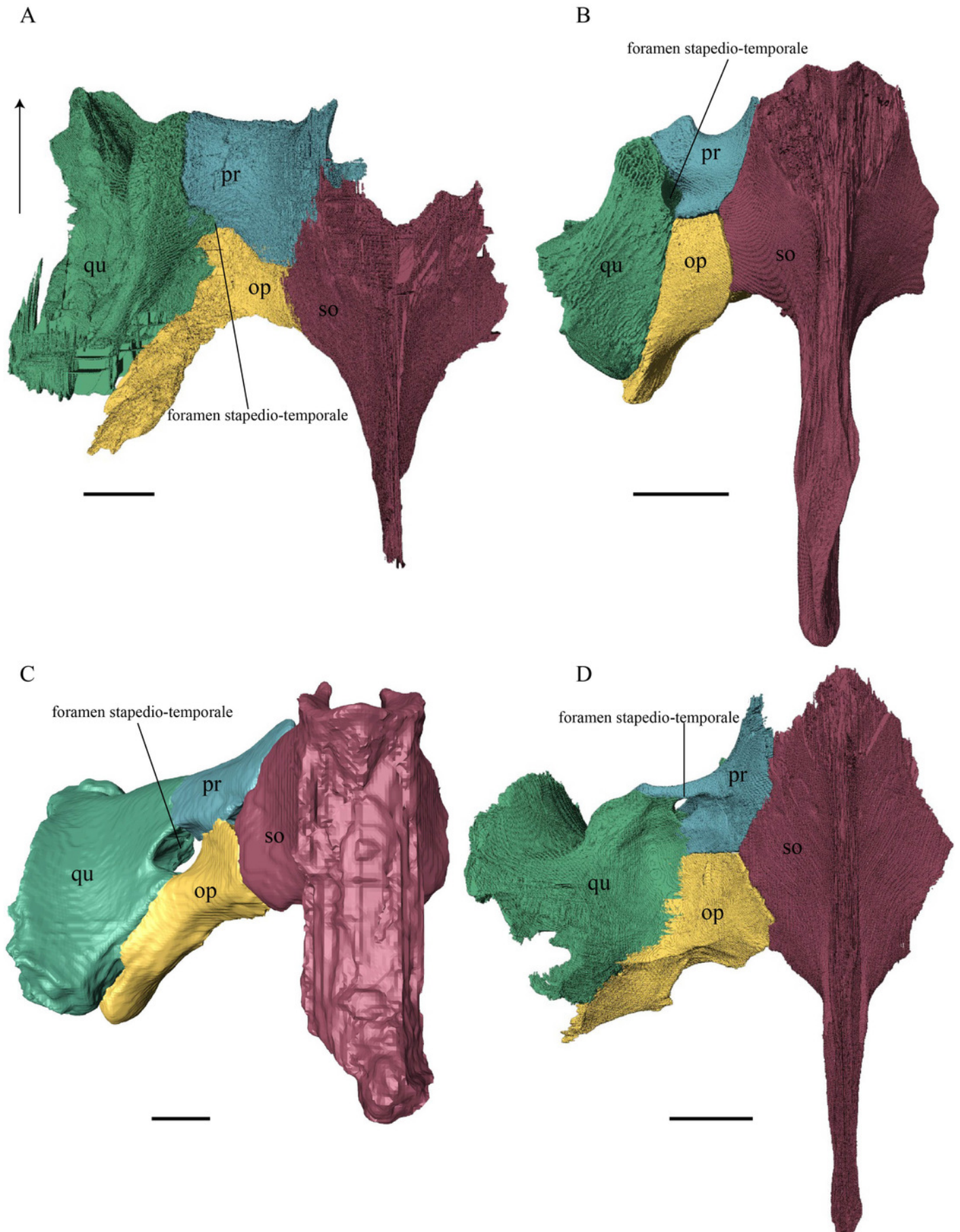
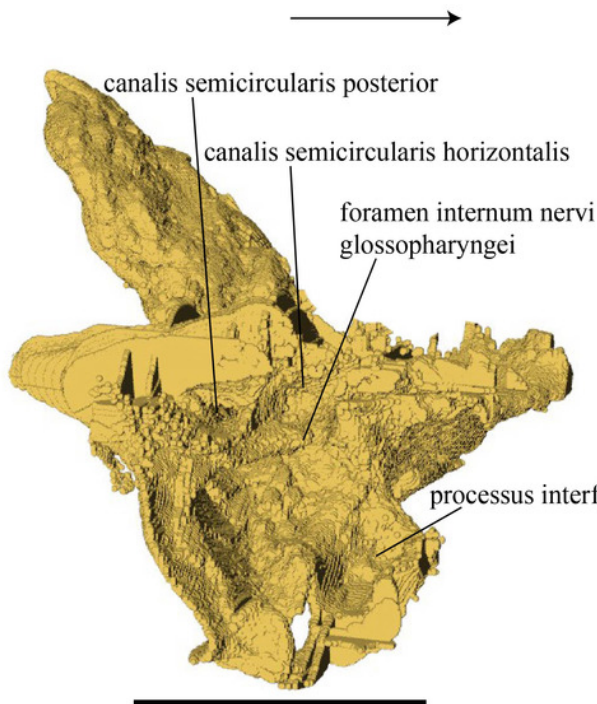


Figure 33

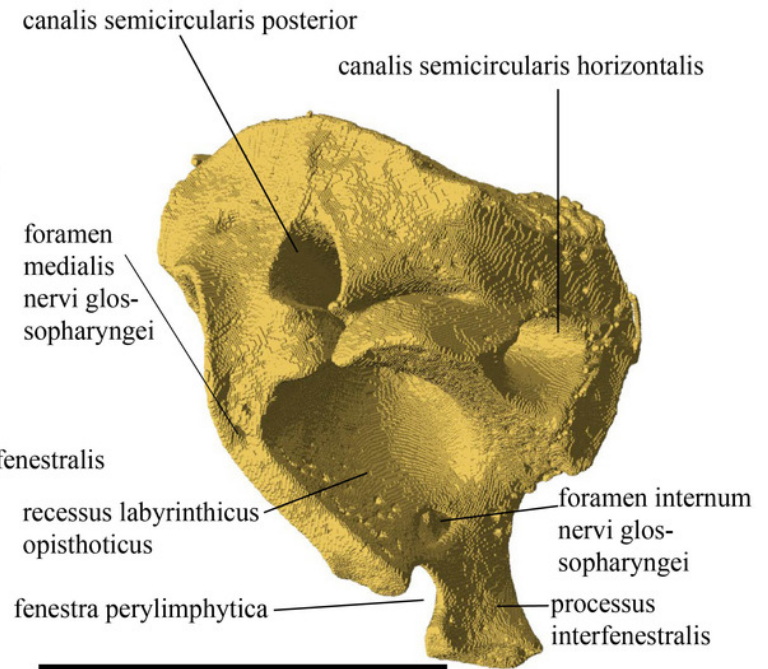
Opisthotic in medial view.

(A) *Desmatochelys lowii*; (B) *Eretmochelys imbricata*; (C) *Dermochelys coriacea*; and (D) *Chelydra serpentina*. The bar marks 10mm.

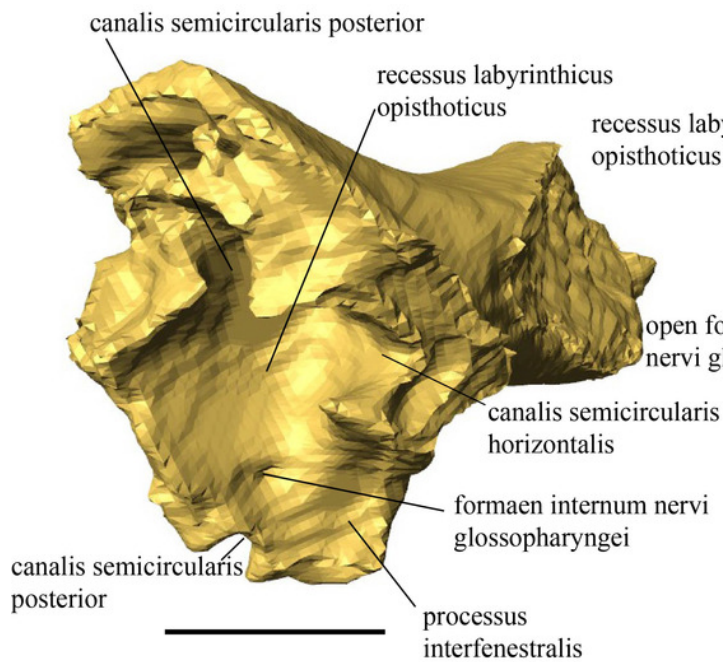
A



B



C



D

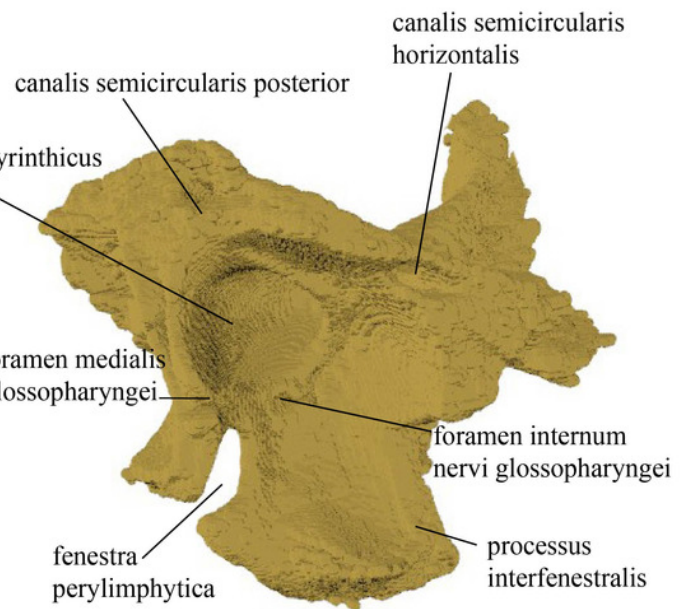


Figure 34

Medial (left) and lateral (right) view of the quadrate.

(A) *Desmatochelys lowii*; (B) *Eretmochelys imbricata*; (C) *Dermochelys coriacea*; and (D) *Chelydra serpentina*. The bar marks 10mm.

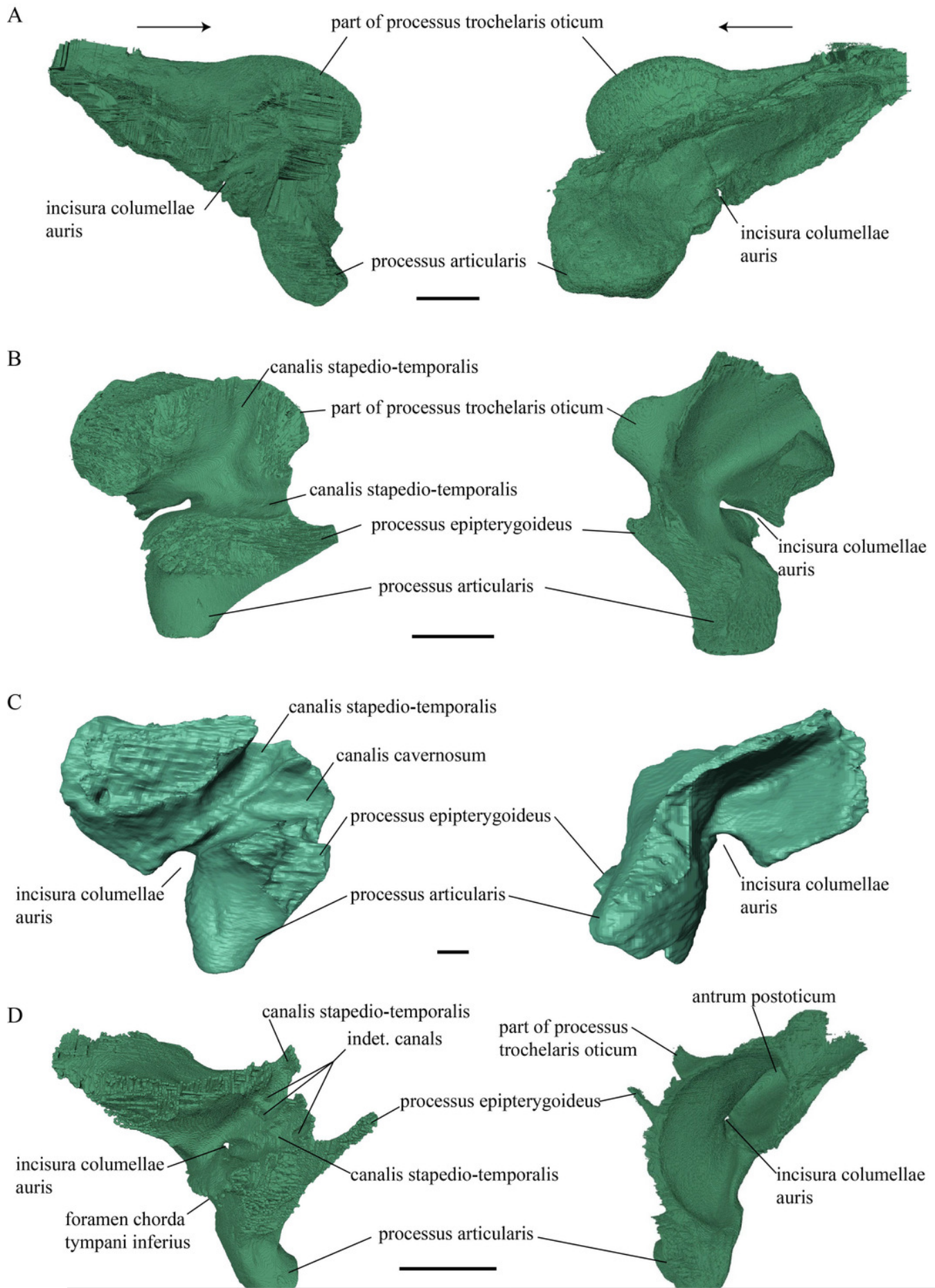


Figure 35

Posterior view of KUVP 1200, type specimen of *Desmatochelys lowii*, highlighting the remains of the columella auris visible through the fenestra postotica.

The bar marks 10mm.

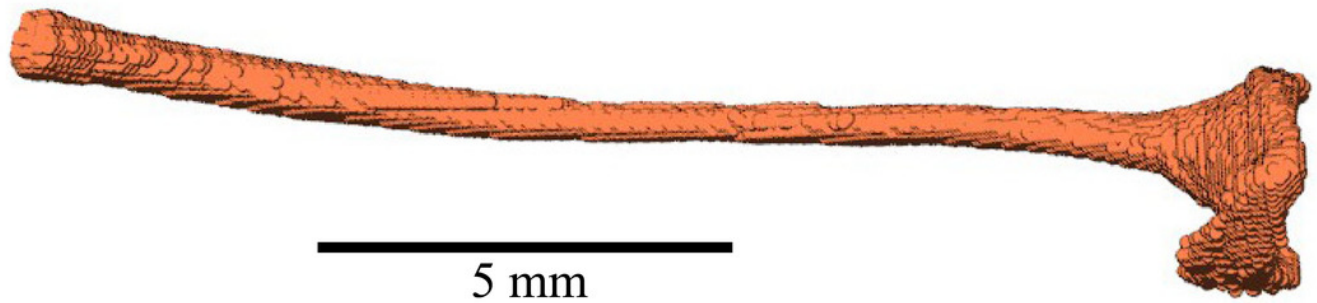


Figure 36

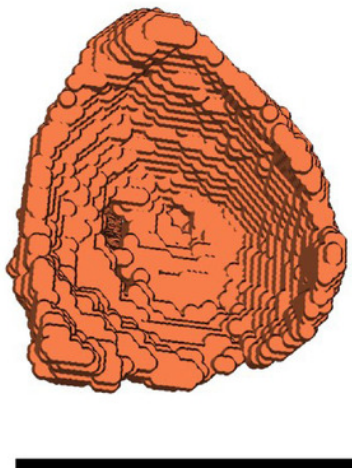
Columella of *Chelydra serpentina*.

(A) "side view"; (B) proximal view; (C) cross-section through the basis columellae in CT scan marking two foramina. The bar marks 10mm, unless noted otherwise.

A



B



C

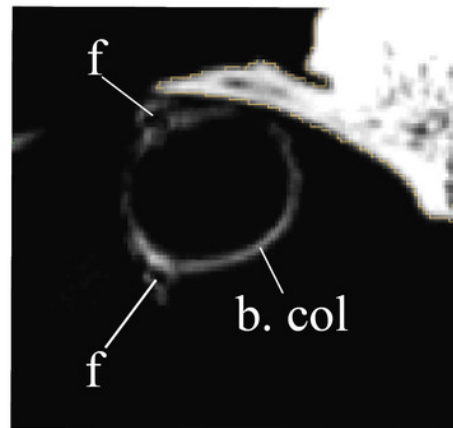


Figure 37

Basioccipital in anterolateral view.

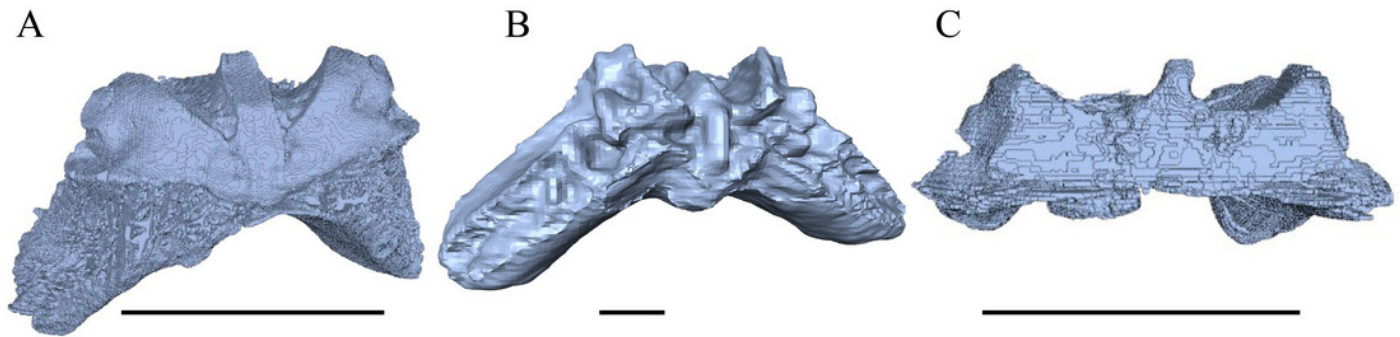


Figure 38

Exoccipital in medial view.

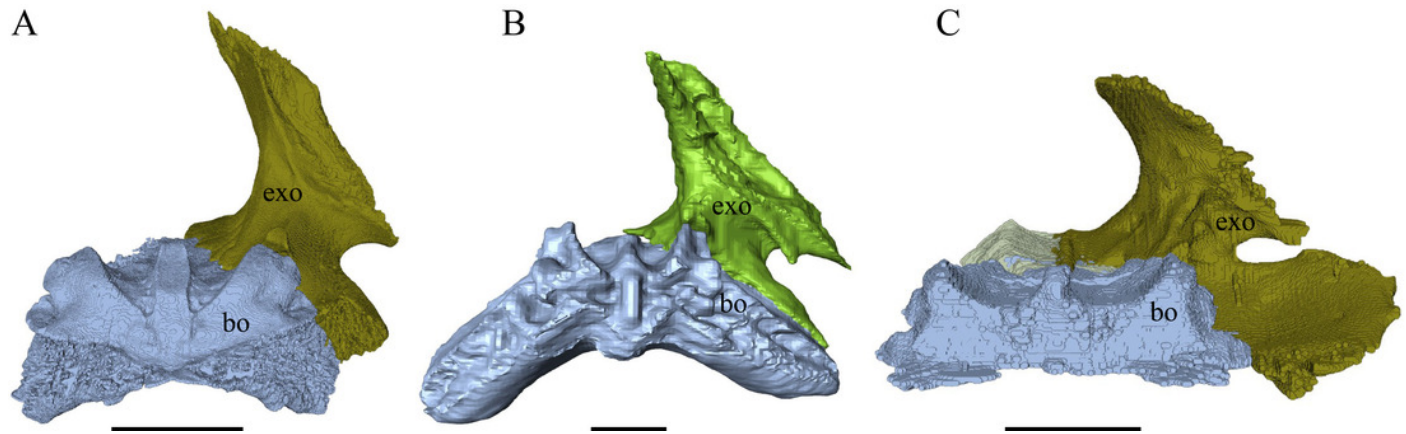


Figure 39

Exoccipital, opisthotic, prootic, basisphenoid, and an unidentifiable posterior portion of the basicranium of *Desmatochelys lowii* in medial view.

The bar marks 10 mm.

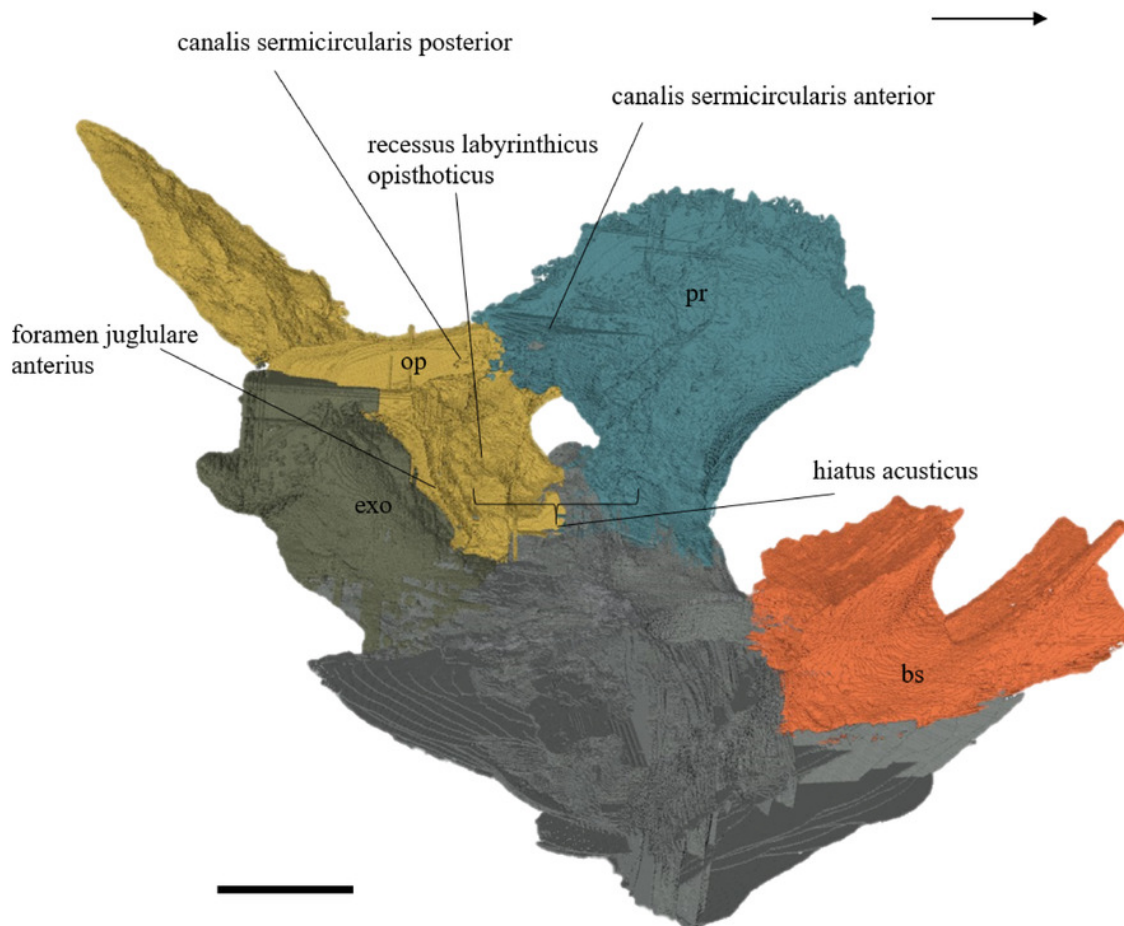


Figure 40

Exoccipital, opisthotic, prootic, and basisphenoid of *Eretmochelys imbricata* in medial view.

The bar marks 10 mm.

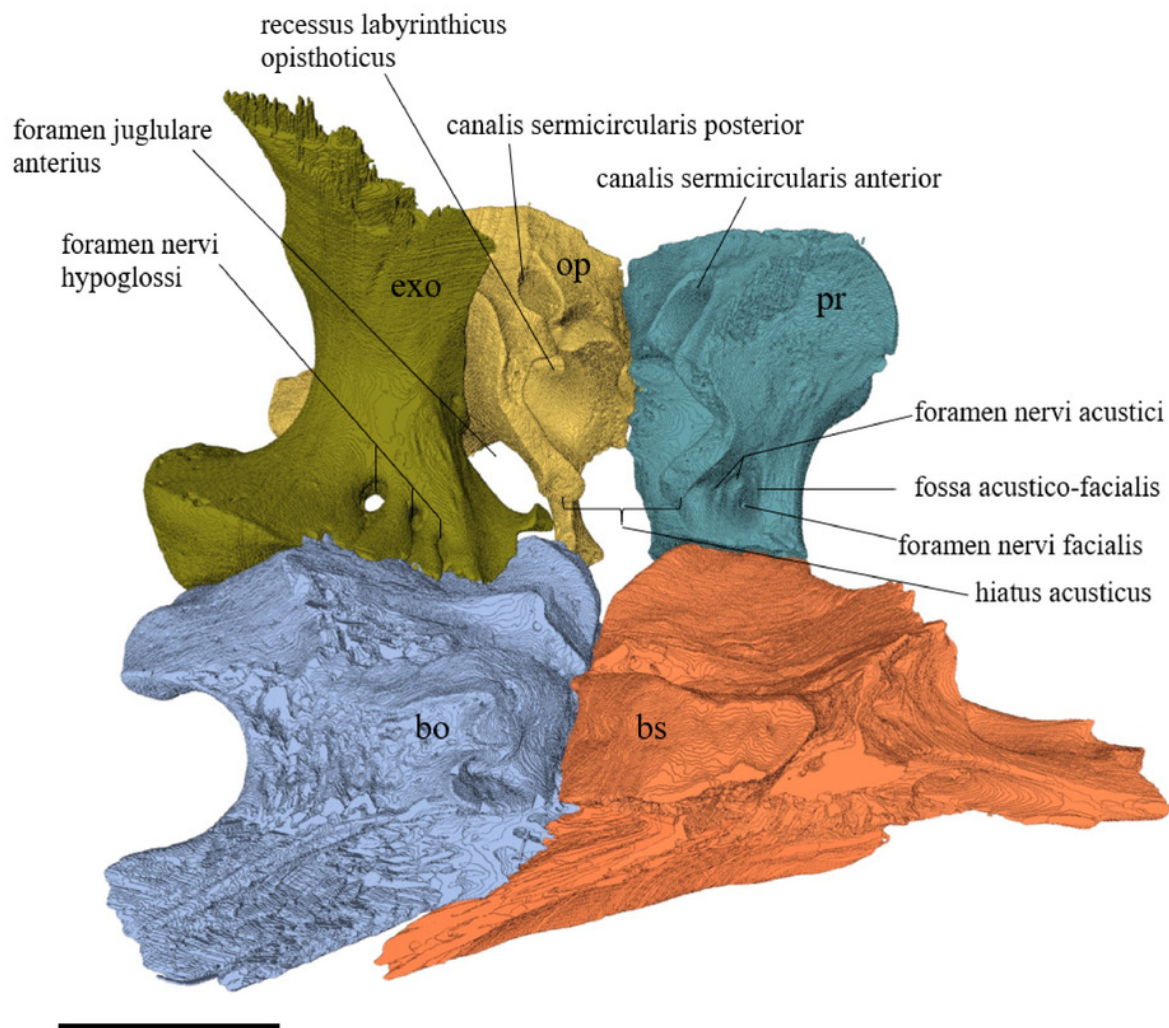


Figure 41

Exoccipital, opisthotic, prootic, basisphenoid, and parasphenoid of *Dermochelys coriacea* in medial view.

The bar marks 10 mm.

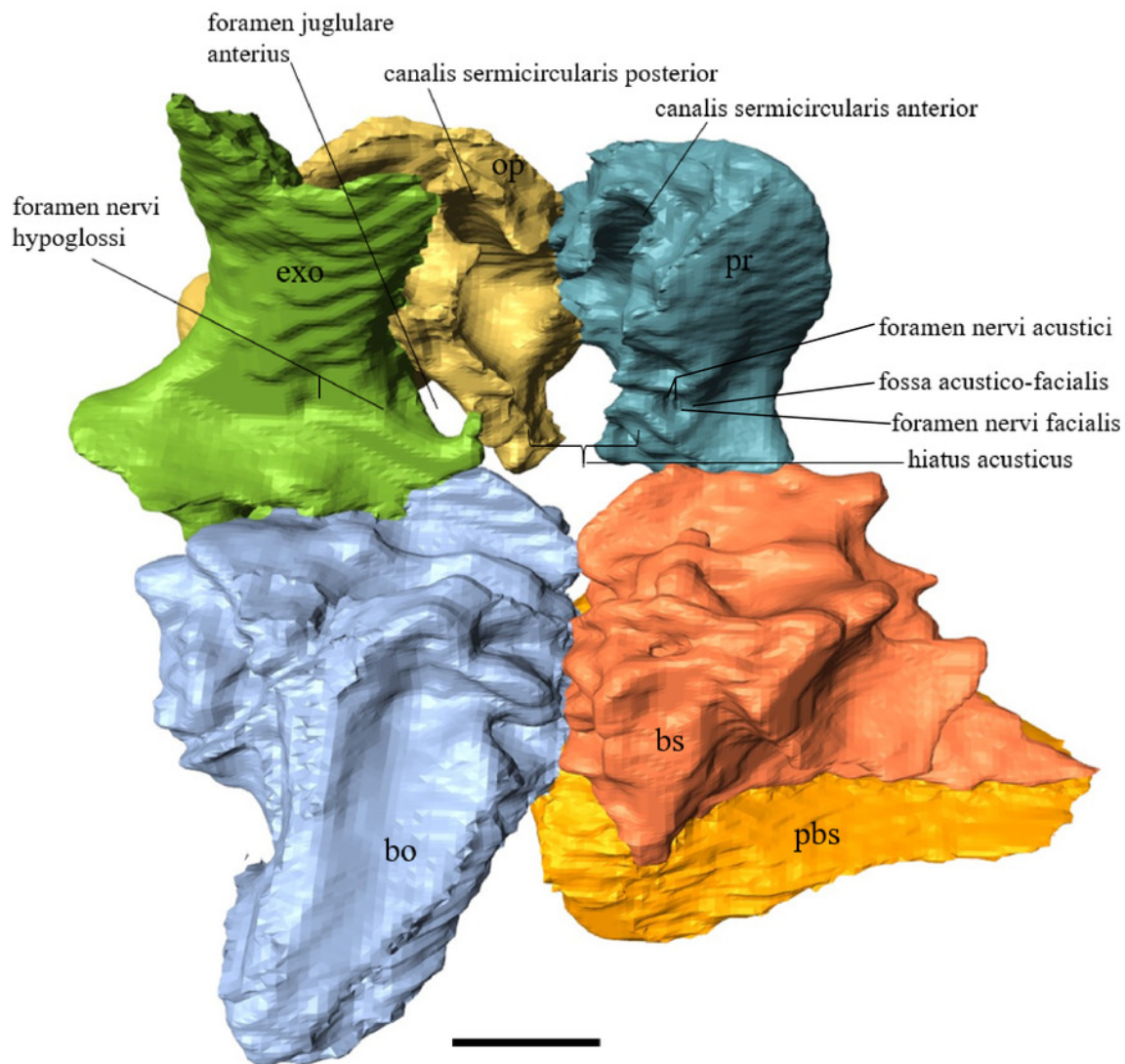


Figure 42

Exoccipital, opisthotic, prootic, basisphenoid, and parasphenoid of *Chelydra serpentina* in medial view.

The bar marks 10 mm.

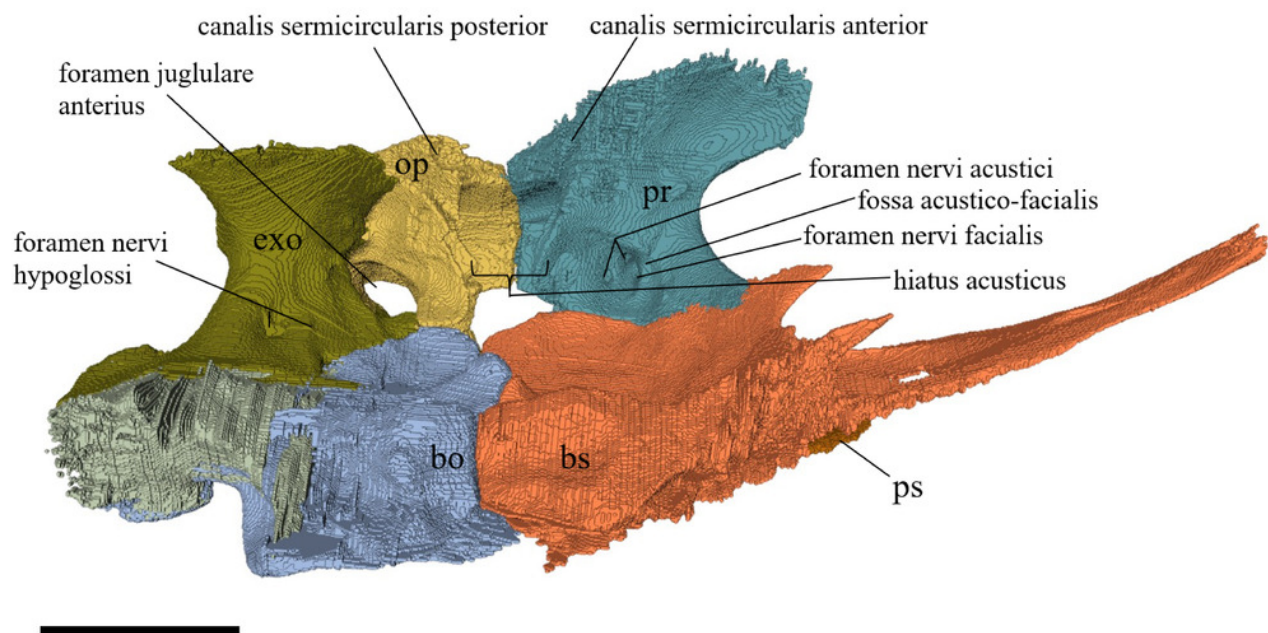


Figure 43

Basioccipital and exoccipital in anterior view.

(A) *Eretmochelys imbricata*; (B) *Dermochelys coriacea*; and (C) *Chelydra serpentina*. The bar marks 10mm.

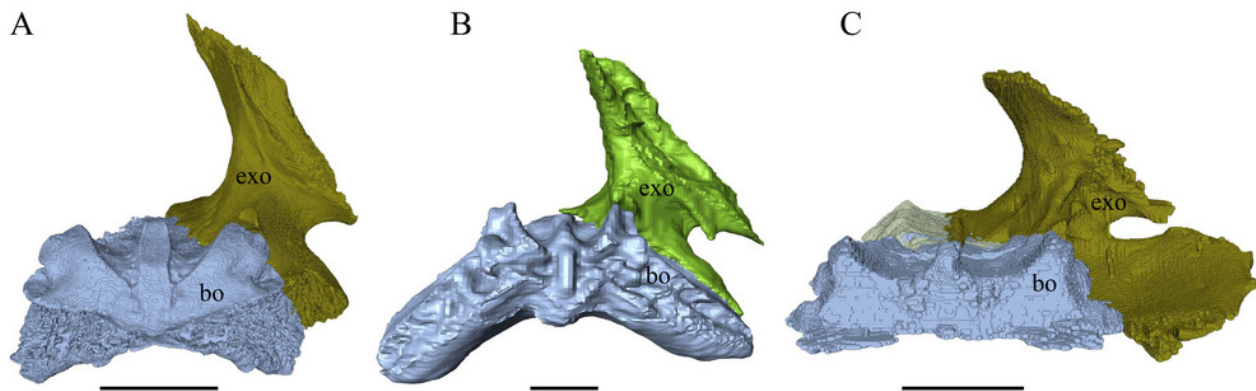


Figure 44

Time calibrated, strict consensus cladogram resulting from the phylogenetic analysis.

The full tree is provided in Supplementary Material (Appendix S7, Figs S7.1-7.3).

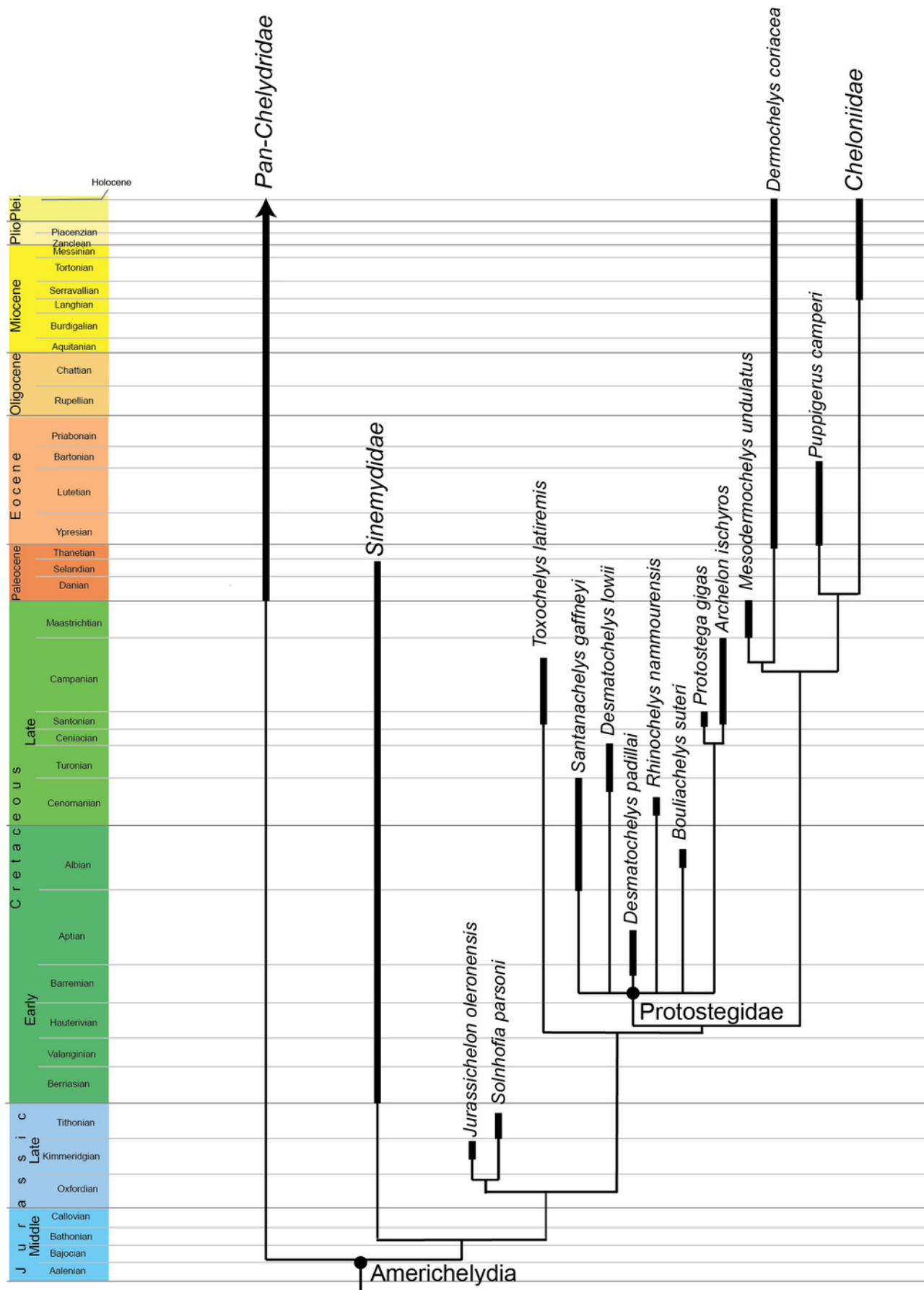


Figure 45

Comparison historical illustrations of KUV 1200, holotype of *Desmatochelys lowii*, in dorsal view.

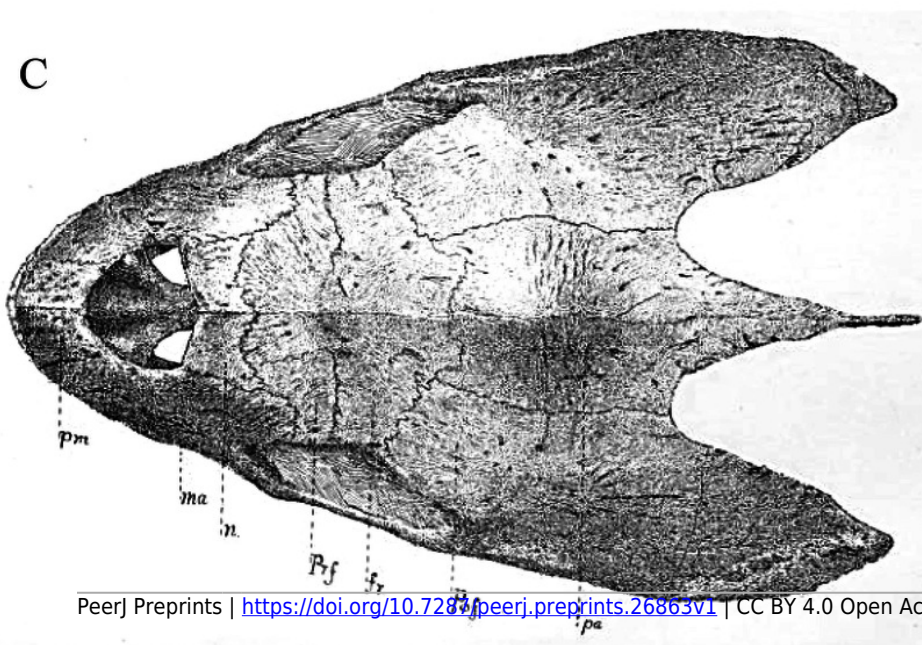
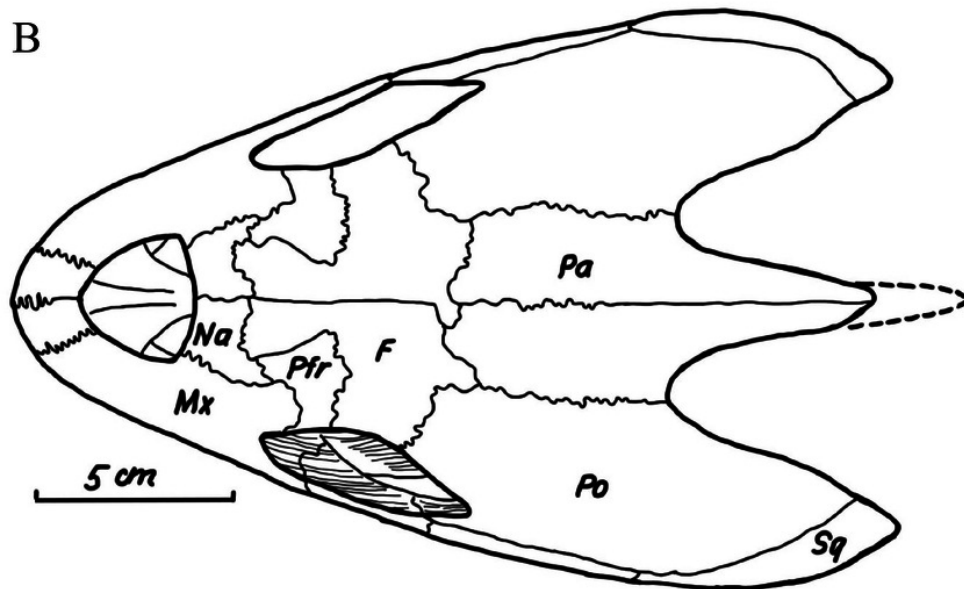
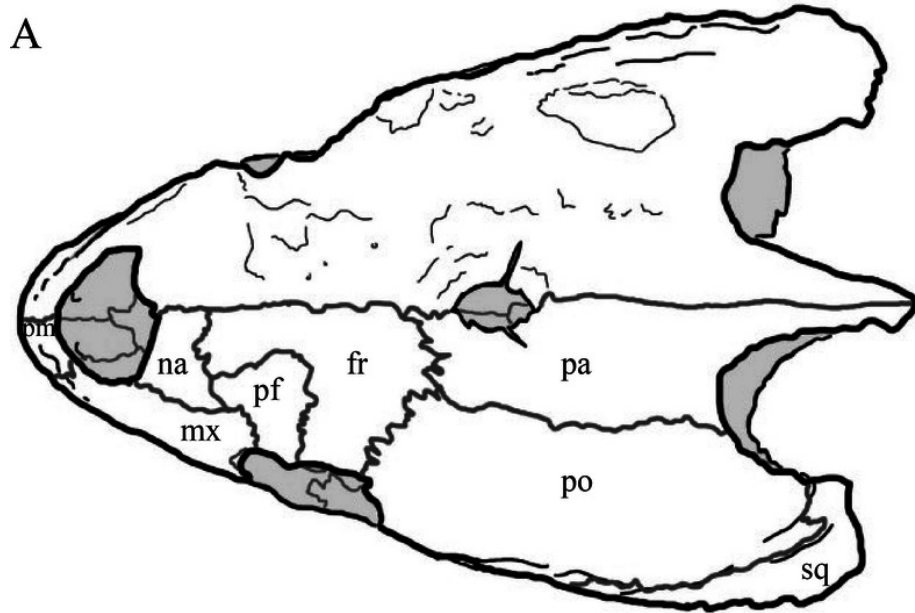


Figure 46

Illustration of KUVP 1200, holotype of *Desmatochelys lowii*, in lateral view, redrawn from Zangerl & Slogan (1960).

Note that crushed basicranium and broken tip of the supraoccipital are marked, but no damage indicated to the dorsal bulge.

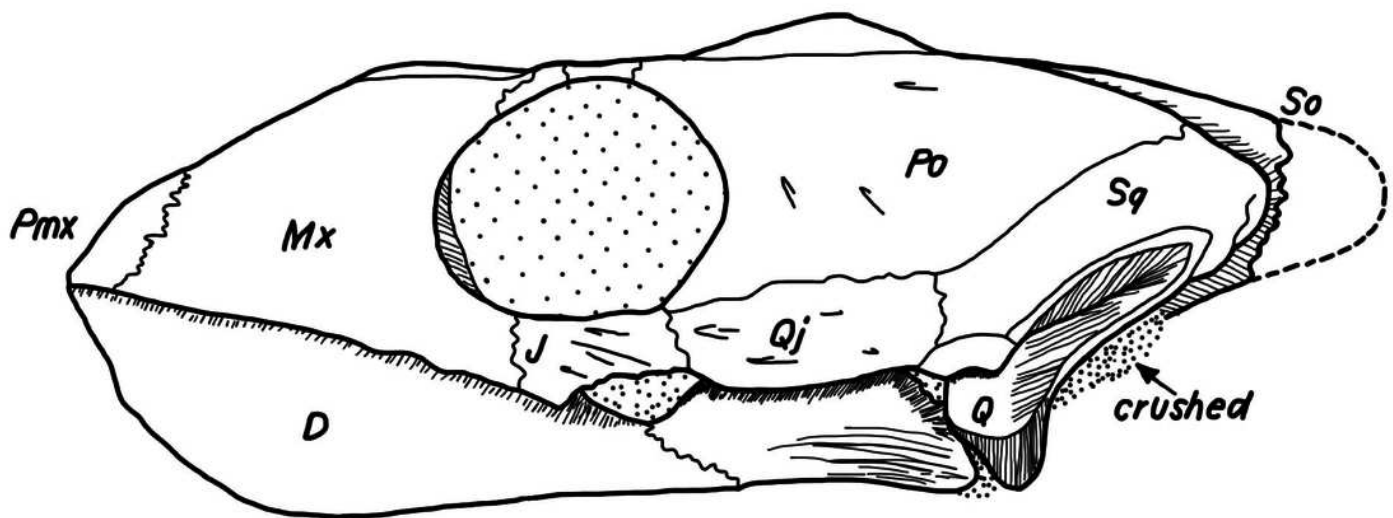


Figure 47

Pictures of the “pink spot” of *Dermochelys coriacea*.

(A) ‘pink spot’ marked with a red arrow on a living *Dermochelys coriacea* (picture by Silvia Bonizzoni, Dolphin Biology and Conservation); (B) skull of a *Dermochelys coriacea* with light shining from the interior through the thinnest part of the parietal’s dorsal plate.

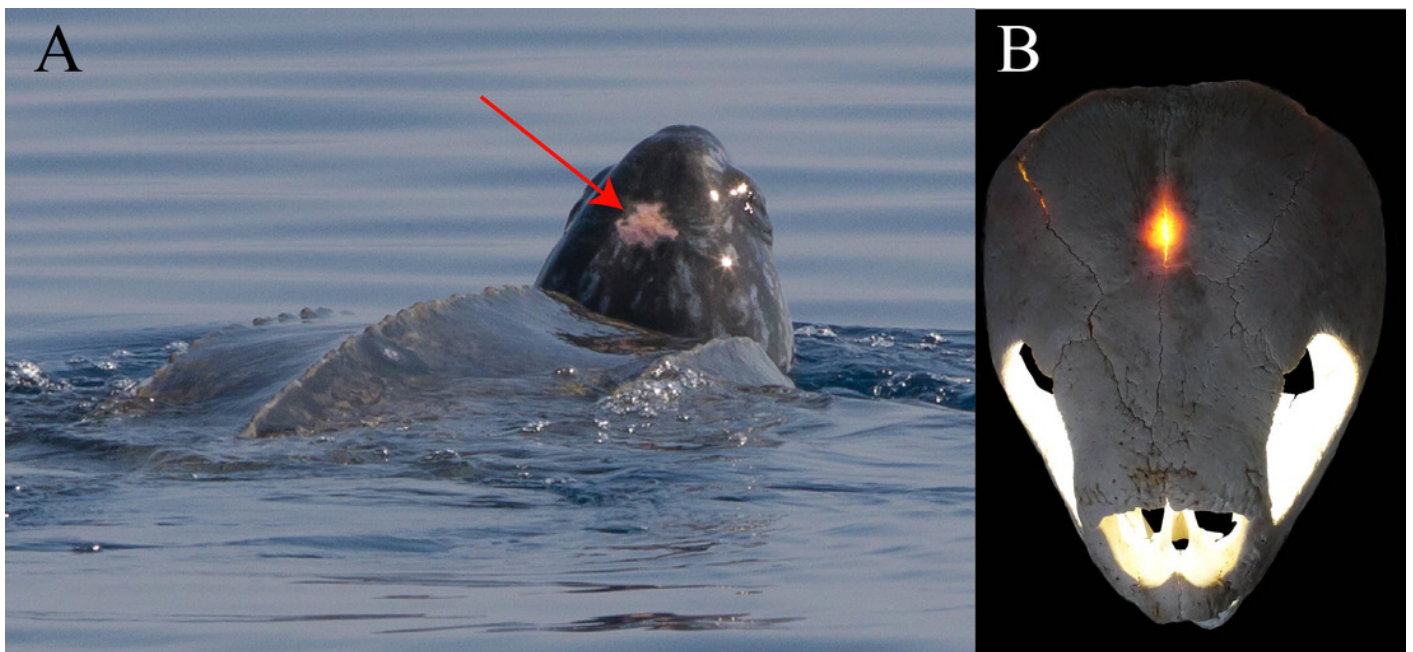


Figure 48

Cross-section image of the basisphenoid of specimen *Eretmochelys imbricata*.

The yellow line marks the outline of the basisphenoid.

**Note: Auto Gamma Correction was used for the image. This only affects the reviewing manuscript. See original source image if needed for review.*

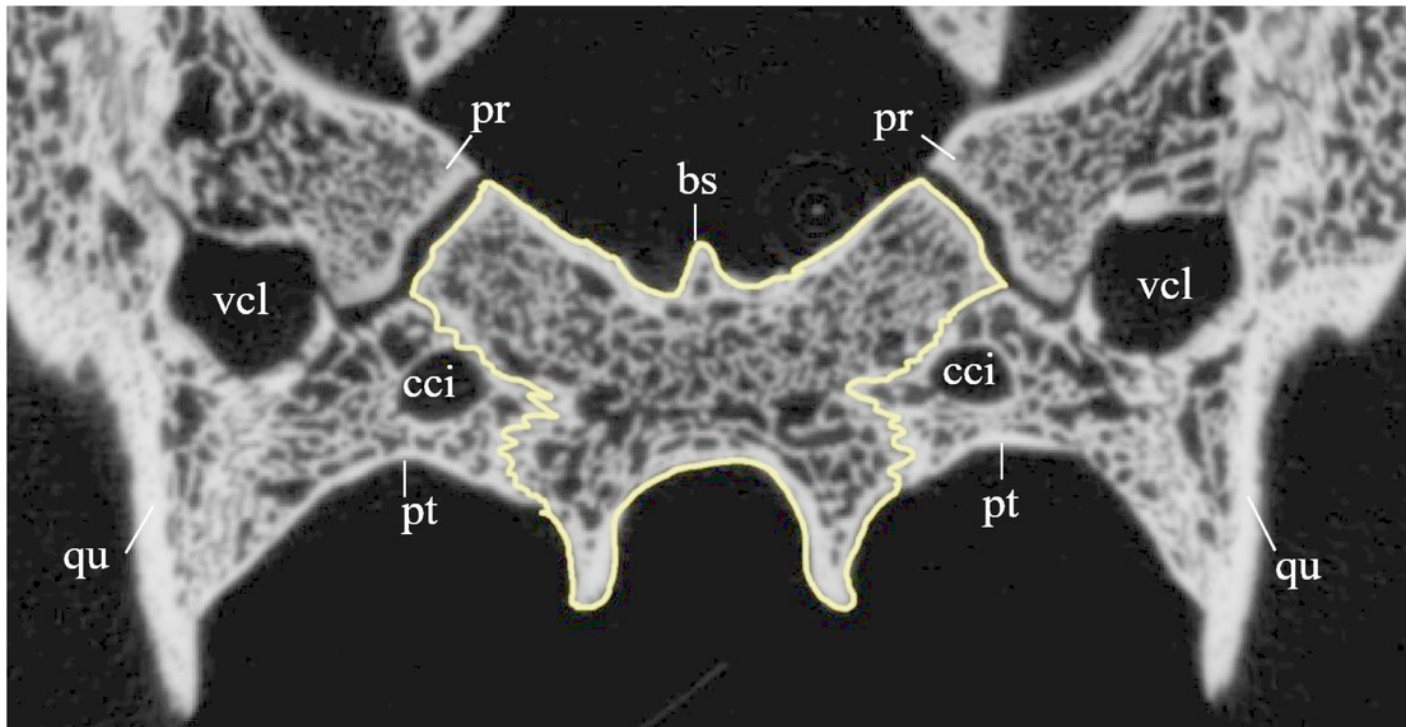
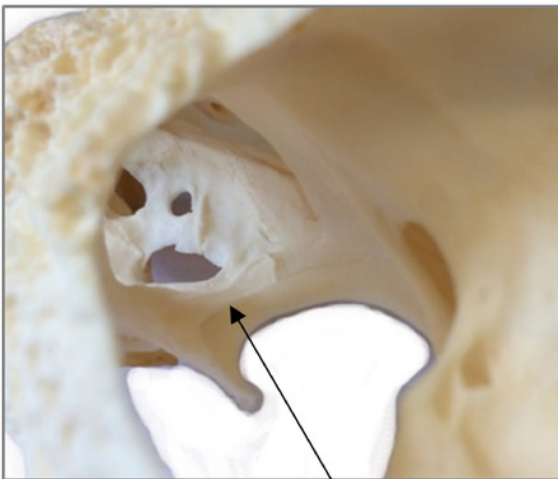


Figure 49

Photography (A) and illustration (B) of the sulcus pro-epipterygoidei.

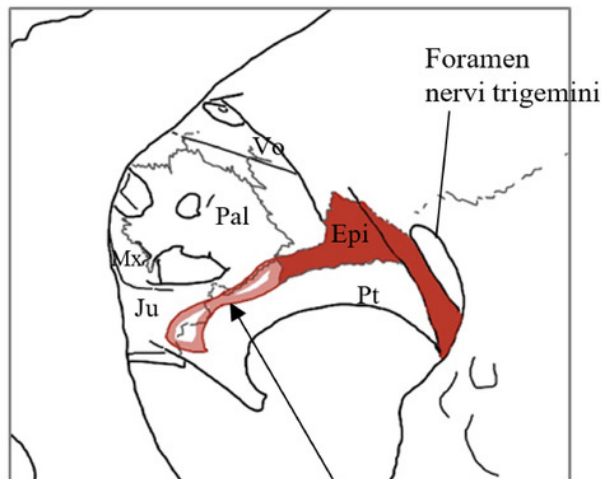
In the illustration, the dark red area marks the epipterygoid, while the anterior to it light red area highlights the extent of the sulcus epipterygoidei.

A



sulcus pro-epipterygoidei

B



sulcus pro-epipterygoidei